New Insights into the Function of the (Pro)Renin Receptor/ATP6ap2 in the Kidney

---

Dissertation

zur

Erlangung der naturwissenschaftlichen Doktorwürde

(Dr. sc. nat.)

vorgelegt der

Mathematisch-naturwissenschaftlichen Fakultät

der

Universität Zürich

von

Marta Raquel Figueiredo

aus Portugal

Promotionskomitee

Prof. Dr. med. Carsten A. Wagner (Vorsitz und Leitung der Dissertation)

Prof. Dr. med. Johannes Loffing

Dr. Nati Hernando

Prof. Dr. med. Erik Ilsø Christensen

Zürich, 2016

Zusammenfassung

Der (Pro)reninrezeptor ((P)RR) ist ein Typ-1-Transmembranprotein verbunden mit dem lokalen Renin-Angiotensin-System (RAS), einem hormonalen System, welches in die Regulation des arteriellen Drucks und der Natriumhomöostase involviert ist. (P)RR hat zwei Liganden: Renin und Prorenin. Renin hat nach Bindung an den (P)RR eine erhöhte Aktivität und Prorenin erlangt enzymatische Aktivität ohne Entfernung des Prosegments. Wenn entweder Prorenin oder Renin mit dem (P)RR interagieren, wird die Angiotensin I und Angiotensin II Produktion initiiert aber auch der MAP-Kinase Signalweg aktiviert und zwar unabhängig von der Angiotensin II Produktion. Eine verkürzte Form des (P)RR assoziiert mit vakuolären H^+-ATPasen; des Weiteren ist der (P)RR ein Adapterprotein zwischen Wnt-Rezeptoren und H^+-ATPasen. Daher ist ATP6ap2, H^+-ATPase associated protein 2, ein anderer Name für den (P)RR.

Die H^+-ATPase ist ein Proteinkomplex aus vielen Untereinheiten der den transmembranären Transport von Protonen vermittelt, welcher durch die Hydrolyse von ATP angetrieben wird. H^+-ATPasen haben zwei Hauptdomänen, eine zytosolische V_1-Domäne und eine membranständige V_0-Domäne. H^+-ATPasen kommen hauptsächlich in intrazellulären Organellen wie Endosomen, Lysosomen, Golgi-Apparat und sekretorischen Vesikeln vor, aber auch in der Plasmamembran von Zellen in Niere, Innenohr, Nebenhoden und Knochen. In intrazellulären Organellen sind H^+-ATPasen notwendig für die Ansäuerung der späten Endosomen und Lysosomen, was Membrantrafficking, Proteindegradation und Proteinreifung ermöglicht. Plasmamembran-assoziierte H^+-ATPasen haben zellspezifische Funktionen wie Körper-pH-Homöostase, Samenreifung, Innenohr-pH-Homöostase und Knochenresorption.

Nieren exprimieren sehr stark H^+-ATPasen in der Plasmamembran des proximalen Tubulus (PT), der Schaltzellen (IC) und in Membranen intrazellularer Organellen. Daher sind H^+-ATPasen in der Niere in

verschiedene Funktionen involviert, wie Endozytose, Membranprotein-Recycling sowie auch in die Ansäuerung des Urins und die Reabsorption von Proteinen mit geringem Molekulargewicht, Bikarbonat und Salz. (P)RR/ATP6ap2 ist in der Niere ebenfalls hoch exprimiert und an den gleichen Orten wie H^+-ATPasen lokalisiert. Jedoch ist die funktionelle Bedeutung der Koexpression von (P)RR und H^+-ATPase im Nieren PT momentan unklar. Diese Dissertation beabsichtigt die Funktion von (P)RR/ATP6ap2 in der Niere, besonders im PT, zu evaluieren und zu verstehen.

Im ersten Kapitel charakterisierten wir die Expression des (P)RR/ATP6ap2 entlang des Nephrons der Mausniere. Wir konnten mit semi-quantitativer real-time PCR (qRT-PCR) zeigen dass *Atp6ap2* mRNA entlang des gesamten Nephrons exprimiert wird, mit höherer Expression im Verbindungstubulus/kortikalen Sammelrohr (CNT/CCD) und im äußeren medullären Sammelrohr (OMCD). Anschliessend haben wir mittels Immunohistochemie die Lokalisation von ATP6ap2 zusammen mit der a4-H^+-ATPase-Untereinheit im proximalen Tubulus gezeigt und die subzelluläre Lokalisation von (P)RR/ATP6ap2 in Schaltzellen untersucht. Wir konnten aufzeigen, dass der (P)RR/ATP6ap2 ausserdem der Expression der H^+-ATPase- Untereinheit a4 in diesen Zellen folgt. Um das H^+-ATPase Trafficking und die Koregulation von (P)RR unter Bedingungen von Säure-Base- oder Elektrolytänderungen zu untersuchen, behandelten wir Mäuse mit NH_4Cl, $NaHCO_3$, $KHCO_3$, NaCl oder dem Mineralocorticoid DOCA für sieben Tage. Wir konnten zeigen, dass der (P)RR/*Atp6ap2* und die H^+-ATPase-Untereinheiten a4 und B1 weder auf dem Protein- noch auf dem mRNA-Level koreguliert sind. Desweiteren konnten wir mittels Immunohistochemie mit Nierengewebe von Kontrollmäusen, NH_4Cl- oder $NaHCO_3$-behandelten Mäusen zeigen, dass der PRR/ATP6ap2 mit H^+-ATPase-Untereinheiten in der Bürstensaummembran von proximalen Tubuli, dem apikalen Pol von Typ-A Schaltzellen und in der basolateralen und/oder apikalen Membran von nicht-Typ A Schaltzellen immer kolokalisiert ist. Mikroperfusion von isolierten kortikalen Sammelrohren und luminale Applikation von Prorenin stimulierten die H^+-ATPase-Aktivität nicht akut. Unsere Ergebnisse zeigen, dass der

PRR/ATP6ap2 möglicherweise einen Komplex mit der H^+-ATPase im proximalen Tubulus und in Schaltzellen bildet und dass Prorenin keinen akuten Effekt auf die H^+-ATPase-Aktivität in Schaltzellen hat.

Im zweiten Kapitel untersuchten wir die (P)RR/ATP6ap2-Funktion im proximalen Tubulus mittels zweier verschiedener Tiermodelle: einem Rattenmodell mit induzierbarer shRNA für *Atp6ap2* und eine induzierbare Nierenepithel-Zellspezifische knockout Maus für (P)RR/ATP6ap2. Im proximalen Tubulus sind H^+-ATPasen an der Rezeptor-vermittelten Endozytose beteiligt, welche die Reabsorption von Proteinen mit geringem Molekulargewicht durch Megalin/Cubilin Rezeptoren gewährleistet. Wir postulierten, dass (P)RR/ATP6ap2 wichtig ist für die H^+-ATPase-Funktion in der Rezeptor-vermittelten Endozytose und somit auch für die Funktion des proximalen Tubulus. Wir zeigten, dass genetische Deletion von (P)RR/ATP6ap2 im proximalen Tubulus in Ratten und Mäusen Albuminurie und Proteinurie von Proteinen mit geringen Molekulargewicht verursacht. Um den endozytotischen Weg genauer zu untersuchen, wurden beide Tiermodelle mit einem Marker für Flüssigphase Endozytose (10 kDA Dextran-FITC) und Rezeptor-vermittelte Endozytose (humanes Transferrin) injiziert. Die Endozytose von injiziertem Dextran-FITC war normal, wohingegen die Prozessierung von rekombinantem Transferrin zu den Lysosomen verzögert war. Dieser Effekt ging mit reduzierter Expression verschiedener H^+-ATPase-Untereinheiten, Akkumulation der LC3-B Untereinheit des Autophagosomens und reduziertem mTOR-signaling einher. Folglich ermöglicht (P)RR/ATP6ap2 die Rezeptor-vermittelte Endozytose, womöglich durch Modulation von H^+-ATPasen im proximalen Tubulus und ist wichtig für die normale lysosomale Funktion.

Zusamemnfassend präsentiert diese Dissertation neue Belege dafür, dass der (P)RR/ATP6ap2 an der Regulation der Nierenhomöostase im proximalen Tubulus beteiligt ist. Weiterhin zeigen wir, dass der (P)RR/ATP6ap2 für die Funktion von Lysosomen und des Autophagosomes relevant ist, und dies möglicherweise aufgrund der Interaktion mit H^+-ATPasen. Diese Rolle von (P)RR/ATP6ap2 in der zellulären Homöostase

scheint auch in anderen murinen Zelltypen wichtig zusein, wie Podozyten, Kardiomyozyten und Schaltzellen. Es gleicht auch Funktionen in anderen Organismen wie Drosophila und Zebrafisch. All diesen Beispielen ist die Interaktion von (P)RR/ATP6ap2 mit H^+-ATPasen gemeinsam. Deshalb untermauert diese Dissertation ausserdem die potentielle, universale, zelluläre Rolle von (P)RR/ATP6ap2 und wir schlagen vor, dass die Regulation der Funktion von H^+-ATPasen vielleicht eine, wenn nicht die Hauptfunktion des (P)RR/ATP6ap2 ist.

Abstract

The (Pro)renin receptor or (P)RR is a type one transmembrane protein linked to the local renin-angiotensin system (RAS), a hormonal system involved in arterial pressure regulation and sodium homeostasis. (P)RR has two ligands: renin and prorenin. Upon binding to (P)RR, renin has its activity increased and prorenin gains enzymatic activity without removal of the pro-segment. When either prorenin or renin interact with the (P)RR, angiotensin I and angiotensin II production is initiated but also MAP kinase signaling is triggered even independent from angiotensin II production. A truncated form of the (P)RR has been shown to associate with vacuolar H^+-ATPases; furthermore, the (P)RR is an adaptor protein between Wnt receptors and H^+-ATPase. Hence, another name for the (P)RR is ATP6ap2 for H^+-ATPase associated protein 2.

The H^+-ATPase is a multi-subunit protein complex that mediates the transport of protons driven by hydrolysis of ATP. H^+-ATPases have two main domains, a cytosolic V_1 domain, and a membrane-inserted V_0 domain. H^+-ATPases are mainly located in intracellular organelles like endosomes, lysosomes, golgi apparatus and secretory vesicles but it can also be found in the plasma membrane in cells in kidney, inner ear, epididymis, and bone. In intracellular organelles, H^+-ATPases are fundamental for acidification of late endosomes and lysosomes allowing for membrane trafficking, protein degradation, and protein maturation. Plasma membrane H^+-ATPases carry cell specific functions such as regulation of body pH homeostasis, sperm maturation, inner ear pH homeostasis, and bone resorption.

Kidneys express very high levels of H^+-ATPases in the plasma membrane of proximal tubules (PT), intercalated cells (IC), and in membranes of intracellular organelles. Therefore, H^+-ATPases in the kidney are involved in multiple functions such as endocytosis, membrane protein recycling as well as urine acidification and reabsorption of low molecular weight proteins,

bicarbonate, and salt. The (P)RR/ATP6ap2 is also highly expressed in the kidney sharing the same locations with H^+-ATPases. However, the functional significance for (P)RR and H^+-ATPase co-expression in the kidney PT is currently unclear. This thesis aims to evaluate and understand the function of the (P)RR/ATP6ap2 in kidney, in particular in the PT.

In chapter 1 we characterized thoroughly (P)RR/ATP6ap2 expression along the mouse nephron. We could show using semi-quantitative real-time PCR (qRT-PCR) that *Atp6ap2* mRNA is expressed along the entire nephron with higher expression in the connecting tubule/ cortical collecting duct (CNT/CCD) and outer medullary collecting duct (OMCD). Next, using immunohistochemistry, we demonstrated localization of the (P)RR/ATP6ap2 together with the a4 H^+-ATPase subunit in the proximal tubule and studied subcellular localization of the (P)RR/ATP6ap2 in intercalated cells. We could demonstrate that the (P)RR/ATP6ap2 also follows H^+-ATPase subunit a4 expression in these cells. To investigate H^+-ATPase trafficking and co-regulation of the (P)RR/ATP6ap2 under conditions of acid-base or electrolyte changes, we treated mice with NH_4Cl, $NaHCO_3$, $KHCO_3$, NaCl, or the mineralocorticoid DOCA for 7 days. We could demonstrate that the (P)RR/*Atp6ap2* and H^+-ATPase subunits a4 and B1 are not co-regulated at protein and mRNA levels. However, immunohistochemistry using kidney tissues from control, NH_4Cl or $NaHCO_3$ treated mice allowed us to demonstrate that (P)RR/ATP6ap2 with H^+-ATPase subunits always colocalized at the brush border membrane of proximal tubules, the apical pole of type A intercalated cells, and at basolateral and/or apical membranes of non-type A intercalated cells. Microperfusion of isolated cortical collecting ducts and luminal application of prorenin did not acutely stimulate H^+-ATPase activity. Our results suggest that the (P)RR/ATP6ap2 may form a complex with H^+-ATPase in proximal tubule and intercalated cells and also that prorenin has no acute effect on H^+-ATPase activity in intercalated cells.

In chapter 2 we investigated the function of the (P)RR/ATP6ap2 in the proximal tubule using two different animal models. A rat model with an inducible shRNA for *Atp6ap2* and an inducible kidney epithelial cell-specific

knockout mouse for the (P)RR/ATP6ap2. The latter model resulted in a partial deletion of the (P)RR/ATP6ap2 which was mostly occurring in proximal tubules but left (P)RR/ATP6ap2 expression in intercalated cells widely intact. In the proximal tubule, H^+-ATPase are involved in receptor-mediated endocytosis allowing for the reabsorption of low molecular weight proteins via the megalin/cubilin receptors. We hypothesize, that the (P)RR/ATP6ap2 is important for H^+-ATPases function in receptor mediated endocytosis, being also important for proximal tubule function. We reported that genetic deletion of the (P)RR/ATP6ap2 from the proximal tubule in rats and mice causes albuminuria and low molecular weight proteinuria. To study in more detail the endocytic pathway, we injected both animal models with a marker for fluid phase endocytosis (10 kDA Dextran-FITC) and receptor-mediated endocytosis (human transferrin). Endocytosis of injected Dextran-FITC was normal whereas processing of recombinant transferrin to lysosomes was delayed. This defect was paralleled by reduced expression of several H^+-ATPases subunits, accumulation of the LC3-B subunit of the autophagosome and reduced mTOR signaling. Thus, the the (P)RR/ATP6ap2 facilitates receptor-mediated endocytosis in the proximal tubule possibly by modulating H^+-ATPases and is important for normal lysosomal function.

Overall this thesis presents new evidence for (P)RR/ATP6ap2 function in the proximal tubule in regulating kidney homeostasis. It further suggests that the (P)RR/ ATP6ap2 is relevant for lysosomal/ autophagy function and that this role may be due to the interaction with H^+-ATPases. This role of (P)RR/ATP6ap2 in cellular homeostasis seems to be consistent with data from other murine cell types such as podocytes, cardiomyocytes and intercalated cells. It parallels also functions in other organisms like drosophila and zebrafish. In all these examples the interaction of the (P)RR/ATP6ap2 with H^+-ATPases is common. Thus, this thesis additionally corroborates this potential universal cellular role of the (P)RR/ATP6ap2 and suggests that the regulation of H^+-ATPase function may be one if not the major function of the (P)RR/ATP6ap2.

Table of content

1.Introduction

1.1 Kidney: overview of the nephron segments

The kidney plays an essential role in maintaining body homeostasis via the regulation of electrolytes, acid-base balance, and blood pressure regulation. It achieves this vital function by filtering blood and excreting metabolic waste. The functional unit of the kidney is the nephron that is organized in several distinct segments (Figure 1). The nephron consists of the glomerulus, the proximal tubule (PT), the loop of Henle, and the distal tubule. Different tubular segments present different ultrastructures, different cell types and even different transporters according to their specific functions.

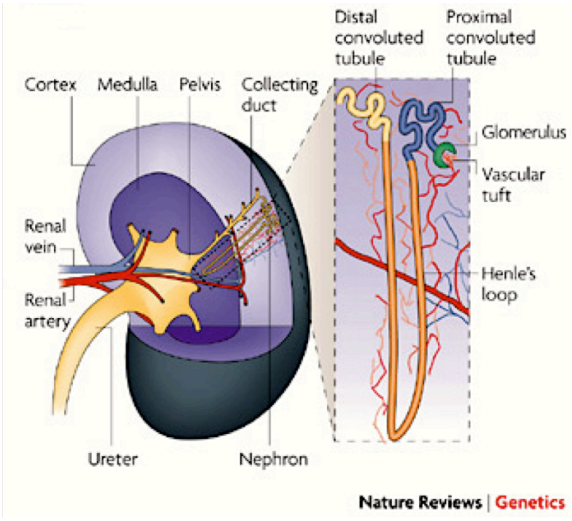

Figure 1. Kidney general anatomy and nephron organization. The kidney is grossly organized into renal cortex and the renal medulla. The kidney functional units is the nephron represented in the insert. Edited from Schedl A., 2007

The glomerulus and Bowman's capsule are part of the kidney filtering unit, localized at the beginning of the nephron. Blood is filtered through glomerular capillaries into the space of Bowman's capsule. The glomerular filtration barrier has three components: capillary endothelium, basement membrane and podocytes. Podocytes are highly differentiated cells lining the outer part of the glomerular capillaries facing the Bowman's capsule [1]. From

the capillary endothelium to the podocytes, the strigency of the filtration barrier increases, allowing the passage of cationic molecules, electrolytes and small and intermediate solutes like urea (60 Da) and glucose (180 Da). This barrier is then selective according to molecular size, electrical charge but also molecular radius. Plasma cells and higher molecular weight plasma proteins (cut off limit for passage of proteins is 60 kDa) are retained by the glomerular filtration barrier [2,3]. In physiological conditions a small amount of intermediate molecular weight proteins like albumin (66 kDa) and transferrin (81 kDa) are allowed to pass the glomerular filtration barrier to a limited extent while all low molecular weight proteins (between10- 40 kDa) have less restrictions in their passage through the filtration barrier [4].

Following the glomeruli is the proximal tubule (PT), which can be segmented according to its gross anatomy into convoluted PT and straight PT. The PT is responsible for reabsorbing the bulk of the ultrafiltrate that passes through the glomerular filter. Due to its reabsorbing functions PT cells exhibit a well-developed apical brush border membrane (BBM), tight junctions, abundance of large mitochondria, an enriched endosome system, and infoldings at the basolateral side [5]. This segment will be discussed in more detail in section 1.2.

The proximal tubule progresses to the loop of Henle (LOH), which can be further subdivided into thin descending and ascending limbs of LOH and thick ascending limb of LOH (TAL). The LOH segment is the nephron part responsible for creating a cortico-medullary concentration gradient, which in turn makes possible to concentrate urine.

The distal tubule is the part of the nephron between the LOH and the collecting duct system (CD). The distal tubule is constituted by the distal convoluted tubule (DCT) and the connecting tubule (CNT). The CD system consists of a number of tubules and ducts that connect nephrons to the pelvis. This region is responsible for fine-tuning urine concentration, regulating pH body homeostasis and is target for several hormones like aldosterone. The CD is characterized by three cell types based on ultrastructure features, transporters composition and function. These cell types are: principal cells

(PC), intercalated cells type-A (IC-A) and type-B (IC-B). PCs are the majority of cells and play a role in water and electrolyte balance while intercalated cells are mostly responsible for acid-base excretion. IC-A is more common in the outer medulla, whereas IC-B are restricted to the renal cortex.

From the CD, filtrate is collected into the pelvis and ureter and finally proceeds to the bladder.

1.2. Proximal tubule

1.2.1 The Structure of the Proximal tubule

The PT can be further segmented according to its ultrastructure. The first segment (S1) is located in the initial part of the convoluted PT, the second segment (S2) spans between the end of the convoluted PT and beginning of straight PT and finally the third segment (S3) is located in the remaining straight PT. S1 cells are characterized by taller BBM, abundant mitochondria and vacuolar system (mainly endosomes and lysosomes) and several ridges in both the basal and lateral side. S2 cells share a few characteristics with the S1 segment cells but S2 cells have a reduced amount of mitochondria, vacuolar system and darker lysosomes. The S2 cell structure, as it can be observed in Figure 2, reflects a transition between S1 to S3 segment. S3 cells show smaller, lesser number of mitochondria with random distribution, less number of vacuoles and a prominent number of peroxisomes.

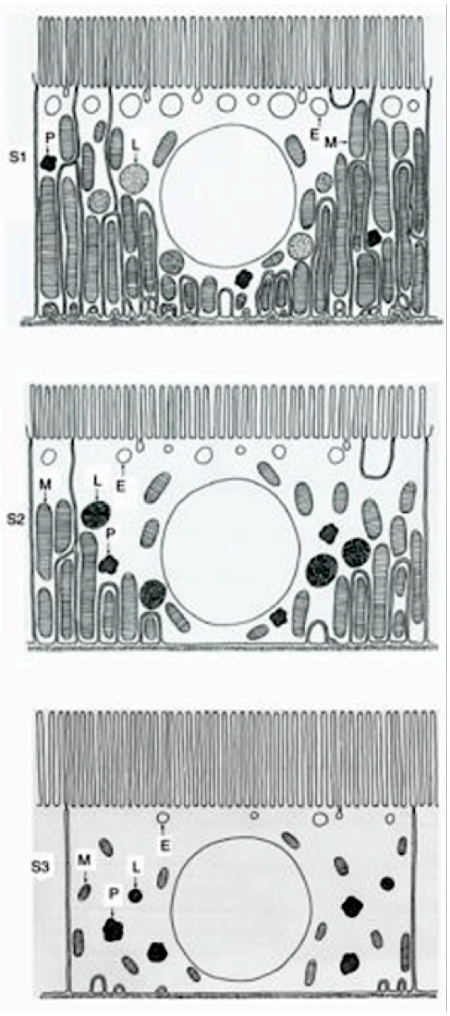

Figure 2. Schematic drawings of proximal tubule ultrastructure, illustrating the three segments of the proximal tubule, S1,S2 and S3. Edited from Christensen et al. 2012

The PT segment ultrastructure reflects its function [5,6].Thus, the S1 segment is concerned with solute reabsorption via sodium dependent transporters, which requires a high reabsorption surface demonstrated by the well-developed brush border membrane and the presence of abundant mitochondria for energy demanding transport. The segments S2 and S3 also contribute to solute reabsorption but their main function is in the excretion of xenobiotics. Therefore, segments S2 and S3 play an important role in the kidney detoxification functions.

1.2.2 Functions of the Proximal Tubule: Low molecular weight proteins retrieval

The PT plays a fundamental role in reabsorbing filtered ions and solutes like glucose and amino acids through its well-developed brush border

membrane and polarized transport system. The PT is also responsible for reabsorbing low molecular weight proteins (LMWPs) like: albumin (66 kDa), transferrin (81 kDa), as well as hormones like parathyroid hormone (6 kDa) and insulin (5,8 kDa) but also vitamin carriers like retinol binding protein (21 kDa) or vitamin D binding protein (55 kDa), enzymes such as α-amylase (55 kDa), immunoglobulin light chains and cell surface antigens [7]. Considering that final urine is almost devoid of proteins, PT reabsorbs and metabolizes an extensive amount of LMWPs. LMWPs uptake by the PT is mainly via receptor-mediated endocytosis, clathrin-dependent endocytosis and possibly by fluid-phase endocytosis [8-10]. A general overview of receptor- mediated endocytosis is represented in figure 3.

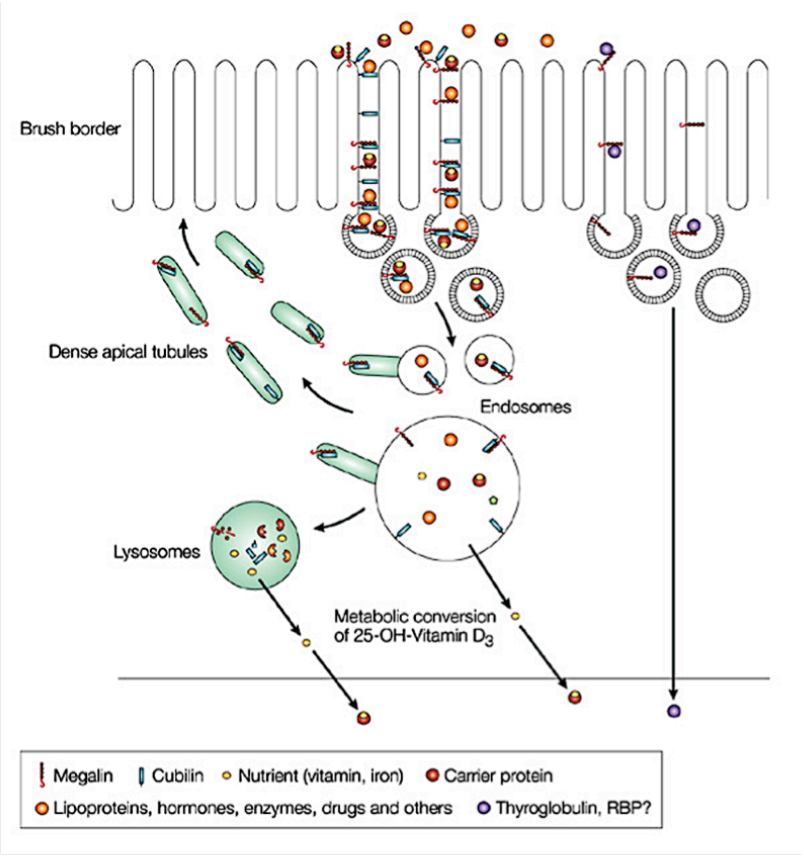

Figure 3. Schematic representation of an PT epithelial cell, which shows possible pathways by which megalin and cubilin can mediate endocytosis and transcellular transport.. Edited from Christensen et al 2002

1.2.3 General structure of the apical endocytic pathway in the proximal tubule

The key features of the endosomal organization are common to all cell types. Internalization of cargos begins with membrane invagination following either a clathrin-dependent, a caveolin-dependent or a clathrin- and caveolin-independent internalization. Thus, glomerular filtrate reaches the PT BBM where it is internalized. Subsequently, internalized cargo arrives at early endosomes where it is sorted either back to membrane (recycling pathway) or moves to the next compartments, the late endosomes. Late endosomes fuse transiently with lysosomes to deliver cargo for degradation (degradative pathway) [11,12]. From early endosomes to lysosomes, this vesicular system goes through several steps of maturation, transformation, fusion and fission. Lipid content and protein content changes according to each step in a transient fashion. Small GTP binding proteins termed Rabs are sequentially recruited onto these compartments regulating formation, transport, tethering, targeting and fusion of vesicular compartments. Rabs switch determines the compartment identity along the endocytic pathway. For example in most of the cells Rab5 is characteristic of early endosomes while Rab7 is localized in the late endosomes [11,13,14].

The present knowledge about the organization of the proximal tubule apical endocytic machinery comes from studies using immortalized and primary cell culture models of proximal tubules, but also from *in vivo* studies using filtered fluid phase and receptor mediated markers [15-18].. In these studies, rats, mice or rabbits were administered intravenal injections of markers for the receptor-mediated and fluid phase endocytosis, and kidneys were fixed at different time intervals to visualize the markers progression along the endocytic pathway [19-23]. Briefly, these studies showed that:

- ✓ Initially both fluid phase and receptor-mediated markers are internalized into clathrin coated structures located at the base of BBM microvilli.
- ✓ These vesicles then lose their clathrin coating and fuse with dense subapical network of tubules.

- ✓ Within 1 to 15 min, both markers are trafficked to a larger vacuolar compartment called apical vacuoles.
- ✓ Receptors that are recycled back to the membrane travelled from the subapical tubule and from apical vacuoles while its respective ligands go to lysosomes for degradation. The structure of the lysosomes changes from species to species and according to the PT segment.

1.2.4 Receptor-mediated endocytosis in proximal tubule: megalin and cubilin.

Receptor- mediated endocytosis in the PT relies on a low affinity, high capacity system, represented by its two main membrane receptors: megalin and cubilin [24-27]. Ligands bound to megalin or cubilin are internalized as a receptor-ligand complex, in the endosomes upon acidification ligands are separated from megalin and cubilin. Ligands are usually transferred to lysosomes and the receptors are recycled back to the proximal tubule apical membrane.

Megalin is a large glycoprotein (approximately 600 kDa) that belongs to the low-density lipoprotein receptor family and is present in several plasma membranes and in the endocytic apparatus of epithelial cells. Megalin is characterized by a large extra-cellular domain containing three types of repeats: four cysteine-rich complement repeats interspaced by growth factor repeats and one epidermal growth factor like repeat (figure 4). The extra-cellular domain is followed by a single transmembrane domain and a small (209 amino acid) cytoplasmic domain which contains two endocytic motifs NPXY which mediate uptake via clathrin coated pits and a NPXY like motif (NQNY) involved in megalin apical delivery [28-30]. Megalin also contains a RXRR motif, which is a target for proteases like furin, leading to secretion of megalin into urine [31]. Besides that, megalin can undergo intramembrane cleavage initiating signaling cascades [32,33].

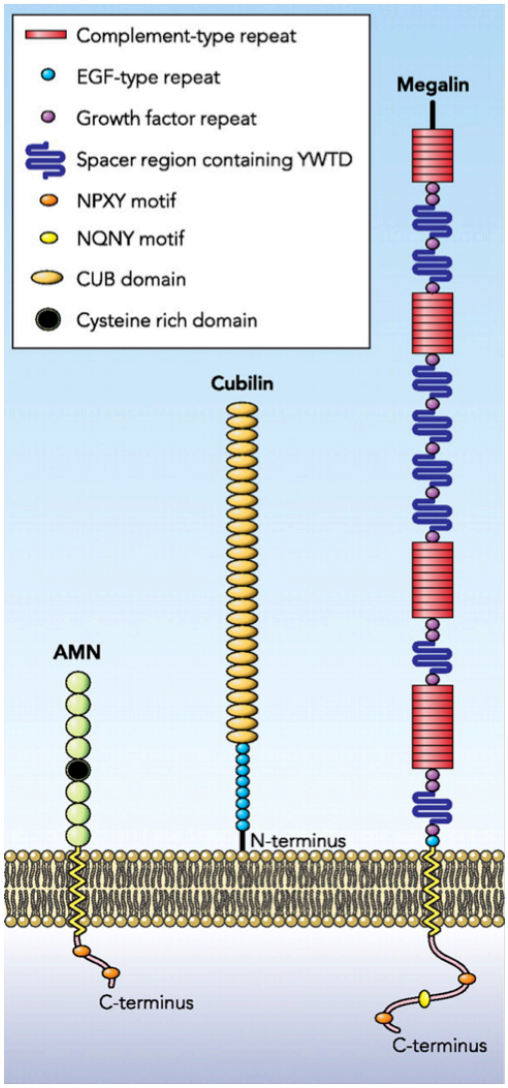

Figure 4. Schematic structure of megalin, cubilin, and amnionless. Figure legend shows domains and motifs of the receptors**.** Edited from Christensen et al 2012

Cubilin shares the same localization of megalin in the BBM of PT and apical endocytic compartments. Cubilin is also known as the intestinal factor B_{12} receptor [34,35]. Cubilin is a 460 kDa glycosylated protein containing 23 complement sub-component domains (CUB) and no transmembrane domain or cytoplasmic domain. The latter implies that cubilin needs to interact with other proteins in order to be positioned at the outer surface of the plasma membrane and to function in endocytosis. Megalin is thought to be the main interacting partner forming a two-receptor complex [36,37]. Cubilin trafficking to the apical membrane is also dependent on another 38-50 kDa single transmembrane protein called amnionless. This functional link was proven *in vivo* in dogs containing mutations in ammnionless, amnionless deficient mice and patients with Imerslund-Gräsbeck syndrome that showed intracellular accumulation of cubilin [38,39].

Megalin and cubilin in the PT have functions that are directly connected to protein/ligand re-uptake from the filtrate. Table 1 shows some main ligands for megalin and cubilin in the PT. Megalin and cubilin are involved in vitamin metabolism like for vitamin D in which vitamin D is reabsorbed together with its carrier vitamin D binding protein and activated after transfer to mitochondria [40]. Megalin is also a receptor for the degradation of parathyroid hormone playing a role in calcium and phosphate metabolism.

Megalin is also involved in lysosome biogenesis, by allowing lysosome enzymes like cathepsin B reabsorption and delivery to lysosomes where the proenzyme can become functional [41].

Megalin	*Cubilin*
Vitamin carriers	
Transcobalamin-vitamin B12	Transcobalamin-vitamin B12
Vitamin D binding protein	Vitamin D binding protein
Retinol-binding protein	
Other carriers	
Albumin	Albumin
Receptor associated protein	Receptor associated protein
Ig light chains	Ig light chains
Hemoglobin	Hemoglobin
Plasminogen	Transferrin
Lactoferrin	Clara cell secretory protein
Thyroglobulin	
Hormones and signaling proteins	
Parathyroid hormone	
Insulin	
Epidermal growth factor	
Prolactin	
Angiotensin II	
Leptin	
Enzymes	
Lipoprotein lipase	
Plasminogen	
α - amilase	
Cathepsin B	

Table 1. Examples of ligands for megalin and cubilin. Edited from Christensen et al 2012

The importance of megalin and cubilin is well illustrated by knockout animal models. Constitutive knockout megalin mice model, die after birth with pulmonary complications, brains defects and a decreased proximal tubule endocytosis machinery [42]. In a conditional knockout of megalin in the proximal and distal tubules, mice did not show major proximal tubule cellular structure difference. However, knockout mice had a reduced number of coated pits, endosomes, and lysosomes in comparison with control animals. These animals also excreted LMWPs in the urine like lipophilic vitamin carriers[43]. Later, a role for megalin in calcium and phosphate homeostasis was established [27,44-46]. Similarly, studies in pronephros of zebrafish deficient for

megalin showed that fluid phase endocytosis was abolished, endocytic uptake was affected and the structure of the endocytic apparatus was changed [47]. In a study with cubilin cre-lox deleted mice, cubilin was shown to be important for amnionless expression and for albumin uptake in the PT [48]. Megalin and cubulin ligands are described in more detail in table 1. In this thesis, we worked with ligands that are internalized by both megalin and cubilin (albumin and vitamin D binding protein), but also ligands that are specifically transported by megalin (procathepsin B) and by cubilin (transferrin).

1.2.5 Proximal tubule dysfunctions in humans

The general dysfunction of the proximal tubule is a clinical syndrome called De Toni-Debré-Fanconi syndrome, which is characterized by loss of glucose, amino acids, bicarbonate, phosphate and LMWPs in the urine. De-Toni-Debré-Fanconi syndromes can be classified as congenital disorders such as Dent`s disease, Lowe`s disease and cystinosis or can be acquired as a result of toxin or drug exposure [27,49]. Clinical symptoms of De-Toni-Debré-Fanconi Syndromes are a result of solute or LMWPs wasting, like osteomalacia and metabolic acidosis.

Dent's disease is a rare X-linked genetic disease which can be divided into Dent's 1 and Dent`s 2 [49,50]. Dent`s 1 was found to be associated with mutations in the CLCN5 gene, which encodes for a proton/chloride exchanger required for endosome acidification [50-52]. The disease mechanism of Dent`s 1 was elucidated by studies using knockout animals for the CLC-5 exchanger. These animals showed tubular proteinuria due to endosomal acidification impairments and decreased expression of megalin and cubilin in PT BBM [50,53-56]. In these animals a decreased urinary excretion of megalin (megalin sheeding) was observed which was also seen in Dent's disease patients. Dent`s 2 patients have mutations in the OCRL gene which encodes an inositol 5-phosphatase. Lowe syndrome patients also have mutations in OCRL but display extra renal symptoms like congenital cataracts and mental disabilities. OCRL was shown to be localized in several endocytic compartments and to be important for megalin recycling [57].

Proximal tubule proteinuria can also be a consequence of direct mutations in megalin and cubilin genes as for rare genetic diseases like Imerslund-Gräsbeck syndrome and Donnai Barrow Syndrome. The first disease is characterized by the incapacity to absorb vitamin B12 in the small intestine due to mislocation of cubilin. The second syndrome is a facio-oculo-acoustico-renal syndrome caused by mutations in the megalin gene (*LRP2)* leading to *the* absence of a functional megalin protein.

Cystinosis is a rare autosomal genetic disease belonging to the lysosomal storage diseases group, that is caused by mutations in CTNS, a lysosomal cystine transporter. Fanconi syndrome is one of the first manifestations of cystinosis. A recent study in human proximal tubular epithelial cells deficient for the CTNS gene revealed a potential mechanism that could lead to Fanconi syndrome. These cells showed an impaired endosome machinery, reduced expression of megalin associated with reduced trafficking and accumulation of lysosome cargos [58].

1.3. The (Pro)renin receptor / ATP6AP2

The renin angiotensin system (RAS) is a hormonal system involved in arterial pressure regulation and sodium homeostasis [59]. Renin is an aspartic protease that performs the rate limiting step of the RAS by enzymatically cleaving angiotensinogen to angiotensin I. Renin is produced as an inactive precursor, prorenin, which contains a pro-segment that when cleaved releases renin. Renin is synthesized, stored and secreted by specialized cells in the wall of the afferent arteriole of the kidney while prorenin is secreted constitutively mainly in the kidney but also to a much smaller extent by other organs like adrenal gland, eye, and reproductive organs [60].

In line with some studies that point to a local tissue RAS production [61], the (pro)renin receptor ((P)RR) was discovered in 2002 by G. Nguyen [62]. Renin and prorenin can both bind to (P)RR, the first has its activity increased and the latter gains enzymatic activity without removal of the pro-segment (conformational change without cleavage of the pro-segment).

The (P)RR is a 350 amino acid protein that is expressed in the brain, heart, liver, kidney, muscle, adrenal glands, pancreas, ovary, and placenta [62]. In the kidney (P)RR expression was found in mesangial cells [62], podocytes [63] in the proximal tubule and in intercalated cells [64]. At the cellular level (P)RR is mainly found in intracellular organelles but it can also be found in the plasma membrane like for instance in the intercalated cells [64,65].

The (P)RR protein has 4 domains: a N-terminal signal peptide, an extracellular domain that allows renin and prorenin binding, a single transmembrane domain, and a short cytosolic domain [66] (figure 5). It contains also a furin cleavage site that undergoes cleavage in the trans- Golgi network by ADAM19 giving origin to a soluble form, s(P)RR, that is secreted into the extracellular space [67,68]. The (P)RR transmembrane and cytoplasmic domain was found to be identical to the M8-9 protein, a potential accessory subunit of H^+-ATPases and since then (P)RR is also named ATP6ap2 [69].

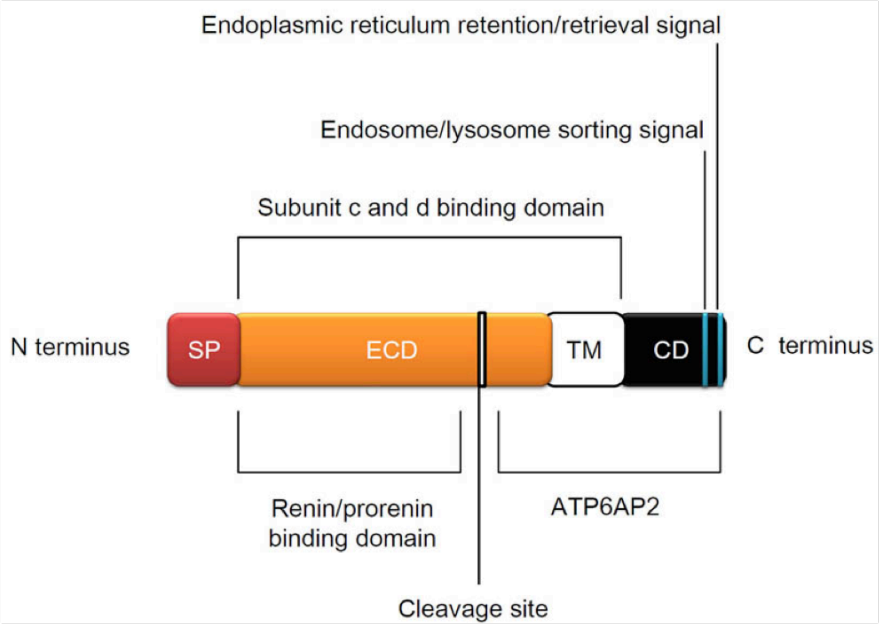

Figure 5. (P)RR/ ATP6AP2 structure. List of abbreviations: SP, signal peptide; ECD, extracellular domain; TM, transmembrane domain; CD, cytosolic domain. Edited from Ichihara, 2011.

1.3.1 (P)RR/ ATP6AP2 functions

The (P)RR/ATP6ap2 has functions dependent and independent from Angiotensin I (ANG I) production. Regarding functions dependent on ANGI production, (P)RR/ATP6ap2 allows activation of prorenin and increase of renin`s catalytically activity[62]. Studies with low sodium diet and ANG II overproduction lead to a increase in (P)RR/ ATP6ap2 expression suggesting that it may be involved in salt and water regulation by the kidney [70,71].In a recent study with a conditional knockout for (P)RR/ATP6ap2 only in kidney epithelial cells, this role of the (P)RR/ATP6ap2 in salt and water homeostasis was investigated in detail. Knockout mice for (P)RR/ATP6ap2 had diluted urine, higher water intake as a consequence of reduced aquaporin 2 and arginine vasopressin levels in renal medulla[72]. However, this may rather be the consequence of loss of medullary tissue and hydronephrosis. In line, Trepiccione et al showed that renal expression of the (P)RR/ATP6ap2 was not necessary for normal activation of the RAS [73].

Apart from the ANG I production when (P)RR/ATP6ap2 ligands bind they may activate mitogen-activated protein kinase (MAPK) signaling and extracellular signal regulated kinase (ERK1/2) [74]. The activation of these kinases per se activates other signaling molecules like transforming growth factor–β1 (TGF-β1) [75], plasminogen–activated inhibitor 1 (PAI-1) [76], cyclooxygenase-2 (COX2) [77,78], interleukin-1 and tumor necrosis factor α (TNFα). The (P)RR/ATP6ap2 seems also to be involved in arginine vasopressin signaling, as it was demonstrated in a study performed in Madin-Darby canine kidney C11 cells [79]. In regard to ANG I independent functions but ligand dependent functions there are some controversies since most of the studies used renin and prorenin in supra-physiological concentrations (nM concentration instead of the physiological picomolar range), leading to the belief that there might be (an)other receptor(s) for these ligands. [80]

During development (P)RR/ATP6ap2 functions independently of its ligands, by serving as a physical adaptor between Fz/LPR6 (canonical elements of Wnt/ β–catenin signaling) and vacuolar H^+-ATPase [81]. It was reported that the (P)RR/ATP6ap2 is also involved in a non-canonical Wnt

signaling or planar cell polarity pathway (PCP) [82,83]. In these two studies (P)RR/ATP6ap2 deletion affected H^+-ATPase function suggesting the importance of the (P)RR/ATP6ap2 for H^+-ATPase function.

The (P)RR/ATP6ap2 was also shown to be important for kidney development via two different embryonic precursor cells: ureteric bud and cap mesenchymal cells [84,85]. These studies demonstrate that the (P)RR/ATP6ap2 is essential for nephron development and renal function postnatally. In another study, involving a inducible conditional knockout in the kidney epithelial cells, the (P)RR/ATP6ap2 was shown to be important for urine concentration [72]. Knockout animals for (P)RR/ATP6ap2 displayed a lower urine osmolality, higher water intake, and higher urine volume compared with control mice. The authors suggested that this could be due to lower levels of AQP2 and arginine vasopressin-induced cAMP in the medulla. Furthermore, in a more recent study using the same animal model, (P)RR/ATP6ap2 deletion resulted in a defect in the TAL, in PCs and ICs in the kidney [73]. Similarly, in this recent study, knockout mice for (P)RR/ATP6ap2 showed polyuria and polydipsia. Furthermore, medullary Na^+-K^+-$2Cl_2$ cotransporter (NKCC2) and AQP2 was reduced in the knockout animals. Interestingly, these mice also suffer from renal distal tubule acidosis due to reduce expression of H^+-ATPase subunit B1. They further show that (P)RR/ATP6ap2 deletion leads to autophagy defects in intercalated cells.

(P)RR/ATP6ap2 also has functions as a putative H^+-ATPase subunit. These functions will be discussed in detail in section 1.5.

1.4. H^+-ATPase

The H^+-ATPase is multisubunit membrane-bound protein complex consisting of two main domains, a cytosolic domain, V_1, and a membrane inserted domain, V_0 (figure 6). The V_1 catalyzes ATP binding and hydrolysis, while the V_0 domain mediates proton translocation [86-88] . The V_1 domain is composed of 8 different subunits (A,B,C,D,E,F,G,H) while V_0 is composed of 6 different subunits (a,d,e,c,c',c''). The A and B subunits of the V_1 domain

facilitate ATP binding and hydrolysis, while the remaining subunits form the central and peripheral stalks connecting the V_1 to the V_0 domain.

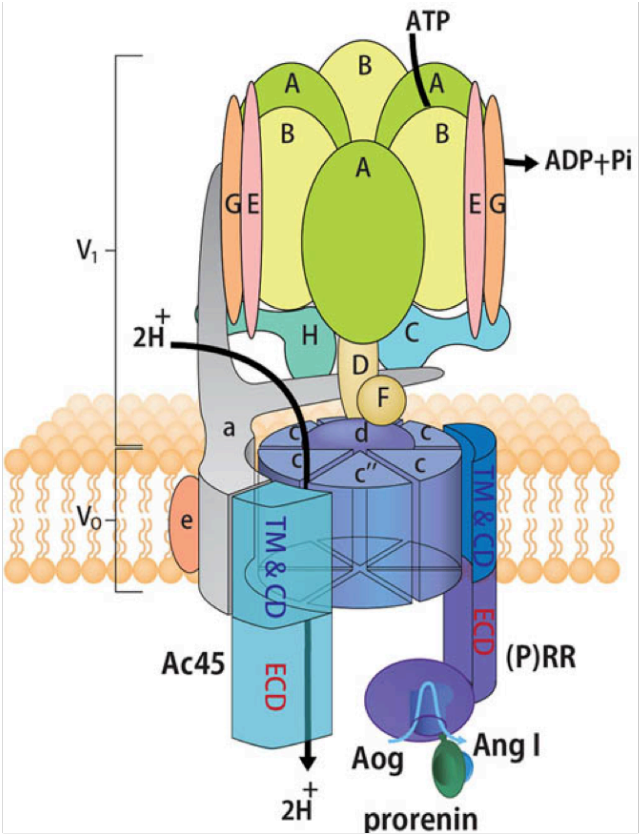

Figure 6. Structure of H^+-ATPase and its accessory subunits. H^+-ATPase is composed of a cytoplasmic domain V_1 responsible for ATP hydrolysis and membrane domain V_0 responsible for proton transport across membrane. Its accessory subunits are ATP6ap1 (Ac45) and ATP6ap2 ((P)RR). Edited from kinouchi et al, 2011

The central stalk transfers the energy generated from the ATP hydrolysis to the rotary ring on the V_0 domain, while the peripheral stalk is essential for preventing the rotation of the V_1 domain. Furthermore, the proteolytic ring in the V_0 domain is involved in proton translocation [80,87,88]. The presence of additional subunit isoforms and splice variants in mammals along with tissue specific expression differences adds to the already existing structural complexity. As an example, expression of a4, B1, and d2 H^+-ATPase subunits have been described to be enriched in the kidney [81,87-89].

1.4.1 H^+-ATPase intracellular functions

H^+-ATPase can be present in intracellular organelles, like lysosomes, endosomes and secretory vesicles. In these organelles, H^+-ATPase has a major function in acidification which allows processes like membrane trafficking, activation of ligand-receptor dissociation, protein processing or degradation and neurotransmitter uptake into secretory vesicles [82,83,88]. The role of H^+-ATPases in receptor-mediated endocytosis has been studied with the aid of pharmacological tools such as ionophores, weak bases and H^+-ATPase specific inhibitors (concanamycin and bafilomycin). In these studies, changes in endosomal pH resulted in non-dissociation of internalized ligand-receptor complexes and blocking of the recycling endosomal pathway that delivers unoccupied receptor back to the plasma membrane [11,90,91]. Furthermore, lysosomal enzymes require a low pH for their optimal activity and function in the degradation of internalized content. H^+-ATPase ensures, maintains and stabilizes an acidic pH in lysosomes. H^+-ATPase also generates pH gradients and positive membrane potential in secretory vesicles necessary for neurotransmitters, like glutamate and noradrenaline, to be taken up into secretory vesicles at the synapses [11,88].

Besides H^+-ATPase functions in membrane trafficking, H^+-ATPase is also thought to be a intracellular or intraorganellar pH sensor [92]. H^+-ATPase was shown to be important for recruitment of the GTPase Arf6 and GDP/GTP exchange factor (GEF) ARNO (ADP-ribosylation factor nucleotide site opener) to endosome membranes. Recruitment of Arf6 and ARNO to their target membranes is important for endosome regulation. Inhibition of interactions between H^+-ATPase–ARNO–Arf6 leads to endosome impairments namely in the transition between early and late endosomes [93]. This study also suggested that H^+-ATPases are not only important for intracellular acidification but also for signaling by helping recruiting other proteins. Furthermore, H^+-ATPases also act as a cytohesin-2 signaling receptor, a protein also known to be a regulator of signaling in the endosomal machinery [94-96]. Cytohensin-2/Arf6 in collaboration with H^+-ATPase are important for regulation of megalin/ cubilin receptor-mediated endocytosis in proximal

tubule cells *in situ.* The H^+-ATPase a2 subunit was indicated as a potential endosomal pH sensor and binding site for the above mentioned signaling molecules [97,98]. It is important to mention that H^+-ATPase interactions with other signaling partners relevant for trafficking happen in a pH dependent manner.

Recent studies, unraveled that H^+-ATPases are a component of the mammalian target of rapamycin 1 complex (mTORC1) and signaling pathway [99]. mTOR complex 1 initiates growth signaling pathways upon stimulation by growth factors, changes in the concentration of specific amino acids, oxygen levels or energy and stress levels. Additionally, H^+-ATPases were shown to be involved in sensing of lysosomal amino acid content which followed by interaction with Ragulator complex drives recruitment of mTOR complex 1 to the lysosome membrane and further activation [100,101]. Therefore, according to these studies, H^+-ATPases play an important role in amino acid sensing in lysosomes and mTOR complex 1 signaling. Interestingly, in a recent study using a drosophila model, it was discovered that H^+-ATPase/mTOR signaling regulates megalin mediated apical endocytosis [102]. In the same study but using a mouse model in which mTOR was pharmacologically inhibited, these animals displayed proteinuria and lower levels of megalin in kidney BBM. This paper suggested that mTOR reduction was a potential reason for tubular proteinuria via megalin [102].

1.4.2 H^+-ATPase plasma membrane functions

Although H^+-ATPases are mainly present in intracellular organelles, they can also be found in the plasma membrane of certain cells like osteoclasts, proximal tubule cells, intercalated cells in the kidney, clear cells in the epididymis, and tumor cells. H^+-ATPases in plasma membranes mediate cell specific functions such as bone reabsorption, regulation of body pH homeostasis, sperm maturation and tumor cell invasiveness [86,88,90].

Bone density is a balance between bone resorption by osteoclasts and bone formation by osteoblasts. Osteoclasts through H^+-ATPases, secrete acid

and digestive enzymes into the extracellular space digesting bone matrix. H^+-ATPases function in these cells is illustrated by genetic defects in the a3 subunit (ATP6V0a3), the responsible subunit for targeting H^+-ATPases to the osteoclast ruffled membrane. Mutations in the a3 subunit result in osteopetrosis that is characterized by excessive bone formation [88,89,103].

Sperm maturation and viability requires low extracellular pH, which is provided by clear cells from the epididymis. Clear cells express specific H^+-ATPase isoforms like E1 in their apical membranes therefore the H^+-ATPase has been suggested as a good contraceptive drug target [88,91].

Recent evidence links tumor invasiveness with the presence of H^+-ATPases in the cell membrane where it produces an acidic environment necessary for cathepsin function. Cathepsins are necessary for extracellular matrix degradation allowing tumors to become more invasive. This evidence is also supported by the overexpression of H^+-ATPases in different cancer cell lines and tumor samples [88,98,104].

1.4.3 H^+-ATPase in the kidney

In the kidney, H^+-ATPases are located in the brush border membrane in the PT, the apical membrane of the thick ascending limb of the loop of Henle and in the plasma membrane of intercalated cells (IC). In the brush border membrane of the PT, H^+-ATPases play an important role in proton secretion, which in turn is essential for bicarbonate reabsorption. In addition, H^+-ATPases are important for absorption and processing of small proteins in the PT by promoting acidification of endocytic vesicles necessary for dissociation of ligands from internalized ligand-receptor complexes (receptor-mediated endocytosis), maturation of endocytic vesicles, and activity of lysosomal enzymes [86]. H^+-ATPase brings protons from the cytoplasm to the intracellular organelle generating a positive potential that is neutralized mainly by Cl^-/H^+ antiporters (CLC-5 in the kidney). While endocytic uptake is regulated by megalin and cubulin in the PT case, the progression through the

endocytic machinery to the lysosome depends on vesicular acidification which in turn is H^+-ATPase dependent [95].

The plasma membrane localization of the H^+-ATPase in IC is responsible for urine acidification which is essential for acid-base homeostasis [87,105]. Based on morphology and function, IC can be further subdivided into type-A intercalated cells (A-IC) and type–B intercalated cells (B-IC). A-IC secrete protons into the urine and transport bicarbonate to blood, and B-IC secrete bicarbonate into urine and protons into blood. Furthermore, A-IC are characterized by the presence of H^+-ATPases at their apical pole and the Cl^-/HCO_3^- exchanger Ae1 (anion exchanger 1, band3 or Slc4a1) at the basolateral side. However, in B-IC the H^+-ATPase is expressed at the basolateral side and a different Cl^-/HCO_3^- exchanger, pendrin, is expressed at the apical side. There is also a third type of IC, non-A non-B, that does not express Ae1 but expresses pendrin in the apical side and H^+-ATPase in both basolateral and apical membranes [106]. The function of this IC type is still unclear.

The relevance of H^+-ATPases for kidney function is reflected by the phenotype of animal models and by the kidney symptoms in human diseases with mutations in specific H^+-ATPase subunits. The H^+-ATPase has kidney enriched subunits like a4, which is expressed in the plasma membrane of IC and the PT (also in intracellular organelles) and B1 that is expressed in IC. Knockout animal models for these specific subunits allow investigating H^+-ATPase function in the kidney [87,91,107].

To illustrate H^+-ATPase function in the PT, a recent study executed with knockout mice for the a4 subunit showed that these mice not only suffer from metabolic acidosis due to loss of this subunit from IC but also had PT dysfunction. a4 knockout mice presented defective endosomal trafficking, proteinuria, phosphaturia and accumulation of lysosomal content [95,108,109].

Mutations in the B1 subunit of the H^+-ATPase cause impairment in acid/base homeostasis leading to a pathological condition referred to as distal renal tubular acidosis (dRTA). The patients suffering from dRTA suffer from

lack of urine acidification, hypokalemia and hypercalciuria [110]. A knockout mouse for the B1 subunit surprisingly had only a mild baseline defect characterized by a slightly alkaline urine and normal blood pH [111]. As a potential explanation for such a phenotype, it was found that these mice had a compensatory overexpression of the B2 H^+-ATPase subunit in IC [111-113].

1.5. (P)RR and H^+-ATPase

The first biochemical interaction between (P)RR/ATP6ap2 and H^+-ATPase was reported in 1998 when H^+-ATPases were copurified together with another protein M8-9 of 9.2 kDa from the chromaffin cells of the adrenal medulla [69]. This protein was subsequently named ATP6ap2 for H^+-ATPase associated protein 2; however, soon it became clear that M8-9 is a truncated form of the (P)RR/ATP6ap2, corresponding to the transmembrane and cytoplasmatic domains. Recent studies have shown that (P)RR/ATP6ap2 colocalizes with H^+-ATPases in the plasma membrane of intercalated cells in the CD [64] and in the Z-disc and dyad of cardiomyocytes [114]. Moreover, B1 subunit immunoprecipitation from mouse kidney lysate and further proteomic analysis identified (P)RR/ATP6ap2 as an interactor of H^+-ATPases [115].

A more direct evidence for the role of the (P)RR/ATP6ap2 in regulating H^+-ATPases comes from functional studies in a (P)RR/ATP6ap2 deletion background which demonstrates a distinct downregulation of H^+-ATPase function [116-119]. It is worthwhile to mention that (P)RR/ATP6ap2 knock-down in cardiomyocytes results in a phenotype similar to pharmacological inhibition of H^+-ATPase, suggesting the importance of the (P)RR/ATP6ap2 for H^+-ATPase function [116]. Furthermore, in podocyte specific (P)RR/ATP6ap2 knock-out mice it was demonstrated that expression of the c subunit of the H^+-ATPase V_0 domain is downregulated [120] giving a hint for possible subunit specific interactions. Both animal models exhibit accumulation of autophagic vesicles suggesting lysosomal defects. Also, (P)RR/ATP6ap2 was shown to be an adaptor protein between H^+-ATPase and frizzle in the Wnt signaling [81,117] . In another study using a drosophila model, lack of (P)RR/ATP6ap2 affected

lysosome acidification leading to accumulation of E-Cadherin, Notch and LAMP1. The authors also suggest that (P)RR/ATP6ap2 function as endosome regulator is independent of its function in Wnt signaling [117]. Moreover, another study in drosophila demonstrates that (P)RR/ATP6ap2 knockdown in pupal wings has a similar phenotype as H^+-ATPase subunits knockdown, leading to defective uptake of dextran (fluid phase endocytosis) and avidin (receptor-mediated endocytosis). The same study could also show that (P)RR/ATP6ap2 knockdown down-regulates expression of megalin [102]. In a more recent study using a inducible conditional knockout mice for (P)RR/ATP6ap2 in kidney epithelial cells, it was shown that (P)RR/ATP6ap2 deletion leads to urinary concentration defects and distal renal tubule acidosis [73]. They could show that deletion of (P)RR/ATP6ap2 does not impair the RAS system and that the observed phenotype results from deficient H^+-ATPase activity. They even went one step further by suggesting that (P)RR/ATP6ap2 should no longer be called (P)RR.

2. Animal models used in the thesis

In the present study, distinct mouse models were used to answer the question whether (P)RR/ ATP6AP2 is important for kidney function.

Chapter 1:

We used models to induce chronic metabolic acidosis and chronic metabolic alkalosis. Metabolic acidosis in C57/Bl6 wildtype mice was induced with NH_4Cl (0.28 M) while metabolic alkalosis was induced with $NaHCO_3$ (0.28 M) or $KHCO_3$ (0.28 M) in the drinking water for 7 days. Furthermore wild type mice also received NaCl (0.28 M) in the drinking water during 7 days. Animals received an aldosterone analogue desoxycorticosterone acetate (DOCA) via subcutaneous injections at day 1 and 4 (2 mg/mouse). These treatments have been shown to induce metabolic acidosis or alkalosis in rodents and induce regulation of major transport proteins expressed in intercalated cells like H^+-ATPase [107,121,122]. All diets except of DOCA were given in drinking water supplemented with 1% sucrose and maintained on a standard diet. The control group received only 1% sucrose in drinking water.

Chapter 2:

To bypass the lethal effects of early developmental loss of (P)RR we used an inducible (P)RR/*Atp6ap2* knock-down rat model .These transgenic rats expressed a small hairpin RNA (shRNA) that specifically target the (P)RR/ATP6ap2 transcript in the whole body [123]. To induce expression of shRNA against (P)RR/*Atp6ap2*, animals were treated with 0.5 g/l doxycycline in the drinking water for 8 days. We used as control littermates wildtype rats not expressing *Atp6ap2* shRNA but also receiving doxycycline. To overcome the problem of a full knock-down, we produced another animal model in-house in which (P)RR is deleted in an inducible fashion only in the epithelial cells along the nephron. We generated this mice by crossing Pax8rtTA [124] with mice flox(P)RR/ATP6AP2 (the *Atp6ap2* gene is on the X chromosome)

[118]. Expression of Cre-recombinase was induced in male (P)RR flox/y,Pax8Cre+ and (P)RR +/+,Pax8Cre+ transgenic mice by administration of 0.5 mg/ml of doxycycline in drinking water containing 2% of sucrose for 5 days followed by 5 days induction with 0.25mg/ml doxycycline in 2% sucrose drinking water and 4 days recovery without doxycycline. This caused a partial knock-out of the (P)RR/ATP6ap2, mostly in the proximal tubule but left residual expression in intercalated cells reducing overall morbidity in animals due to loss of function of medullary collecting ducts.

3. Aim of the thesis

Given that the H^+-ATPase is highly expressed in the kidney in the plasma membrane of PT, IC cells and intracellular organelles, and that (P)RR/ATP6ap2 is coexpressed at high levels in the kidney, it is likely that the (P)RR/ATP6ap2 and H^+-ATPases are functionally coupled. Thus, in this thesis, we aimed at study (P)RR/ATP6ap2 functions in the kidney in particular in the PT cells.

In the chapter 1, we studied the localization of (P)RR/ATP6ap2 protein along the murine nephron and its co-localization with plasma membrane associated H^+-ATPases. Furthermore, we looked at co-regulation of (P)RR/ATP6ap2 and main kidney specific H^+-ATPase subunits B1 and a4 on mRNA and protein level. Finally, we also tested whether acute application of prorenin could regulate native plasma membrane H^+-ATPase activity in intercalated cells in freshly isolated and microperfused mouse collecting ducts.

In the chapter 2, we investigated the (P)RR/ATP6AP2 function in the PT using two different animal models. A rat model with an inducible shRNA for *Atp6ap2* and an inducible kidney epithelial cell-specific knockout mouse for (P)RR/ATP6ap2. To study in more detail the endocytic pathway we injected both animal models with fluid phase endocytosis marker (dextran-FITC, 10 kDa) and receptor mediated endocytosis marker (human transferrin). We report that (P)RR/ATP6ap2 plays a role in cargo reabsorption and processing via receptor-mediated endocytosis, hence, contributing to kidney proximal tubule function.

4. Experimental part/ manuscripts

Chapter 1: Colocalization of the (Pro)renin Receptor/Atp6ap2 with H+-ATPases in Mouse Kidney but Prorenin Does Not Acutely Regulate Intercalated Cell H+-ATPase Activity.

Marta F.L. Figueiredo contributions: performed immunohistochemistry for figure 4 and figure 8.

Colocalization of the (Pro)renin receptor/Atp6ap2 with H^+-ATPases in mouse kidney but prorenin does not acutely regulate intercalated cell H^+-ATPase activity

Arezoo Daryadel[1], Soline Bourgeois[1], Marta F. L. Figueiredo[1], Ana Gomes Moreira[1], Nicole B. Kampik[1], Lisa Oberli[1], Nilufar Mohebbi[1,2], Xifeng Lu[3], Marcel E. Meima[3], A. H. Jan Danser[3], Carsten A. Wagner[1]

[1]Institute of Physiology, University of Zurich, Switzerland; [2]Divison of Nephrology, University Hospital Zurich, Switzerland, [3]Division of Vascular Medicine and Pharmacology, Department of Internal Medicine, Erasmus Medical Center, Rotterdam, Netherland

Corresponding author:

Carsten A. Wagner
Institute of Physiology and Zurich Center for
Integrative Human Physiology (ZIHP)
University of Zurich
Winterthurerstrasse 190
CH-8057 Zurich
Switzerland
Phone: +41-44-63 55023
Fax: +41-44-63 56814
E-Mail: Wagnerca@access.uzh.ch

ABSTRACT

The (Pro)renin receptor (P)RR/Atp6ap2 is a cell surface protein capable of binding and non-proteolytically activate prorenin. Additionally, (P)RR is associated with H^+-ATPases and alternative functions in H^+-ATPase regulation as well as in Wnt signalling have been reported. Kidneys express very high levels of H^+-ATPases which are involved in multiple functions such as endocytosis, membrane protein recycling as well as urinary acidification, bicarbonate reabsorption, and salt absorption. Here, we wanted to localize the (P)RR/Atp6ap2 along the murine nephron, exmaine whether the (P)RR/Atp6ap2 is coregulated with other H^+-ATPase subunits, and whether acute stimulation of the (P)RR/Atp6ap2 with prorenin regulates H^+-ATPase activity in intercalated cells in freshly isolated collecting ducts. We localized (P)PR/Atp6ap2 along the murine nephron by qPCR and immunohistochemistry. (P)RR/Atp6ap2 mRNA was detected in all nephron segments with highest levels in the collecting system coinciding with H^+-ATPases. Further experiments demonstrated expression at the brush border membrane of proximal tubules and in all types of intercalated cells colocalizing with H^+-ATPases. In mice treated with NH_4Cl, $NaHCO_3$, $KHCO_3$, NaCl, or the mineralocorticoid DOCA for 7 days, (P)RR/Atp6ap2 and H^+-ATPase subunits were regulated but not co-regulated at protein and mRNA levels. Immunolocalization in kidneys from control, NH_4Cl or $NaHCO_3$ treated mice demonstrated always colocalization of PRR/Atp6ap2 with H^+-ATPase subunits at the brush border membrane of proximal tubules, the apical pole of type A intercalated cells, and at basolateral and/or apical membranes of non-type A intercalated cells. Microperfusion of isolated cortical collecting ducts and luminal application of prorenin did not acutely stimulate H^+-ATPase activity. However, incubation of isolated collecting ducts with prorenin non-significantly increased

ERK1/2 phosphorylation. Our results suggest that the PRR/Atp6ap2 may form a complex with H^+-ATPases in proximal tubule and intercalated cells but that prorenin has no acute effect on H^+-ATPase activity in intercalated cells.

Key words: (Pro)renin receptor (P)RR, H^+-ATPases, ATP6ap2, prorenin, angiotensin II, kidney, proximal tubule, intercalated cells

Short title: The prorenin receptor/Atp6ap2 and renal H^+-ATPases

INTRODUCTION

The (pro)renin receptor (P)RR is a protein spanning the membrane once and with a large extracellular domain. The extracellular domain can be cleaved to yield a soluble, shorter fragment of approximately 28 kDa [1,2,3]. The (P)RR was initially identified as a receptor for renin and prorenin, inducing non-proteolytical activation of prorenin and thus allowing local production of angiotensin I from angiotensinogen by both renin and prorenin. In addition, binding of prorenin and renin may activate an angiotensin-independent intracellular signaling cascade leading to enhanced ERK1/2 phosphorylation [4].

(P)RR is identical to ATP6AP2, a protein that associates and co-immunoprecipitates with vacuolar-type H^+-ATPases (V-ATPases) [5]. H^+-ATPases are membrane-associated multi-protein complexes mediating the transport of protons by hydrolyzing ATP [6,7]. In the kidney, H^+-ATPases are localized at the plasma membrane of most epithelial cells lining the nephron and mediate proton extrusion into urine or blood [8]. Moreover, H^+-ATPases are found in many intracellular organelles such as endosomes and lysosomes and play there a critical role in endocytosis, e.g. receptor-mediated endocytosis in the proximal tubule [7,9]. The activity of plasma membrane-associated H^+-ATPases is regulated by various hormones and factors including angiotensin II, aldosterone, acidosis or alkalosis [7]. Some of these effects are mediated by intracellular signaling cascades involving cAMP/PKA, PKC, ERK1/2 or AMPK [10,11,12,13,14]. Activation of these signaling pathways can result in enhanced trafficking and localization of H^+-ATPases at the plasma membrane associated with increased activity. Disruption of signaling or the

actin cytoskeleton-dependent trafficking reduces plasma membrane H^+-ATPase localization and stimulation [15,16,17,18,19,20,21].

In various model organisms such as *Drosophila* or *Xenopus laevis* larvae, the (P)RR/Atp6ap2 is critical for fundamental cellular processes such as endocytic retrieval of proteins and Wnt signaling [22,23,24]. Whether these functions of the (P)RR/Atp6ap2 are related to its possible role as accessory subunit of the H^+-ATPase or due to other functions has not been fully elucidated. However, endocytosis as well as Wnt signaling (e.g. the recycling of Wnt receptors) are sensitive to the disruption of other *bona fide* H^+-ATPase subunits and H^+-ATPase inhibitors providing a strong argument for a role of the (P)RR/Atp6ap2 in H^+-ATPase trafficking, regulation, or function [22,24]. However, limited information is available about the localization of the (P)RR/Atp6ap2 in kidney, an organ with very intense expression of H^+-ATPases, and whether H^+-ATPase activity itself can be affected by acute application of prorenin.

The main questions addressed in this manuscript are 1) the localization of (P)RR/Atp6ap2 protein along the murine nephron and its colocalization with plasma membrane associated H^+-ATPases, 2) the coregulation of (P)RR/Atp6ap2 and two major H^+-ATPase subunits on mRNA and protein level, and 3) to test whether acute application of prorenin could regulate native plasma membrane H^+-ATPase in intercalated cells in freshly isolated murine collecting ducts.

MATERIALS AND METHODS

Animals

Experiments were performed in 8-12 weeks old male C57BL/6 (body weight 25-30 g) mice. All animal experiments were conducted according to Swiss laws for the welfare of animals and were approved by local authorities (Swiss Veterinary Authority of the Kanton Zurich, permission no 03/2011). The animals had free access to food and tap water. Where indicated NaCl (0.28 M), $NaHCO_3$ (0.28 M), $KHCO_3$ (0.28 M), or NH_4Cl (0.28 M) were added to the drinking water for 7 days. Animals receiving the aldosterone analogue desoxycorticosterone acetate (DOCA) received subcutaneous injections at day 1 and 4 (2 mg/mouse). These treatments have been shown to induce metabolic acidosis or alkalosis in rodents and induce regulation of major transport proteins expressed in intercalated cells [25]. Each group consisted of at least 5 animals and was compared to the time-, age- and gender-matched corresponding control groups. All diets except of DOCA were given in drinking water supplemented with 1% sucrose and maintained on a standard diet. The control group received only 1% sucrose in drinking water.

For some experiments, mice were used expressing eGFP under the control of the Atp6v1b1 (B1) H^+-ATPase subunit promoter inducing high levels of eGFP expression in intercalated cells along the collecting duct system (B1-eGFP mice) [26]. B1-eGFP mice were kindly provided by Dr. Lance Miller and Dr. Raoul Nelson, University of Utah, Salt Lake City..

Isolation of mouse nephron segments and mRNA extraction

Defined segments of mouse nephrons were isolated from the kidneys of untreated male C57BL/6 mice or B1-eGFP, 10 – 12 weeks old using hand-dissection

under a stereo microscope illuminated with normal light or fluorescent light (Leica M165FC).

mRNA extraction of organs and hand-dissected isolated nephron segments with subsequent quantitative real time RT-PCR was performed as described previously [27]. Enrichment of the hand-dissected nephron segment preparation was ensured, by testing each sample for the most dominantly expressed segment specific mRNA transcripts (Podoplanin, NaPi-IIa, NKCC2, NCC, AQP2, and Pendrin).

RNA extraction from kidney and semi-quantitative RT-qPCR analysis

To determine (P)RR/ATP6AP2, ATP6V1B1, ATP6V0A4, and HPRT relative mRNA abundance in dissected tissues, total RNA was extracted from dissected kidney cortex and medulla using an RNeasy kit (Qiagen, Basel, Switzerland). RNA was bound to columns and treated with DNase for 15 min at room temperature to reduce genomic DNA contamination. Quantity and purity of total eluted RNA was assessed by spectrometry. To generate complementary DNA (cDNA), total RNA was reverse transcribed (RT reaction) by Taqman Reverse Transcription Kit (Applied Biosystems, USA). The thermal cycle conditions used were 25°C (10 min), 48°C (30 min) and 95° (5 min). Primers and probes were designed using Primer Express (Applied Biosystems, USA) and purchased from Microsynth, Switzerland (Supplementary Table S1). The specificity of the primers was tested using adult mouse kidney cDNA by conventional PCR. Each pair of primers resulted only in a single band of the expected size (data not shown). Probes were labelled with the reporter dye FAM at the 5' end and the quencher dye TAMRA at the 3' end. RT-PCR reactions were performed using Taqman Universal PCR Master Mix (Applied Biosystems, USA) 17 µl reactions were prepared using 3 µl of cDNA-template. Reactions were run in 96-well Optical reaction plates and caps (Applied Biosystems,

USA). Thermal cycles were set at 50°C (2 min) 95°C (10 min) and then 40 cycles at 95°C (15 sec) and 60°C (1 min). Each reaction was made in triplicates and the average taken. Samples without enzyme in the RT reaction were used as negative controls to exclude contamination with genomic DNA. Only results with less than 1 cycle difference were taken into consideration. Cross point threshold (C_t value) was taken as the earliest cycle number in the PCR amplification, when fluorescence rises significantly above the background fluorescence.

The expression of candidate genes was normalized to the reference gene, HPRT giving comparable results and analyzed by the delta delta C_t method.

MDCK cells and cell culture

MDCK cells (C11 clone, kindly provided by Dr. H. Oberleithner, University of Münster, Germany) [28] were cultured at 37°C and 5 % CO_2 in DMEM (no. E15-810, GE Healthare, Glattbrugg, Switzerland) supplemented with 10 % heat-inactivated fetal bovine serum (FBS, Sigma-Aldrich, Buchs, Switzerland), 2 mM L-glutamine, and 1 % non-essential amino acids (no. M11-003, GE Healthcare). After cells had reached 80-90 % confluency, they were starved for 24 hrs and thereafter treated with the AT_1R blocker losartan (10 μM, Sigma-Aldrich, Buchs Switzerland) and the AT_2R blocker PD123319 (10 μM, Sigma-Aldrich, Buchs, Switzerland) for 30 min at 37°C followed by human prorenin (1 and 20 nM, a kind gift of Dr. Walter Fischli, Actelion, Allschwil, Switzerland) and angiotensin II (10 nM, Sigma-Aldrich, Buchs Switzerland) stimulation for 10 min.

Membrane preparation from kidney and western blot analysis

For total membrane preparations, kidneys were dissected into cortex and medulla. Samples were homogenized in an ice-cold K-HEPES buffer (200 mM

mannitol, 80 mM HEPES, 41 mM KOH, pH 7.5) containing a protease inhibitor mix (Complete Mini, Roche Diagnostics, Germany) at a final concentration of 1 tablet in a volume of 10 ml solution. Samples were centrifuged at 2000 rpm for 20 min at 4°C. Subsequently, the supernatant was transferred to a new tube and centrifuged at 41'000 rpm for 1 h at 4°C. The resultant pellet was resuspended in K-HEPES buffer containing protease inhibitors.

MDCK cells were lysed with ice-cold Radio-Immunoprecipitation Assay (RIPA) buffer (150 mM NaCl, 50 mM Tris, pH 7.4, 1% NP-40, 0.5 % Na-Deoxycholate, 2 mM Phenylmethylsulfonylfluoride) supplemented with a protease inhibitor mix (Complete Mini, Roche Diagnostics, Germany, at a final concentration of 1 tablet in a volume of 10 ml solution) and incubated for 30 min on ice. Cellular debris was pelleted by centrifugation at 2500 g for 10 min at 4 °C.

After measurement of the total protein concentration (Bio-Rad D_c protein Assay; Bio-Rad, Hercules, CA, USA), 10 µg of crude membrane proteins from cortex or medulla or 20 µg of MDCK extracts were solubilised in Laemmli buffer, and SDS-PAGE was performed on 10% polyacrylamide gels.

For immunoblotting, proteins were transferred electrophoretically to polyvinylidene difluoride membranes (Immobilon-P; Millipore, Bedford, MA, USA). After blocking with 5% milk powder in Tris-buffered saline/0.1% Tween-20 for 60 min; the blots were incubated with the respective primary antibodies: goat anti mouse (P)RR 1:1000, Novus Biologicals, USA (NB100-1318), rabbit anti mouse ATP6V1B1 1:5000 [29], rabbit anti-human ATP6V0A4 1:5000 [30], rabbit anti-pERK1/2 1:1000 (Cell Signaling, 9101, Danvers, MA, USA), rabbit anti-total ERK1/2 1:1000 (Cell Signaling, 9102, Danvers, MA, USA , and mouse monoclonal anti-β-actin antibody

(42 kDa; Sigma, St. Louis, MO, USA) 1:5000, diluted in 1% milk/TBS-T) either for 2 h at room temperature or overnight at 4°C. After washing, the membranes were incubated for 1 h at room temperature with the secondary antibodies: donkey anti-goat, goat anti-rabbit and goat anti-mouse IgG-conjugated with alkaline phosphatase 1:5000 (Promega, WI, USA) and sheep anti-mouse IgG-conjugated with horseradish peroxidase (Amersham Life Sciences, 1:10000). Antibody binding was detected with enhanced chemiluminescence ECL kit (Amersham Pharmacia Biotech) or the CDP-Star Western chemiluminescence Kit (Roche Diagnostics, Mannheim, Germany) using the DIANA III-chemiluminescence detection system (Raytest; Straubenhardt, Germany). All images were analyzed using appropriate software (Advanced Image Data Analyzer, Raytest, Straubenhardt, Germany) to calculate the protein of interest/β-actin ratio.

Immunohistochemistry

Mice were anesthetized with Ketamine/Xylazine and perfused through the left ventricle with phosphate-buffered saline (PBS) followed by paraformaldehyde-lysine-periodate (PLP) fixative [31]. Kidneys were removed and fixed overnight at 4°C by immersion in PLP. Kidneys were washed 3 times with PBS and 5 µm cryosections were cut after cryoprotection with 2.3 M sucrose in PBS for at least 12 h. Immunostaining was carried out as described previously [32,33,34]. Briefly, sections were incubated with 10 mM TRIS (Trizma Base, Sigma, pH 10 at 100 °C for 20 min in a microwave, washed 3 times with PBS and incubated with 5 % (v/v) donkey serum in PBS for 15 min prior to the primary antibody. The primary antibodies (goat anti-(P)RR (Novus Biologicals, USA) 1:100), rabbit anti-ATP6V0A4 (a4) serum 1:1000 [29,30], rabbit polyclonal anti ATP6V1B1 (B1) 1:150 [29], guinea-pig anti-pendrin 1:1000 [35], guinea-pig anti-AE1 1:500 [36], and rabbit-anti-AQP2 (kindly

provided by J. Loffing, Zurich)[37] 1:1000 were diluted in PBS and applied either for 75 min at room temperature or overnight at 4°C. Sections were then washed twice for 5 min with high NaCl PBS (PBS + 18 g NaCl/l), once with PBS, and incubated with dilutions of the secondary antibodies (donkey anti-rabbit 586 (1:1000), donkey anti-goat 488 (1:1000), donkey anti-guinea-pig Dylight 649 (Jackson ImmunoResearch Lab Inc) (1:1000) mixed with DAPI (Molecular Probes, Oregon, USA) 1:1000 for 1 h at room temperature. Sections were again washed twice with high NaCl PBS and once with PBS before mounting with glycergel mounting medium (Dako, USA). Sections were viewed with a Leica DM5500B epifluorescence microscope and for images comparing localization and intensity of stainings pictures were taken on the same day and with identical settings for gain, intensity, and fluorescence filters. Images were processed (overlays) using Adobe Photoshop.

In vitro microperfusion experiments

Mice were anesthetized with Xylazin/Ketamin i.p., both kidneys were cooled in situ with control bath solution containing in mM (138 NaCl, 1.5 $CaCl_2$ 1.2 $MgSO_4$, 2 K_2HPO_4, 10 HEPES, 5.5 glucose, 5 alanine, pH 7.4) for 1 min and then removed and cut into thin coronal slices for tubule dissection. Cortical collecting ducts (CCDs) were dissected under a stereo microscope from the cortex at 10°C in the control solution.

Intracellular pH measurement

The isolated cortical collecting ducts were transferred into the bath chamber on the stage of an inverted microscope (IX81, Olympus, Japan) in the control solution and then mounted on concentric pipettes and perfused *ex vivo* with Na^+-free, ammonium-free solution where N-methyl-D-Glutamine$^+$ ($NMDG^+$) replaced Na^+. The average tubule length exposed to bath fluid was limited to 300 – 350 µm in order to

prevent motion of the tubule. CCDs were loaded with 5 µM of the fluorescent probe BCECF-AM (2',7'-bis(2-carboxyl)-5-(and-6)-carboxyfluorescein acetoxymethyl ester, Invitrogen, Switzerland) for ~20 min at 37°C in the control bath solution. The loading solution was then washed out by initiation of bath flow and the tubule was equilibrated with dye-free control bath solution for 5 min. Luminal incubation with prorenin (20 pM and 1 nM) was initiated during the BCECF loading and prorenin was presented throughout the incubation period and experiment (approx.40 min). Bath solution was delivered at a rate of 20 ml/min and warmed to 37°C by water jacket immediately upstream to the chamber. After temperature equilibration in control solution, tubules were first transiently acidified by peritubular Na^+ removal (Na-free, ammonium-free solution) (10 min duration), where sodium was replaced by $NMDG^+$ to avoid exit of NH_4^+ by basolateral Na^+-coupled transport. This maneuver was done in the luminal absence of Na^+. During the fluorescence recording, perfusion solution was delivered to the perfusion pipette via a chamber under an inert gas (N_2) pressure (around 1 bar) connected through a manual 6-way valve. With this system, opening of the valve instantaneously activates flow of solutions. The majority of the fluid delivery to the pipette exits the rear of the pipette system through a drain port at 4 ml/min. This method results in a smooth and complete exchange of the luminal or the peritubular solution in less than 3 to 4 s [38].

After the fluorescence signal stabilization, luminal fluid was instantly (at the rate of 4 ml/min in the draining) replaced by a Na^+-free solution containing 20 mM NH_4Cl (and 118 mM NMDG-Cl) that elicited a rapid intracellular alkalinization, followed by a sharp acidification. The rate of intracellular alkalinization has been associated with the entry of NH_3 whereas the subsequent phase of intracellular acidification in the continous presence of extracellular NH_4Cl reflects mostly NH_4^+ entry [39]. Intracellular dye was excited alternatively every 2 seconds at 434 and 494

nm with a MT fluorescence light source (150W Xenon/Mercury mixed gas burner) including a light guide and coupling to a disk scan Unit (Olympus, Japan). Emitted light was collected through a dichroïc mirror, passed through a 530 nm filter and focused onto a EM-CCD camera (Hamamatsu, Japan) connected to a computer. The measured light intensities were digitized with the $Cell^M$&$Cell^R$ Imaging hardware system (Olympus, Japan) for further analysis. Intracellular dye was calibrated at the end of each experiment using the high [K^+]-nigericin technique. Tubules were perfused and bathed with a HEPES-buffered, 95-mM K^+-solution containing 10 µM of the K^+/ H^+-exchanger nigericin. Four different calibration solutions, titrated to pH 6.3, 6.9 ,7.5, or 7.8 were used.

Statistical analysis

Data are provided as means ± SEM; *n* represents the number of independent experiments. All data were tested for significance using Student's unpaired two-tailed t-test, or ANOVA, where applicable. The level of statistical significance was set at * $p < 0.05$, ** $p < 0.01$ and *** $p < 0.001$.

RESULTS

Localization of the (pro)renin receptor/Atp6ap2 in mouse kidney

The distribution of (pro)renin receptor/Atp6ap2 mRNA was examined in mouse kidney using hand-dissected nephron segments by semi-quantitative RT-qPCR. (P)RR/Atp6ap2 mRNA was detected in the glomerulus and all other segments, with highest levels in the connecting tubule/cortical collecting duct (CNT/CCD) and outer medullary collecting duct (OMCD) (Figure 1). The high mRNA abundance of (P)RR/Atp6ap2 in CNT/CCD and OMCD was paralleled by high mRNA levels of the B1 (Atp6v1b1) H^+-ATPase subunit which is selectively enriched in intercalated cells [40,41]. The enrichment of nephron segments was ascertained by RT-qPCR for segment specific markers (Podoplanin for the glomerulum, NaPi-.IIa for the S1 /S2 , S3 segments of the proximal tubule and DCT, NKCC2 for the TAL, NCC for the DCT, AQP2 for the collecting duct system, and pendrin for the CNT/CCD). Patterns of expression are in good agreement with previous transcript analyses along the mouse nephron [42].

Immunohistochemistry detected weak (P)RR/Atp6ap2 related staining in the glomerulus as described before [43,44]. However, clear signals were detected in the proximal tubule at the brush border membrane and in cells in the collecting duct system (Figure 2 A,B). Costaining of (P)RR/Atp6ap2 with the a4 (Atp6v0a4) H^+-ATPase subunit, which is expressed along the entire nephron [32,45,46], showed strong overlay at the apical side of proximal tubular cells (Figure 2 D-F). In the collecting duct, costaining with the principal cell specific marker AQP2 demonstrated that the (P)RR/Atp6ap2 was expressed in intercalated cells (Figure 2 C). Further studies demonstrated that the (P)RR/Atp6ap2 colocalized in intercalated cells with

the a4 (Atp6v0a4) H^+-ATPase subunit that forms part of the plasma membrane H^+-ATPase (Figure 3) [9,47].

H^+-ATPases in intercalated cells can be associated with the luminal membrane in type A intercalated cells and with either the basolateral and/or luminal membrane in non-type A intercalated cells [7,8,32,48,49]. Type A intercalated cells were identified by the presence of AE1 specifically expressed at the basolateral membrane of these cells. In AE1 positive cells, (P)RR/Atp6ap2 staining was always detected at the luminal side of cells (Fig. 4A, B). In cells expressing pendrin, a marker of non-type A intercalated cells which is localized at the luminal membrane, (P)RR/Atp6ap2 staining was observed either at the basolateral membrane and/or colocalizing with pendrin at the luminal pole (Fig. 4C, D).

Thus, the (P)RR colocalizes with H^+-ATPases at the plasma membrane in various nephron segments and can be found both at the apical side of cells in the proximal tubule and in type A and non-type A intercalated cells as well as at the basolateral side of some non-type A intercalated cells as previously described for other H^+-ATPase subunits [32,40,41,46,48,49].

Regulation of (P)RR/Atp6ap2 mRNA and protein abundance in kidney by acid-base status and electrolyte intake

Mice were treated with different diets to alter activity of the different subtypes of intercalated cells and renal handling of bicarbonate and protons, conditions that have been associated with altered activity, expression, and/or localization of H^+-ATPases along the nephron [32,48].

Semi-quantitative qPCR was used to assess the relative abundance of mRNAs encoding (P)RR, B1 and a4 subunits of the vacuolar H^+-ATPase in dissected cortex and medulla from control mice and animals that had received NaCl, $NaHCO_3$,

$KHCO_3$, NH_4Cl, or the mineralocorticoid DOCA for 7 days (n = 5 per group). The abundance of (P)RR/Atp6ap2 mRNA was significantly increased in kidney cortex from $NaHCO_3$ treated mice and reduced with NH_4Cl treatment (Fig. 5). Atp6v1b1 mRNA was higher in cortex with $NaHCO_3$ treatment and Atp6v0a4 mRNA increased with NH_4Cl supplementation (Fig. 5). In kidney medulla, (P)RR/Atp6ap2 mRNA was not altered by any of the diets, whereas Atp6v1b1 mRNA decreased with NaCl, NH_4Cl, and DOCA treatments. Similarly, Atp6v0a4 mRNA expression in medulla was reduced with $NaHCO_3$ or DOCA treatments. Thus, these data provided no evidence for coordinated regulation of mRNA expression of these three genes.

Next we assessed protein abundance of (P)RR/Atp6ap2, and the B1 and a4 H^+-ATPase subunits separately in kidney cortex and medulla. In cortex, $NaHCO_3$ treatment resulted in a significant increase in the protein abundance of (P)RR protein whereas all other treatments had no influence (Fig. 6). The expression of the B1 (Atp6v1b1) subunit was reduced by NaCl intake and increased by alkali treatment such as $NaHCO_3$ or $KHCO_3$, whereas $NaHCO_3$, $KHCO_3$, and NH_4Cl increased the a4 (Atp6v0a4) subunit. In contrast, DOCA reduced a4 protein expression. In medulla, (P)RR/Atp6ap2 abundance was not regulated, whereas B1 abundance increased with $KHCO_3$ and decreased with $NaHCO_3$ treatment. Moreover, a4 expression decreased with $NaHCO_3$, $KHCO_3$, NH_4Cl and DOCA treatments (Fig. 7). Similar to the mRNA data, these experiments did not indicate coordinated regulation of protein abundance of H^+-ATPase subunits and (P)RR/Atp6ap2.

Trafficking of H^+-ATPase and (P)RR/Atp6ap2 in response to alkali and acid loading

Loading of rodents with either alkali/bicarbonate or acid (NH_4Cl) provokes increased trafficking of H^+-ATPase subunits to the basolateral membrane of non-type A intercalated cells or luminal membrane of type A intercalated cells, respectively [32,48,49]. We performed immunohistochemistry for the a4 H^+-ATPase subunit together with the (P)RR/ Atp6ap2 and AE1 as a marker of type A intercalated cells on kidneys from control mice and mice receiving $NaHCO_3$ or NH_4Cl for 7 days (Figure 8). In the proximal tubule, the signals for (P)RR/Atp6ap2 (green) and a4 H^+-ATPase (red) showed a high degree of colocalization as indicated by the strong yellow color (Figure 8 B, E, H). Similarly, in intercalated cells, (P)RR and a4 H^+-ATPase strongly colocalized at the luminal and/or basolateral side (Figure 8 A, C, D, F, G, I). In AE1 positive intercalated cells, yellow staining was confined mostly to the luminal membrane, whereas in intercalated cells negative for AE1, yellow staining was detected at the luminal and/or basolateral side. Neither $NaHCO_3$ nor NH_4Cl treatment did alter the apparent costaining, at least at the level of light microscopy.

Acute exposure of *ex vivo* microperfused collecting ducts to prorenin does not stimulate H^+-ATPase activity and ERK1/2 phosphorylation

The (P)RR/Atp6ap2 has been identified because of its ability to bind prorenin and experiments in MDCK cells demonstrated increased ERK1/2 phosphorylation and stimulated H^+-ATPase activity when incubated with prorenin [50,51] . Thus, we tested in freshly isolated and microperfused mouse cortical collecting ducts whether luminal application of prorenin could stimulate H^+-ATPase activity also in *ex vivo* preparations (Fig. 9). However, luminal microperfusion with two different concentrations of prorenin (20 pM and 1 nM) for 15 minutes did not alter H^+-ATPase

activity measured as pH_i recovery rates after intracellular acidification with a NH_4Cl prepulse (20 mM) as described previously [13,20,21,29]. Next, we incubated hand-dissected connecting tubules and cortical collecting ducts with prorenin (1 and 20 nM) for 10 min at 37 °C *in vitro*. For these experiments, we used mice expressing eGFP in intercalated cells [26] to facilitate isolation of large enough quantities of these nephron segments for experiments. In three independent preparations, no difference in pERK1/2 abundance could be detected (Figure 10 A, B), however, 20 nM prorenin caused a strong trend towards increased ERK1/2 phosphorylation ($p = 0.08$). We performed parallel experiments in MDCK cells incubated for 10 minutes with prorenin (20 nM) or angiotensin II (10 nM) in the absence or presence of the AT_1 and AT_2 receptor blockers losartan (10 μM) and PD123310 (10 μM) (Figure 10). In the combined presence of losartan and PD123310 a non-significant tendency to more pERK1/2 abundance ($p = 0.2$) was detected in MDCK cells incubated with prorenin (Figure 10 C, D).

DISCUSSION

Our study provides new insights into the localization of the prorenin receptor/Atp6ap2 and its regulation in mouse kidney by confirming and expanding previous observations reporting the expression and localization of the (P)RR/Atp6ap2 in the vasculature and podocytes of the glomerulus [4,43,44,52], in proximal tubule [52,53], and in the collecting duct [52] and intercalated cells [50,54,55,56].

Here, we present the detailed expression and localization of the (P)RR along the entire nephron. Semi-quantitative qPCR showed abundant expression of (P)RR/Atp6ap2 mRNA in hand-dissected mouse nephron segments spreading from glomerulus to the distal segments including the collecting duct. Of note, the highest mRNA levels were found in the collecting duct system coinciding with the localization of intercalated cells. Previous experiments using in-situ hybridization in rat kidney had detected signals in proximal tubule and thick ascending limb of the loop of Henle (TAL) but with much weaker intensity than in the collecting duct supporting our observations [50]. Immunohistochemistry shows (P)RR/Atp6ap2 localization at the luminal membrane of proximal tubules and in all subtypes of intercalated cells. Weak immunohistochemical signals for (P)RR/Atp6ap2 were also detected in TAL and distal convoluted tubule (DCT) and were very weak or absent from segment-specific cells (principal cells) in the collecting duct system. In intercalated cells, localization of the (P)RR/Atp6ap2 differed between specific cell subtypes. In type A intercalated cells, identified by positive basolateral localization of AE1 [57], (P)RR/Atp6ap2 staining was detected only at the luminal pole consistent with the luminal localization of H^+-ATPases in these cells [7,49]. Consistently, Advani and colleagues had reported the localization of immunogold-labeled (P)RR/Atp6ap2 at the luminal membrane of rat type A intercalated cells with electron microscopy [50]. In contrast,

intercalated cells expressing pendrin (type B and non-A/non-B intercalated cells) [58,59] showed luminal, basolateral or combined (P)RR/Atp6ap2 staining as reported previously also for other H^+-ATPase subunits [32,46,48,49]. Accordingly, (P)RR/Atp6ap2 staining colocalized at the level of light microscopy with the a4/Atp6v0a4 H^+-ATPase subunit at the brush border membranes of proximal tubule cells and in all subtypes of intercalated cells. Thus, the (P)RR/Atp6ap2 is apparently localized to kidney cells where plasma membrane-associated H^+-ATPases are also expressed such as in the proximal tubule and intercalated cells.

Next we examined whether mRNA and protein abundance of the (P)RR/Atp6ap2 paralleled mRNA and protein expression levels of two H^+-ATPase subunits, a4/Atp6v0a4 and B1/Atp6v1b1, in membrane preparations from kidney cortex and kidney medulla from mice subjected to different treatments known to affect acid-base status and H^+-ATPase regulation [25,32,35,48,60,61]. Changes in acid-base and electrolyte balance caused changes in mRNA and protein expression of all three molecules but did not show an uniform and obvious pattern of coregulation. At the level of the kidney cortex this may not be surprising since the preparation contains a mixture of proximal tubules, connecting tubules, and cortical collecting ducts which may have differential patterns of regulation. The medullary preparations (from outer and inner medulla) are more homogenous and thus representative for medullary collecting ducts even though containing also fractions from the late proximal tubule and medullary TALs [62]. Nevertheless, no consistent coregulation of the H^+-ATPase subunits and the (P)RR/atp6ap2 was observed. Along the same line, B1 and a4 subunit isoforms showed varying responses which may reflect different expression patterns. Part of the changes in H^+-ATPase subunit isoform expression and (PRR/Atp6ap2 may also be due to remodeling of the collecting duct that during chonic changes in electrolyte and acid-base status can

affect the relative abundance of principal versus intercalated cells as well as the relative frequency of the different intercalated cell subtypes [25,63].

Regulation of the (P)RR/Atp6ap2 has been shown in rodent models subjected to low or high salt intake [52,64]. Similar to our results no effect of high salt intake on (P)RR/Atp6ap2 mRNA was detected [52] whereas low salt diet increased (P)RR/Atp6ap2 mRNA [64,65]. In contrast, on protein level high salt diet was associated with increased full length (P)RR/Atp6ap2 protein expression in cortex and medulla which was attributed to changes in glomerular and proximal tubular abundance [52]. But also low salt intake caused higher expression of (P)RR/Atp6ap2 protein at the level of the total kidney [64,65,66]. The functional relevance of the seemingly same response of the (P)RR/Atp6ap2 to both high and low salt intake are not known to date.

Regulation of H^+-ATPase activity occurs on several levels involving assembly and disassembly of V_0 and V_1 sectors, trafficking of pumps into and from the membrane, and phosphorylation of subunits [6,7]. Changes in acid-base status or electrolyte homeostasis as well as aldosterone or its analogue DOCA have been shown to induce marked redistribution of H^+-ATPases in intercalated cells with more pronounced membrane association at the luminal membrane in type A intercalated cells upon NH_4Cl or DOCA treatment [13,20,32,48,67]. Likewise, supplementation with bicarbonate leads to a strong staining of basolateral and/or luminal membranes in type B and non-A/non-B intercalated cells [32,48,67]. Thus, we tested whether the (P)RR/Atp6ap2 would colocalize with the a4/Atp6v0a4 H^+-ATPase subunit that has been previously shown to participate in the trafficking of H^+-ATPases to the different membrane domains in type A and non-type A intercalated cells [32]. Detailed

analysis of intercalated cells in the connecting tubule and medullary collecting duct showed that (P)RR/Atp6ap2 and the a4/Atp6v0a4 H^+-ATPase subunit showed a high degree of colocalization both in intercalated cells stained for AE1 (type A intercalated cells) and intercalated cells negative for AE1 (non-type A intercalated cells). In the latter cell population, (P)RR/Atp6ap2 and a4/Atp6v0a4 were detected at the basolateral and luminal membrane as expected and consistent with the detection of (P)RR/Atp6ap2 in pendrin positive cells (Figure 4C,D). Also in the proximal tubule, (P)RR/Atp6ap2 and a4/Atp6v0a4 strongly colocalized at the brush border membrane under all treatments. Thus, the (P)RR/Atp6ap2 appears to colocalize with H^+-ATPases under different conditions inducing a subcellular redistribution of pumps.

In a last set of experiments we addressed the question whether prorenin would acutely affect basal H^+-ATPase function in type A intercalated cells. Isolated cortical collecting ducts microperfused *in vitro* were exposed to two different concentrations of luminal prorenin that had previously been shown to induce cellular responses in other preparations [50,51]. However, we detected no differences between tubules microperfused with prorenin or left untreated in the realkalinization rates after washing out the NH_4Cl prepulse. The rate of realkalinization represents mostly proton extrusion by H^+-ATPases as indicated by its sensitivity to typical H^+-ATPase inhibitors such as bafilomycin or concanamycin [20,29,68]. Moreover, we and others have previously shown that various stimuli including aldosterone, angiotensin II, or cAMP can stimulate H^+-ATPase activity in such preparations [12,13,20,21,69]. In a previous study using MDCK cells as model for intercalated cells we had shown that prorenin was able to stimulate H^+-ATPase activity, albeit at high concentrations, and that siRNA mediated suppression of (P)RR/Atp6ap2 expression reduced expression of the a2 but not the a4, d2, and B1/2 H^+-ATPase

subunits and diminished stimulation of H^+-ATPase activity by the antidiuretic hormone [51]. The discrepancy between our present study and the previous experiments in MDCK cells may be explained by differences in the composition of proton pump subunits present in MDCK and the native murine cortical collecting duct or by more general differences between the MDCK cell culture system and freshly isolated intercalated cells. Some subclones of the original MDCK cell line, namely the C7 and C11 clones, are believed to resemble principal and intercalated cells [28]. However, we performed qPCR for typical markers expressed by intercalated cells (e.g. pendrin, AE1, Foxi1, CP2L1, B1/ATP6V1B1) and by principal cells (e.g. AQP2) on these clones and found only very low or inconsistent expression of specific intercalated cell markers in these clones (Kampik, Wagner, unpublished data) suggesting that MDCK cells may not represent a very faithful model to investigate intercalated cell functions and regulation. Along the same line, Advani et al had reported that incubation of MDCK cells with renin and prorenin stimulated ERK1/2 phosphorylation and that this effect was blocked by the H^+-ATPase inhibitor bafilomycin [50]. We thus incubated freshly isolated cortical collecting ducts and MDCK cells with prorenin. In both preparations, cortical collecting ducts and MDCK cells, only a weak but not significant increase of ERK1/2 phosphorylation was found. In freshly isolated murine collecting ducts ERK1/2 participates in the stimulatory effect of aldosterone on H^+-ATPase activity [13]. Hence, an increase in pERK1/2 might directly stimulate H^+-ATPase activity or be permissive for other positive stimuli. Therefore, the absence of a stimulatory effect of prorenin on H^+-ATPase activity is consistent with the absence of an effect on ERK1/2 phosphorylation in the same preparation and possibly also in MDCK cells. Of note, all batches of prorenin were extensively tested for *in vitro* activity before use in microperfusion or *in vitro* incubation experiments ruling out that an inactive form of prorenin was used [70,71].

In summary, we extend previous observations on the localization of the (P)RR/Atp6ap2 along the entire murine nephron and provide detailed information on its subcellular localization in the various types of intercalated cells. (P)RR/Atp6ap2 and two other H^+-ATPase subunits did not show coordinated regulation of mRNA and protein expression in kidneys from mice receiving different treatments. Nevertheless, immunolocalization of (P)RR/Atp6ap2 and the a4/Atp6v0a4 H^+-ATPase subunit showed colocalization under all conditions suggesting that (P)RR/Atp6ap2 may be closely linked to or an integral part of the pump. In freshly isolated collecting ducts, prorenin had no effect on basal H^+-ATPase activity and ERK1/2 phosphorylation indicating that prorenin and possibly also renin are not directly regulating H^+-ATPase activity under the conditions used in this assay. Whether prorenin may have a permissive effect on the regulation of H^+-ATPase function by other stimuli cannot be ruled out. Our data do not provide any answer to the question whether the (P)RR/Atp6ap2 is a functionally relevant part of the H^+-ATPase in the proximal tubule or intercalated cells. Experiments in *Drosophila* suggest that the (P)RR/Atp6ap2 might participate in endocytic retrieval of proteins from urine in the proximal tubule [22]. Genetic deletion of (P)RR/Atp6ap2 in other tissues and cells suggests that the absence of (P)RR/Atp6ap2 impairs the expression and function of the proton pump complex [44,51,72]. Also, the genetic deletion of (P)RR/Atp6ap2 from the entire collecting duct in mice causes hydronephrosis and more alkaline urine consistent with an important role of the protein in the collecting duct [73]. The timed and specific deletion of (P)RR/Atp6ap2 from renal cells will have to address the specific function(s) of the (P)RR/Atp6ap2 in these cells and its relationship to H^+-ATPase function.

ACKNOWLEDGEMENTS

This work was supported by the Swiss National Science Foundation (grant No. 31003A_138143) to C.A. Wagner and the Hartmann-Müller Stiftung (Zurich, Switzerland) to A. Daryadel.

Competing interests and financial disclosure

The authors declare that they have no competing interests and no financial disclosures.

FIGURE LEGENDS

Figure 1. Expression of (P)RR/Atp6ap2 mRNA along the mouse nephron

Nephron segments were dissected from mouse kidney and relative mRNA abundance of the (P)RR and the B1 (Atp6v1b1) subunit of the vacuolar H^+-ATPase assessed. Segment-specific enrichment of nephron fragments was tested by qPCR for various transcripts: Podoplanin for the glomerulum, NaPi-.IIa for the S1 /S2 , S3 segments of the proximal tubule and DCT, NKCC2 for the TAL, NCC for the DCT, AQP2 for the collecting duct system, and pendrin for the CNT/CCD. Data are mean ± SEM (n= 4 mice/segments). Glom glomerulus, S1/S2 convoluted part of the proximal tubule, S3 straight part of the proximal tubule, thin limb thin descending and ascending limb of the loop of Henle, TAL thick ascending limb of the loop of Henle, DCT distal convoluted tubule, CNT/CCD connecting tubule/cortical collecting duct, OMCD outer medullary collecting duct, IMCD inner medullary collecting duct, WT M 12 wk C57BL/6 male mouse 12 weeks old.

Figure 2. Localization of the (P)RR/Atp6ap2 in mouse kidney

Immunoflourescence staining for the (P)RR/Atp6p2 in mouse kidney (green). **(A)** Overview showing (P)RR/Atp6ap2 (green), the principal cell specific AQP2 water channel (red), and nuclei (blue), original magnification 40 x. **(B)** A cortical field with glomerulus (G), and (P)RR/Atp6ap2 staining (green) in the proximal tubule (PT) and connecting tubules (CNT), 400 x magnification. **(C)** Cortical and outer medullary collecting duct stained for (P)RR/Atp6ap2 (green) and the principal cell specific AQP2 water channel (red), 400 x magnification. **(E,D,F)** (P)RR staining (D: green) was detected in the proximal tubule (PT) in the brush border membrane and colocalized with the a4 H^+-ATPase subunit (ATP6V0A4)(E: red) as indicated by the yellow color (F), original magnification 400x.

FIGURE 3

Colocalization of the (P)RR/Atp6ap2 with the a4 H^+-ATPase subunit in intercalated cells

Staining of mouse kidney sections with antibodies against the a4 (Atp6v0a4) H^+-ATPase subunit (red, upper panels) and the (P)RR/Atp6ap2 (green, middle panels) demonstrates colocalization (yellow, lower panels) in intercalated cells at the light microscopy level. Original magnification 400x.

FIGURE 4

Subcellular localization of the (P)RR/Atp6ap2 in type A and non-type A intercalated cells

(A,B) Staining of mouse kidney sections with antibodies against the (P)RR/Atp6ap2 (green), the type A intercalated cell specific marker AE1 (red) and nuclei with DAPI (blue). In cells expressing AE1, (P)RR/Atp6ap2 related staining is found and localizes to the apical side of cells (insert in B), original magnification 630-1000 x. (C,D) Staining of mouse kidney sections with antibodies against the (P)RR/Atp6ap2 (green), the non-type A intercalated cell specific marker pendrin (red) and nuclei with DAPI (blue). In cells positive for pendrin, (P)RR/Atp6ap2 staining is detected either at the basolateral side of cells (asterisks in D) and/or luminal side (yellow overlay, arrow in D). Original magnification 400 - 630 x.

FIGURE 5

Regulated mRNA expression of (P)RR/Atp6ap2 and the B1/Atp6v1b1 and a4/Atp6v0a4 H^+-ATPase subunits in mouse kidney.

Mice were treated with NaCl, $NaHCO_3$, $KHCO_3$, NH_4Cl or DOCA for 7 days, and relative mRNA expression levels of (P)RR/Atp6ap2, and the B1/Atp6v1b1 and a4/Atp6v0a4 H^+-ATPase subunits were assessed by semi-quantitative real-time RT-PCR in cortex and medulla. N = 5 animals/ group, *p ≤ 0.05, **p ≤ 0.01, ***p ≤ 0.001.

FIGURE 6

Regulated protein abundance of (P)RR/Atp6ap2 and the B1/Atp6v1b1 and a4/Atp6v0a4 H^+-ATPase subunits in mouse kidney cortex.

Mice were treated with NaCl, $NaHCO_3$, $KHCO_3$, NH_4Cl or DOCA for 7 days, and protein expression levels of (P)RR/Atp6ap2, and the B1/Atp6v1b1 and a4/Atp6v0a4 H^+-ATPase subunits were examined by immunoblotting of total membrane fractions prepared from kidney cortex **(A)**. All blots were stripped and reprobed for β-actin. (42 kDa), and the ratio of (P)RR : β-actin was calculated. Bar graphs **(B)** summarize data from the blots. Arithmetic means ± SD are shown, n = 5 animals/ group, *p ≤ 0.05, **p ≤ 0.01, ***p ≤ 0.001.

FIGURE 7

Regulated protein abundance of (P)RR/Atp6ap2 and the B1/Atp6v1b1 and a4/Atp6v0a4 H^+-ATPase subunits in mouse kidney medulla.

Mice were treated with NaCl, $NaHCO_3$, $KHCO_3$, NH_4Cl or DOCA for 7 days, and protein expression levels of (P)RR/Atp6ap2, and the B1/Atp6v1b1 and a4/Atp6v0a4 H^+-ATPase subunits were examined by immunoblotting of total membrane fractions prepared from kidney outer and inner medulla **(A)**. All blots were stripped and reprobed for β-actin. (42 kDa), and the ratio of (P)RR to β-actin was calculated. Bar

graphs **(B)** summarize data from the blots. Arithmetic means ± SD are shown, n = 5 animals/ group, *p ≤ 0.05, **p ≤ 0.01, ***p ≤ 0.001.

FIGURE 8

Colocalization of (P)RR/Atp6ap2 and the a4/Atp6v0a4 H^+-ATPase subunit under conditions of acidosis and alkalosis

Mice were left untreated or received NH_4Cl (0.28 M) or $NaHCO_3$ (0.28 M) in drinking water for 7 days to induce metabolic acidosis or alkalosis, respectively. Kidney sections were stained with antibodies against the (P)RR/Atp6ap2 (green), the a4/Atp6v0a4 H^+-ATPase subunit (red), the type A intercalated cell specific anion exchanger AE1 (white), and with DAPI (blue) to mark nuclei. **(A-C)** Kidney sections from control mice with a cortical field (A) (400x), convoluted proximal tubules (B)(630 x), and an outer medullary collecting duct (C)(630x). The insert in (C) shows a higher magnification of type A intercalated cells in the outer medulla. **(D-F)** Kidney sections from mice receiving NH_4Cl showing a cortical field (D) (400x), convoluted proximal tubules (E)(630 x), and an outer medullary collecting duct (F)(630x). The insert in (F) shows a higher magnification of type A intercalated cells in the outer medulla. **(G-I)** Kidney sections from mice treated with $NaHCO_3$ showing a cortical field (G) (400x), convoluted proximal tubules (H)(630 x), and an outer medullary collecting duct (I)(630x). The insert in (I) shows a higher magnification of type A intercalated cells in the outer medulla. N = 4 animals/group.

FIGURE 9

Prorenin does not acutely stimulate H^+-ATPase activity in microperfused mouse outer medullary collecting ducts

Cortical collecting ducts were prepared by hand-dissection from mouse kidney and microperfused *ex vivo*. H^+-ATPase activity was assessed from pH_i recovery rates in BCECF loaded intercalated cells using the NH_4Cl prepulse technique. 1 nM or 20 pM Prorenin was applied from the luminal side and pH_i recovery rates were measured. N = 4 to 6 tubules/group

FIGURE 10

Prorenin stimulates ERK1/2 phosphorylation in isolated mouse collecting ducts and MDCK cells

(A) Outer medullary collecting ducts were prepared by hand-dissection from kidneys of mice expressing EGFP under the control of the intercalated cell specific Atp6v1b1 promoter [26] and incubated *in vitro* with or without prorenin for 10 min. Immunoblots were performed for pERK1/2 and total ERK1/2. **(B)** Three independent experiments were performed and are summarized as bar graph showing the ratio of pERK1/2 over total ERK1/2. **(C, D)** MDCK cells were incubated for 10 minutes with prorenin (20 nM) or angiotensin II (10 nM) in the absence or presence of the AT_1 and AT_2 receptor blockers losartan (10 μM) and PD123310 (10 μM). Immunoblots were performed for pERK1/2 and total ERK1/2. Three independent experiments were performed and are summarized as bar graph showing the ratio of pERK1/2 over total ERK1/2.

Supplementary table 1

Sequences of forward and reverse primers and probes used for semi-quantitative real-time RT-PCR.

REFERENCES

1. Nguyen G, Muller DN (2010) The biology of the (pro)renin receptor. J Am Soc Nephrol 21: 18-23.

2. Sihn G, Rousselle A, Vilianovitch L, Burckle C, Bader M (2010) Physiology of the (pro)renin receptor: Wnt of change? Kidney Int 78: 246-256.

3. Krop M, Lu X, Danser AH, Meima ME (2013) The (pro)renin receptor. A decade of research: what have we learned? Pflugers Arch 465: 87-97.

4. Nguyen G, Delarue F, Burckle C, Bouzhir L, Giller T, et al. (2002) Pivotal role of the renin/prorenin receptor in angiotensin II production and cellular responses to renin. J Clin Invest 109: 1417-1427.

5. Ludwig J, Kerscher, S, Brandt, U, Pfeiffer, K, Getlawi, F, Apps, D K, Schagger, H (1998) Identification and characterization of a novel 9.2-kDa membrane sector-associated protein of vacuolar proton-ATPase from chromaffin granules. J Biol Chem 273: 10939-10947.

6. Nishi T, Forgac, M (2002) The vacuolar H^+-ATPases--nature's most versatile proton pumps. Nat Rev Mol Cell Biol 3: 94-103.

7. Wagner CA, Finberg, K E, Breton, S, Marshansky, V, Brown, D, Geibel, J P (2004) Renal vacuolar H^+-ATPase. Physiol Rev 84: 1263-1314.

8. Breton S, Brown D (2013) Regulation of luminal acidification by the V-ATPase. Physiology (Bethesda) 28: 318-329.

9. Hennings JC, Picard N, Huebner AK, Stauber T, Maier H, et al. (2012) A mouse model for distal renal tubular acidosis reveals a previously unrecognized role of the V-ATPase a4 subunit in the proximal tubule. EMBO Mol Med 4: 1057-1071.

10. Pastor-Soler N, Beaulieu, V, Litvin, T N, Da Silva, N, Chen, Y, Brown, D, Buck, J, Levin, L R, Breton, S (2003) Bicarbonate-regulated adenylyl cyclase (sAC) is a sensor that regulates pH-dependent V-ATPase recycling. J Biol Chem 278: 49523-49529.

11. Alzamora R, Thali RF, Gong F, Smolak C, Li H, et al. (2010) PKA regulates vacuolar H+-ATPase localization and activity via direct phosphorylation of the a subunit in kidney cells. J Biol Chem 285: 24676-24685.

12. Paunescu TG, Ljubojevic M, Russo LM, Winter C, McLaughlin MM, et al. (2010) cAMP stimulates apical V-ATPase accumulation, microvillar elongation, and proton extrusion in kidney collecting duct A-intercalated cells. Am J Physiol Renal Physiol 298: F643-654.

13. Winter C, Kampik NB, Vedovelli L, Rothenberger F, Paunescu TG, et al. (2011) Aldosterone stimulates vacuolar H(+)-ATPase activity in renal acid-secretory

intercalated cells mainly via a protein kinase C-dependent pathway. Am J Physiol Cell Physiol 301: C1251-1261.

14. Gong F, Alzamora R, Smolak C, Li H, Naveed S, et al. (2010) Vacuolar H+-ATPase apical accumulation in kidney intercalated cells is regulated by PKA and AMP-activated protein kinase. Am J Physiol Renal Physiol 298: F1162-1169.

15. Brown D, Sabolic, I, Gluck, S (1991) Colchicine-induced redistribution of proton pumps in kidney epithelial cells. Kidney Int Suppl 33: S79-83.

16. Cannon C, van Adelsberg J, Kelly S, Al-Awqati Q (1985) Carbon-dioxide-induced exocytotic insertion of H+ pumps in turtle-bladder luminal membrane: role of cell pH and calcium. Nature 314: 443-446.

17. Gluck S, Cannon, C, Al-Awqati, Q (1982) Exocytosis regulates urinary acidification in turtle bladder by rapid insertion of H^+ pumps into the luminal membrane. Proc Natl Acad Sci U S A 79: 4327-4331.

18. Schwartz GJ, Al-Awqati, Q (1985) Carbon dioxide causes exocytosis of vesicles containing H^+ pumps in isolated perfused proximal and collecting tubules. J Clin Invest 75: 1638-1644.

19. Wagner CA, Giebisch, G, Lang, F, Geibel, J P (1998) Angiotensin II stimulates vesicular H^+-ATPase in rat proximal tubular cells. Proc Natl Acad Sci U S A 95: 9665-9668.

20. Winter C, Schulz, N, Giebisch, G, Geibel, J P, Wagner, C A (2004) Nongenomic stimulation of vacuolar H^+-ATPases in intercalated renal tubule cells by aldosterone. Proc Nat Acad Sci USA 101: 2636-2641.

21. Wagner CA, Mohebbi N, Uhlig U, Giebisch GH, Breton S, et al. (2011) Angiotensin II stimulates H(+)-ATPase activity in intercalated cells from isolated mouse connecting tubules and cortical collecting ducts. Cell Physiol Biochem 28: 513-520.

22. Hermle T, Guida MC, Beck S, Helmstadter S, Simons M (2013) Drosophila ATP6AP2/VhaPRR functions both as a novel planar cell polarity core protein and a regulator of endosomal trafficking. EMBO J 32: 245-259.

23. Hermle T, Saltukoglu D, Grunewald J, Walz G, Simons M (2010) Regulation of Frizzled-dependent planar polarity signaling by a V-ATPase subunit. Curr Biol 20: 1269-1276.

24. Cruciat CM, Ohkawara B, Acebron SP, Karaulanov E, Reinhard C, et al. (2010) Requirement of prorenin receptor and vacuolar H+-ATPase-mediated acidification for Wnt signaling. Science 327: 459-463.

25. Mohebbi N, Perna A, van der Wijst J, Becker HM, Capasso G, et al. (2013) Regulation of two renal chloride transporters, AE1 and pendrin, by electrolytes and aldosterone. PLoS One 8: e55286.

26. Miller RL, Zhang P, Smith M, Beaulieu V, Paunescu TG, et al. (2005) V-ATPase B1-subunit promoter drives expression of EGFP in intercalated cells of kidney, clear cells of epididymis and airway cells of lung in transgenic mice. Am J Physiol Cell Physiol 288: C1134-1144.

27. Nowik M, Lecca MR, Velic A, Rehrauer H, Brandli AW, et al. (2008) Genome-wide gene expression profiling reveals renal genes regulated during metabolic acidosis. Physiol Genomics 32: 322-334.

28. Gekle M, Wunsch S, Oberleithner H, Silbernagl S (1994) Characterization of two MDCK-cell subtypes as a model system to study principal cell and intercalated cell properties. Pflugers Arch 428: 157-162.

29. Wagner CA, Lukewille, U, Valles, P, Breton, S, Brown, D, Giebisch, G H, Geibel, J P (2003) A rapid enzymatic method for the isolation of defined kidney tubule fragments from mouse. Pflugers Arch 446: 623-632.

30. Bonnici B, Wagner CA (2004) Postnatal expression of transport proteins involved in acid-base transport in mouse kidney. Pflugers Arch 448: 16-28.

31. McLean IW, Nakane PK (1974) Periodate-lysine-paraformaldehyde fixative. A new fixation for immunoelectron microscopy. J Histochem Cytochem 22: 1077-1083.

32. Stehberger P, Schulz, N, Finberg, K E, Karet, F E, Giebisch, G, Lifton, R P, Geibel, J P, Wagner, C A (2003) Localization and regulation of the ATP6V0A4 (a4) vacuolar H^+-ATPase subunit defective in an inherited form of distal renal tubular acidosis. J Am Soc Nephrol 14: 3027-3038.

33. Brown D, Lydon J, McLaughlin M, Stuart-Tilley A, Tyszkowski R, et al. (1996) Antigen retrieval in cryostat tissue sections and cultured cells by treatment with sodium dodecyl sulfate (SDS). Histochem Cell Biol 105: 261-267.

34. Wagner CA, Finberg KE, Stehberger PA, Lifton RP, Giebisch GH, et al. (2002) Regulation of the expression of the Cl-/anion exchanger pendrin in mouse kidney by acid-base status. Kidney Int 62: 2109-2117.

35. Hafner P, Grimaldi R, Capuano P, Capasso G, Wagner CA (2008) Pendrin in the mouse kidney is primarily regulated by Cl- excretion but also by systemic metabolic acidosis. Am J Physiol Cell Physiol 295: C1658-1667.

36. Stehberger PA, Shmukler BE, Stuart-Tilley AK, Peters LL, Alper SL, et al. (2007) Distal renal tubular acidosis in mice lacking the AE1 (band3) Cl^-/HCO_3^- exchanger (slc4a1). J Am Soc Nephrol 18: 1408-1418.

37. Wagner CA, Loffing-Cueni D, Yan Q, Schulz N, Fakitsas P, et al. (2008) Mouse model of type II Bartter's syndrome. II. Altered expression of renal sodium- and water-transporting proteins. Am J Physiol Renal Physiol 294: F1373-1380.

38. Watts BA, 3rd, Good DW (1994) Apical membrane Na^+/H^+ exchange in rat medullary thick ascending limb. pH-dependence and inhibition by hyperosmolality. J Biol Chem 269: 20250-20255.

39. Roos A, Boron, W F (1981) Intracellular pH. Physiol Rev 61: 296-434.

40. Finberg KE, Wagner, C A, Stehberger, P A, Geibel, J P, Lifton, R P (2003) Molecular Cloning and Characterization of *Atp6v1b1*, the Murine Vacuolar H^+-ATPase B1-Subunit. Gene 318: 25-34.

41. Nelson RD, Guo, X L, Masood, K, Brown, D, Kalkbrenner, M, Gluck, S (1992) Selectively amplified expression of an isoform of the vacuolar H^+-ATPase 56-kilodalton subunit in renal intercalated cells. Proc Natl Acad Sci U S A 89: 3541-3545.

42. Lee JW, Chou CL, Knepper MA (2015) Deep Sequencing in Microdissected Renal Tubules Identifies Nephron Segment-Specific Transcriptomes. J Am Soc Nephrol 26: 2669-2677.

43. Riediger F, Quack I, Qadri F, Hartleben B, Park JK, et al. (2011) Prorenin receptor is essential for podocyte autophagy and survival. J Am Soc Nephrol 22: 2193-2202.

44. Oshima Y, Kinouchi K, Ichihara A, Sakoda M, Kurauchi-Mito A, et al. (2011) Prorenin receptor is essential for normal podocyte structure and function. J Am Soc Nephrol 22: 2203-2212.

45. Smith AN, Finberg, K E, Wagner, C A, Lifton, R P, Devonald, M A, Su, Y, Karet, F E (2001) Molecular cloning and characterization of Atp6n1b: a novel fourth murine vacuolar H^+-ATPase a-subunit gene. J Biol Chem 276: 42382-42388.

46. Schulz N, Dave MH, Stehberger PA, Chau T, Wagner CA (2007) Differential localization of vacuolar H+-ATPases containing a1, a2, a3, or a4 (ATP6V0A1-4) subunit isoforms along the nephron. Cell Physiol Biochem 20: 109-120.

47. Norgett EE, Golder ZJ, Lorente-Canovas B, Ingham N, Steel KP, et al. (2012) Atp6v0a4 knockout mouse is a model of distal renal tubular acidosis with hearing loss, with additional extrarenal phenotype. Proc Natl Acad Sci U S A 109: 13775-13780.

48. Bastani B, Purcell, H, Hemken, P, Trigg, D, Gluck, S (1991) Expression and distribution of renal vacuolar proton-translocating adenosine triphosphatase in response to chronic acid and alkali loads in the rat. J Clin Invest 88: 126-136.

49. Brown D, Hirsch, S, Gluck, S (1988) An H^+-ATPase in opposite plasma membrane domains in kidney epithelial cell subpopulations. Nature 331: 622-624.

50. Advani A, Kelly DJ, Cox AJ, White KE, Advani SL, et al. (2009) The (Pro)renin receptor: site-specific and functional linkage to the vacuolar H+-ATPase in the kidney. Hypertension 54: 261-269.

51. Lu X, Garrelds IM, Wagner CA, Danser AH, Meima ME (2013) (Pro)renin receptor is required for prorenin-dependent and -independent regulation of vacuolar H(+)-ATPase activity in MDCK.C11 collecting duct cells. Am J Physiol Renal Physiol 305: F417-425.

52. Rong R, Ito O, Mori N, Muroya Y, Tamura Y, et al. (2015) Expression of (pro)renin receptor and its upregulation by high salt intake in the rat nephron. Peptides 63: 156-162.

53. Huang J, Ledford KJ, Pitkin WB, Russo L, Najjar SM, et al. (2013) Targeted deletion of murine CEACAM 1 activates PI3K-Akt signaling and contributes to the expression of (Pro)renin receptor via CREB family and NF-kappaB transcription factors. Hypertension 62: 317-323.

54. Gonzalez AA, Green T, Luffman C, Bourgeois CR, Gabriel Navar L, et al. (2014) Renal medullary cyclooxygenase-2 and (pro)renin receptor expression during angiotensin II-dependent hypertension. Am J Physiol Renal Physiol 307: F962-970.

55. Gonzalez AA, Luffman C, Bourgeois CR, Vio CP, Prieto MC (2013) Angiotensin II-independent upregulation of cyclooxygenase-2 by activation of the (Pro)renin receptor in rat renal inner medullary cells. Hypertension 61: 443-449.

56. Gonzalez AA, Lara LS, Luffman C, Seth DM, Prieto MC (2011) Soluble form of the (pro)renin receptor is augmented in the collecting duct and urine of chronic angiotensin II-dependent hypertensive rats. Hypertension 57: 859-864.

57. Alper SL, Natale J, Gluck S, Lodish HF, Brown D (1989) Subtypes of intercalated cells in rat kidney collecting duct defined by antibodies against erythroid band 3 and renal vacuolar H^+-ATPase. Proc Natl Acad Sci U S A 86: 5429-5433.

58. Royaux IE, Wall, S M, Karniski, L P, Everett, L A, Suzuki, K, Knepper, M A, Green, E D (2001) Pendrin, encoded by the Pendred syndrome gene, resides in the apical region of renal intercalated cells and mediates bicarbonate secretion. Proc Natl Acad Sci U S A 98: 4221-4226.

59. Kim YH, Kwon, T H, Frische, S, Kim, J, Tisher, C C, Madsen, K M, Nielsen, S (2002) Immunocytochemical localization of pendrin in intercalated cell subtypes in rat and mouse kidney. Am J Physiol Renal Physiol 283: F744-754.

60. Aruga S, Wehrli, S, Kaissling, B, Moe, O W, Preisig, P A, Pajor, A M, Alpern, R J (2000) Chronic metabolic acidosis increases NaDC-1 mRNA and protein abundance in rat kidney. Kidney Int 58: 206-215.

61. Nowik M, Kampik NB, Mihailova M, Eladari D, Wagner CA (2010) Induction of metabolic acidosis with ammonium chloride (NH4Cl) in mice and rats--species differences and technical considerations. Cell Physiol Biochem 26: 1059-1072.

62. Christensen EI, Wagner CA, Kaissling B (2012) Uriniferous tubule: structural and functional organization. Compr Physiol 2: 805-861.

63. Welsh-Bacic D, Nowik M, Kaissling B, Wagner CA (2011) Proliferation of acid-secretory cells in the kidney during adaptive remodelling of the collecting duct. PLoS One 6: e25240.

64. Matavelli LC, Huang J, Siragy HM (2012) In vivo regulation of renal expression of (pro)renin receptor by a low-sodium diet. Am J Physiol Renal Physiol 303: F1652-1657.

65. Huang J, Siragy HM (2012) Sodium depletion enhances renal expression of (pro)renin receptor via cyclic GMP-protein kinase G signaling pathway. Hypertension 59: 317-323.

66. Gonzalez AA, Womack JP, Liu L, Seth DM, Prieto MC (2014) Angiotensin II increases the expression of (pro)renin receptor during low-salt conditions. Am J Med Sci 348: 416-422.

67. Schwartz GJ, Barasch, J, Al-Awqati, Q (1985) Plasticity of functional epithelial polarity. Nature 318: 368-371.

68. Biver S, Belge H, Bourgeois S, Van Vooren P, Nowik M, et al. (2008) A role for Rhesus factor Rhcg in renal ammonium excretion and male fertility. Nature 456: 339-343.

69. Pech V, Kim YH, Weinstein AM, Everett LA, Pham TD, et al. (2006) Angiotensin II increases chloride absorption in the cortical collecting duct in mice through a pendrin-dependent mechanism. Am J Physiol Renal Physiol.

70. Krop M, van Gool JM, Day D, Hollenberg NK, Jan Danser AH (2011) Evaluation of a direct prorenin assay making use of a monoclonal antibody directed against residues 32-39 of the prosegment. J Hypertens 29: 2138-2146.

71. Krop M, Lu X, Verdonk K, Schalekamp MA, van Gool JM, et al. (2013) New renin inhibitor VTP-27999 alters renin immunoreactivity and does not unfold prorenin. Hypertension 61: 1075-1082.

72. Kinouchi K, Ichihara A, Sano M, Sun-Wada GH, Wada Y, et al. (2010) The (pro)renin receptor/ATP6AP2 is essential for vacuolar H+-ATPase assembly in murine cardiomyocytes. Circ Res 107: 30-34.

73. Song R, Preston G, Ichihara A, Yosypiv IV (2013) Deletion of the prorenin receptor from the ureteric bud causes renal hypodysplasia. PLoS One 8: e63835.

FIGURE 1

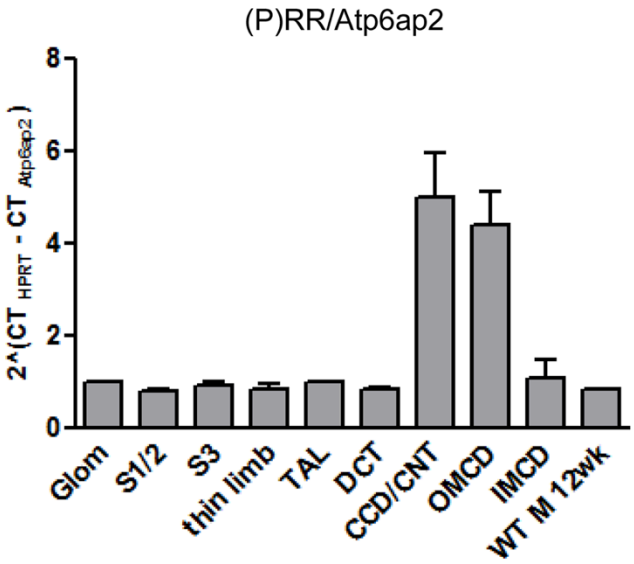
(P)RR/Atp6ap2
2^(CT HPRT - CT Atp6ap2)
8
6
4
2
0
Glom
S1/2
S3
thin limb
TAL
DCT
CCD/CNT
OMCD
IMCD
WT M 12wk

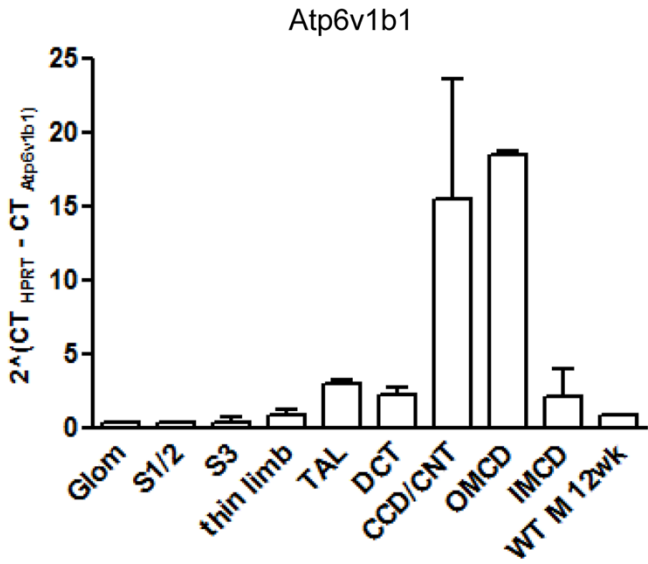
Atp6v1b1
2^(CT HPRT - CT Atp6v1b1)
25
20
15
10
5
0
Glom
S1/2
S3
thin limb
TAL
DCT
CCD/CNT
OMCD
IMCD
WT M 12wk

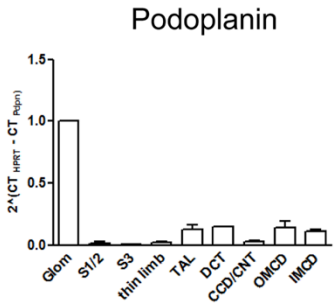
Podoplanin
1.5
1.0
0.5
0.0
Glom
S1/2
S3
thin limb
TAL
DCT
CCD/CNT
OMCD
IMCD

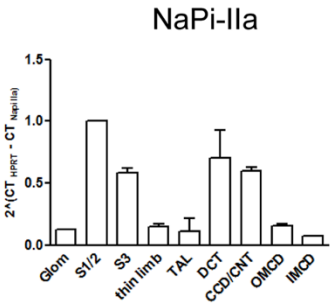
NaPi-IIa
1.5
1.0
0.5
0.0
Glom
S1/2
S3
thin limb
TAL
DCT
CCD/CNT
OMCD
IMCD

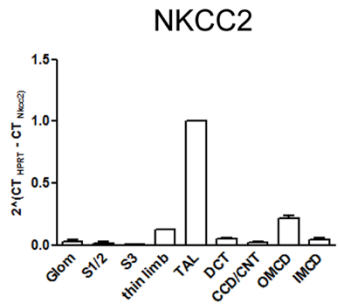
NKCC2
1.5
1.0
0.5
0.0
Glom
S1/2
S3
thin limb
TAL
DCT
CCD/CNT
OMCD
IMCD

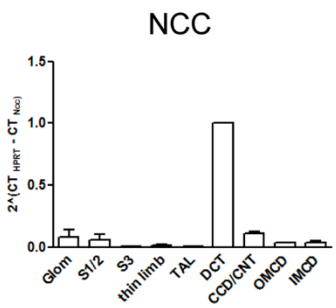
NCC
1.5
1.0
0.5
0.0
Glom
S1/2
S3
thin limb
TAL
DCT
CCD/CNT
OMCD
IMCD

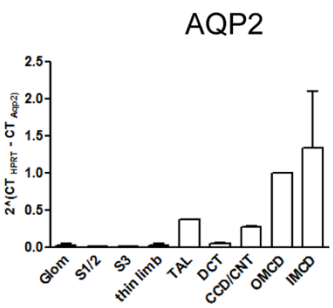
AQP2
2.5
2.0
1.5
1.0
0.5
0.0
Glom
S1/2
S3
thin limb
TAL
DCT
CCD/CNT
OMCD
IMCD

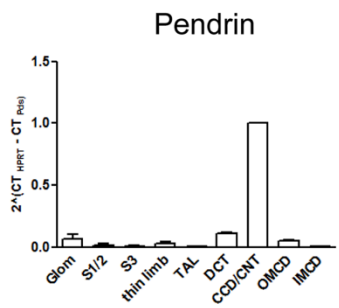
Pendrin
1.5
1.0
0.5
0.0
Glom
S1/2
S3
thin limb
TAL
DCT
CCD/CNT
OMCD
IMCD

FIGURE 2

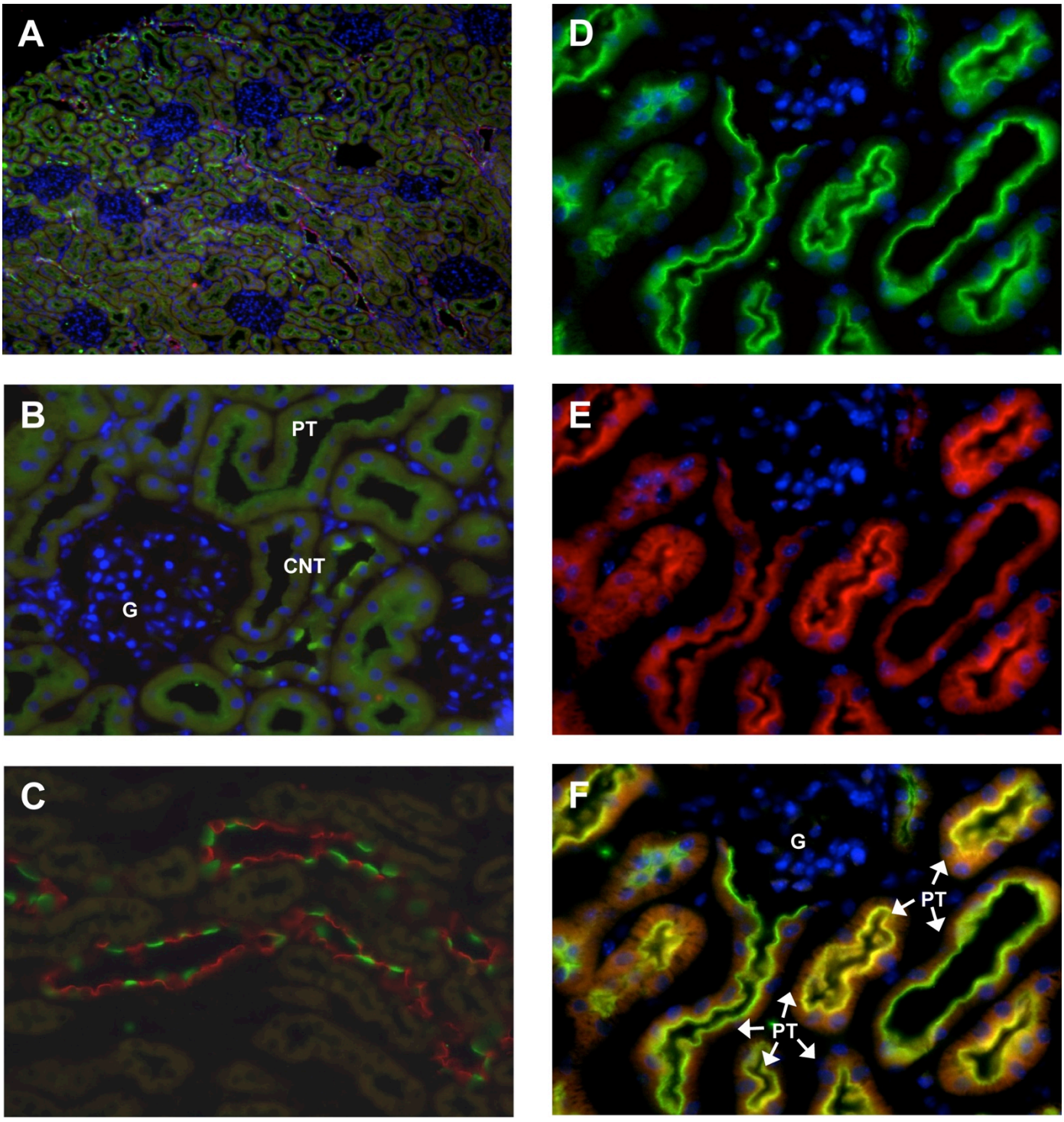

FIGURE 3

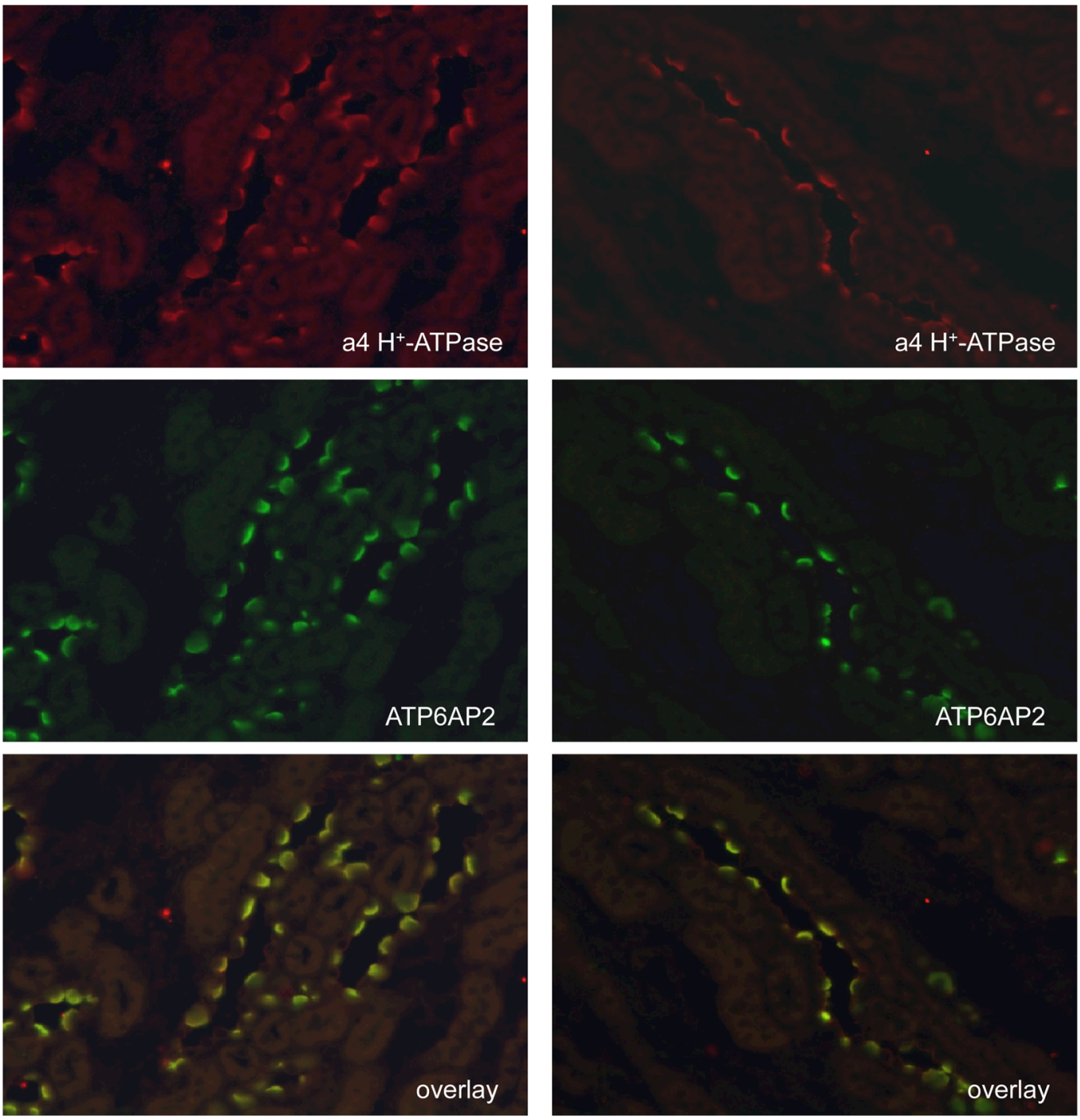

FIGURE 4

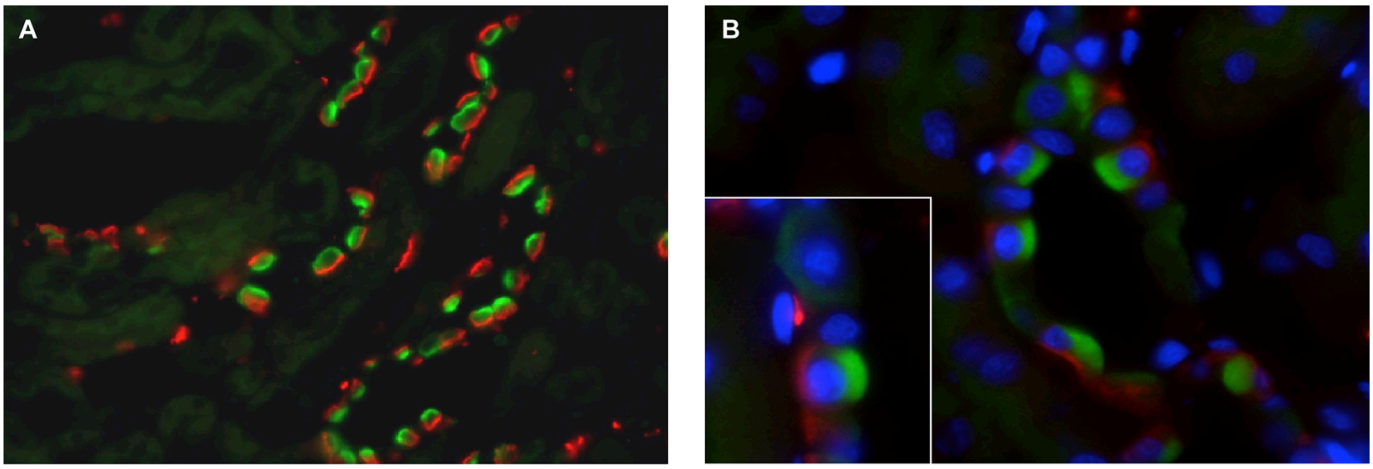

ATP6AP2: green, AE1: red, Nuclei: blue

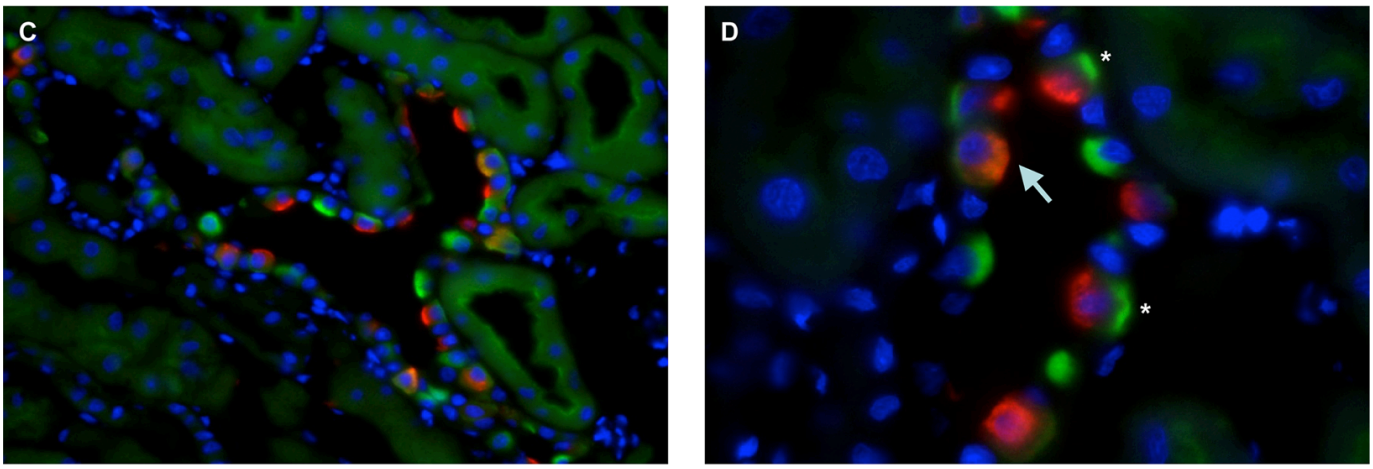

ATP6AP2: green, Pendrin: red, Nuclei: blue

FIGURE 5

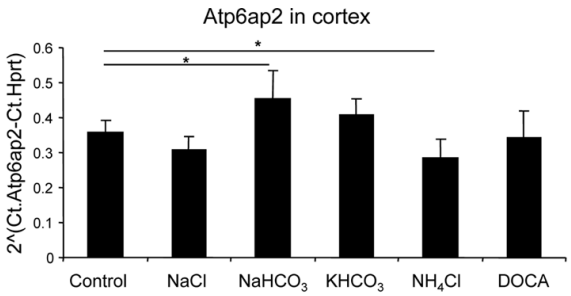
Atp6ap2 in cortex
2^(Ct.Atp6ap2-Ct.Hprt)
0.6
0.5
0.4
0.3
0.2
0.1
0
*
*
Control
NaCl
NaHCO3
KHCO3
NH4Cl
DOCA

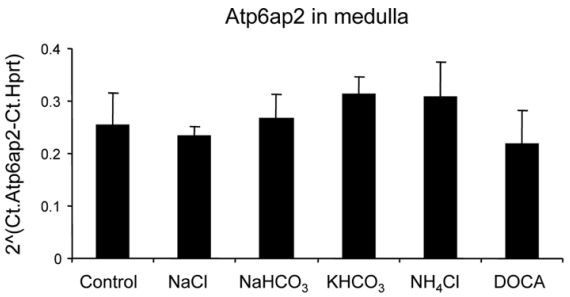
Atp6ap2 in medulla
2^(Ct.Atp6ap2-Ct.Hprt)
0.4
0.3
0.2
0.1
0
Control
NaCl
NaHCO3
KHCO3
NH4Cl
DOCA

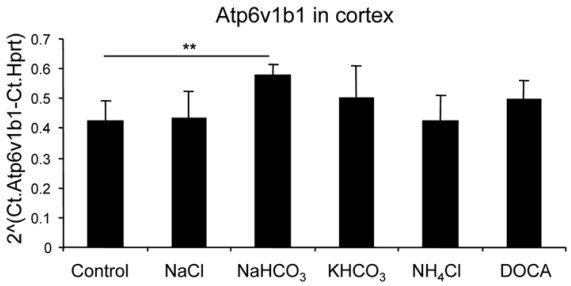
Atp6v1b1 in cortex
2^(Ct.Atp6v1b1-Ct.Hprt)
0.7
0.6
0.5
0.4
0.3
0.2
0.1
0
**
Control
NaCl
NaHCO3
KHCO3
NH4Cl
DOCA

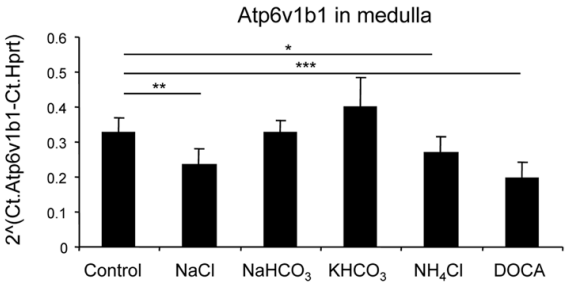
Atp6v1b1 in medulla
2^(Ct.Atp6v1b1-Ct.Hprt)
0.6
0.5
0.4
0.3
0.2
0.1
0
*
***
**
Control
NaCl
NaHCO3
KHCO3
NH4Cl
DOCA

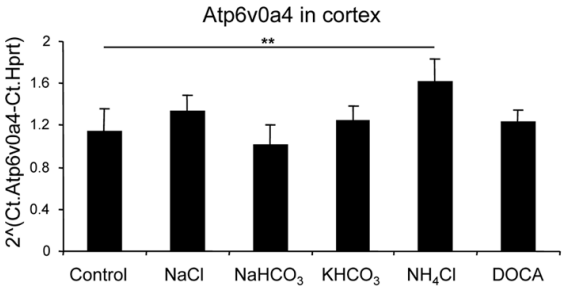
Atp6v0a4 in cortex
2^(Ct.Atp6v0a4-Ct.Hprt)
2
1.6
1.2
0.8
0.4
0
**
Control
NaCl
NaHCO3
KHCO3
NH4Cl
DOCA

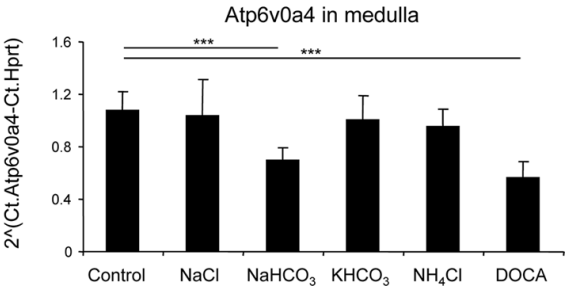
Atp6v0a4 in medulla
2^(Ct.Atp6v0a4-Ct.Hprt)
1.6
1.2
0.8
0.4
0
***
***
Control
NaCl
NaHCO3
KHCO3
NH4Cl
DOCA

FIGURE 6

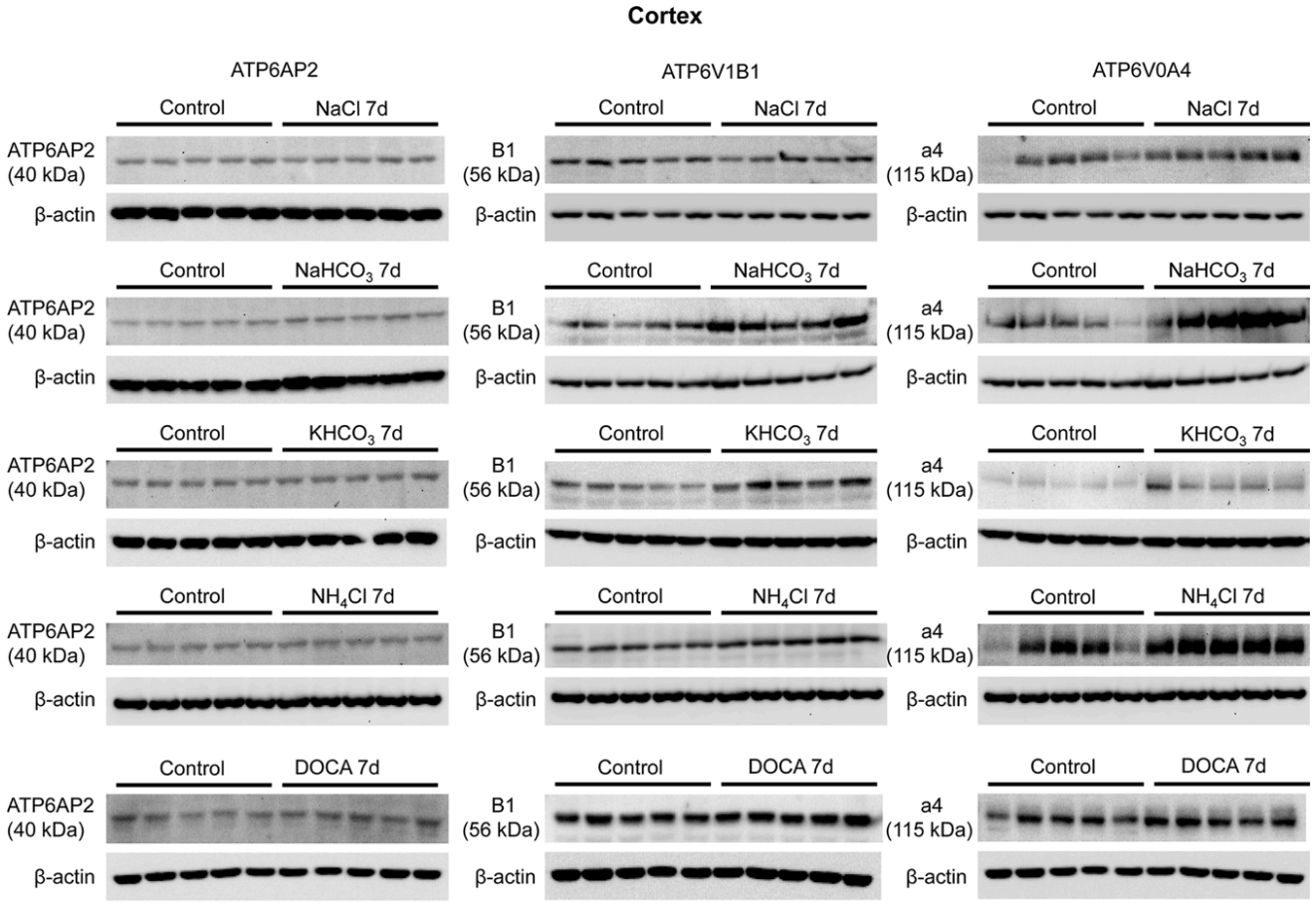
Cortex
ATP6AP2
ATP6V1B1
ATP6V0A4
Control
NaCl 7d
NaHCO3 7d
KHCO3 7d
NH4Cl 7d
DOCA 7d
ATP6AP2 (40 kDa)
B1 (56 kDa)
a4 (115 kDa)
β-actin

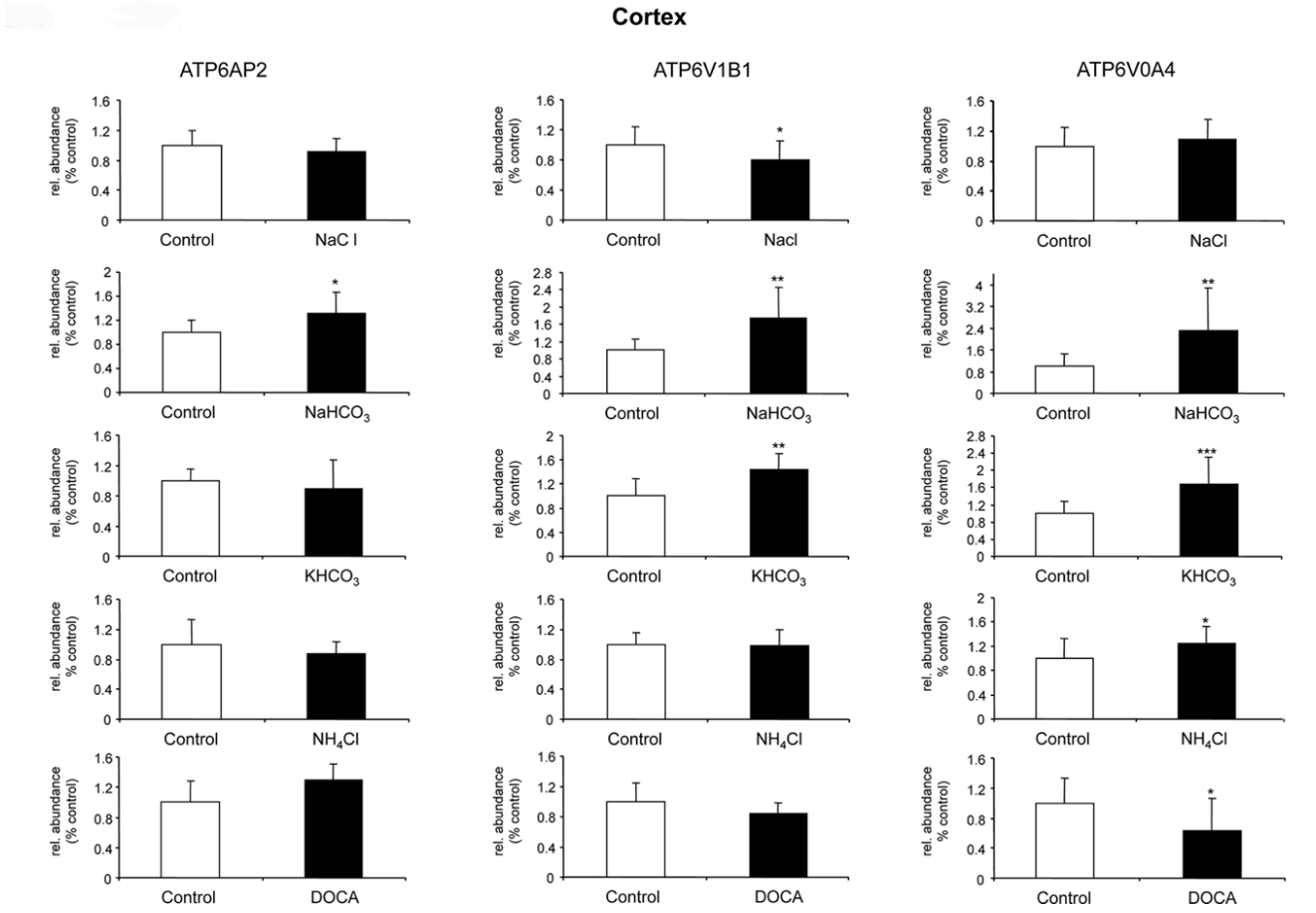
Cortex
ATP6AP2
ATP6V1B1
ATP6V0A4
rel. abundance (% control)
Control
NaC l
Nacl
NaCl
NaHCO3
KHCO3
NH4Cl
DOCA

FIGURE 7

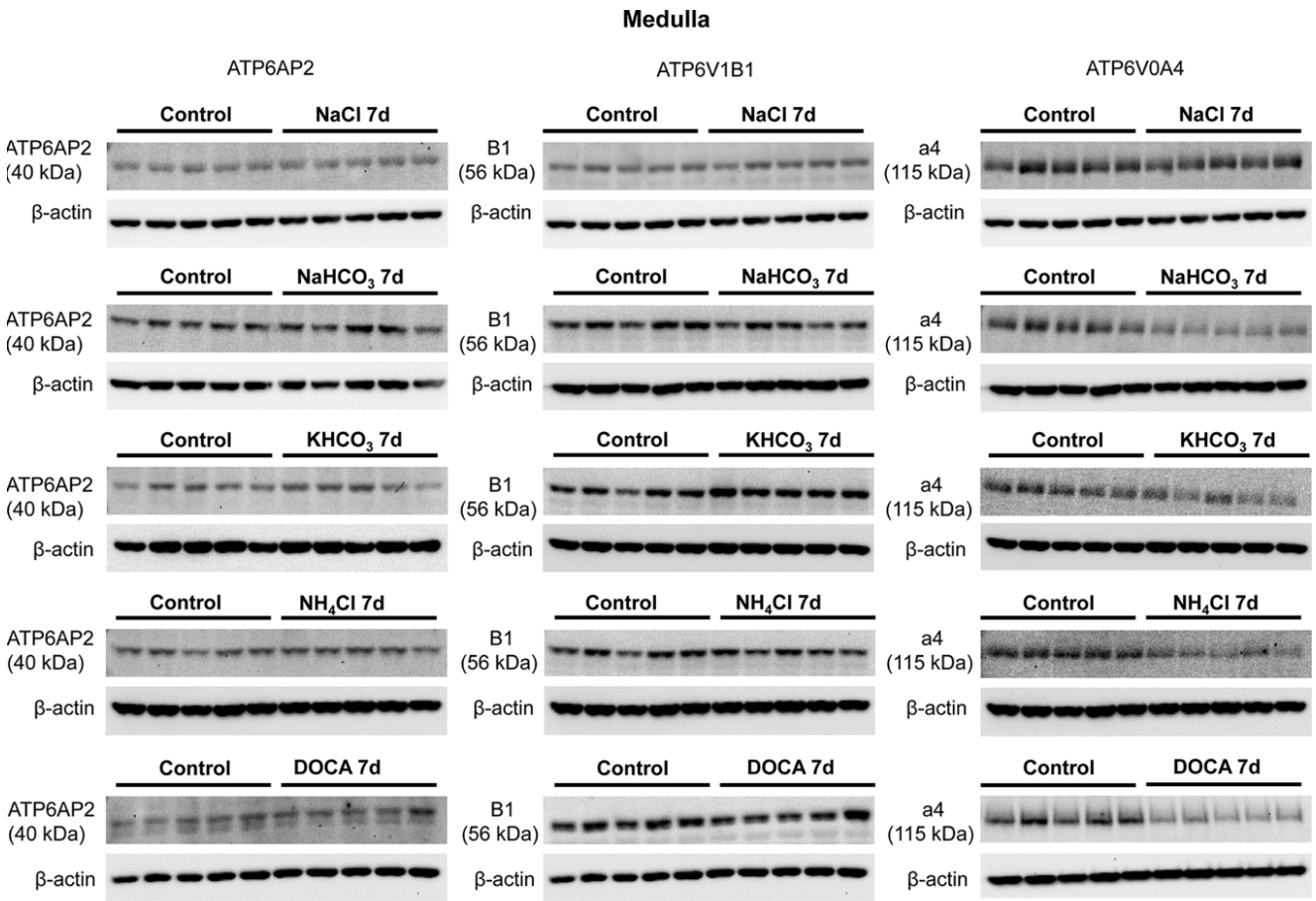
Medulla
ATP6AP2
ATP6V1B1
ATP6V0A4
Control
NaCl 7d
NaHCO3 7d
KHCO3 7d
NH4Cl 7d
DOCA 7d
ATP6AP2 (40 kDa)
B1 (56 kDa)
a4 (115 kDa)
β-actin

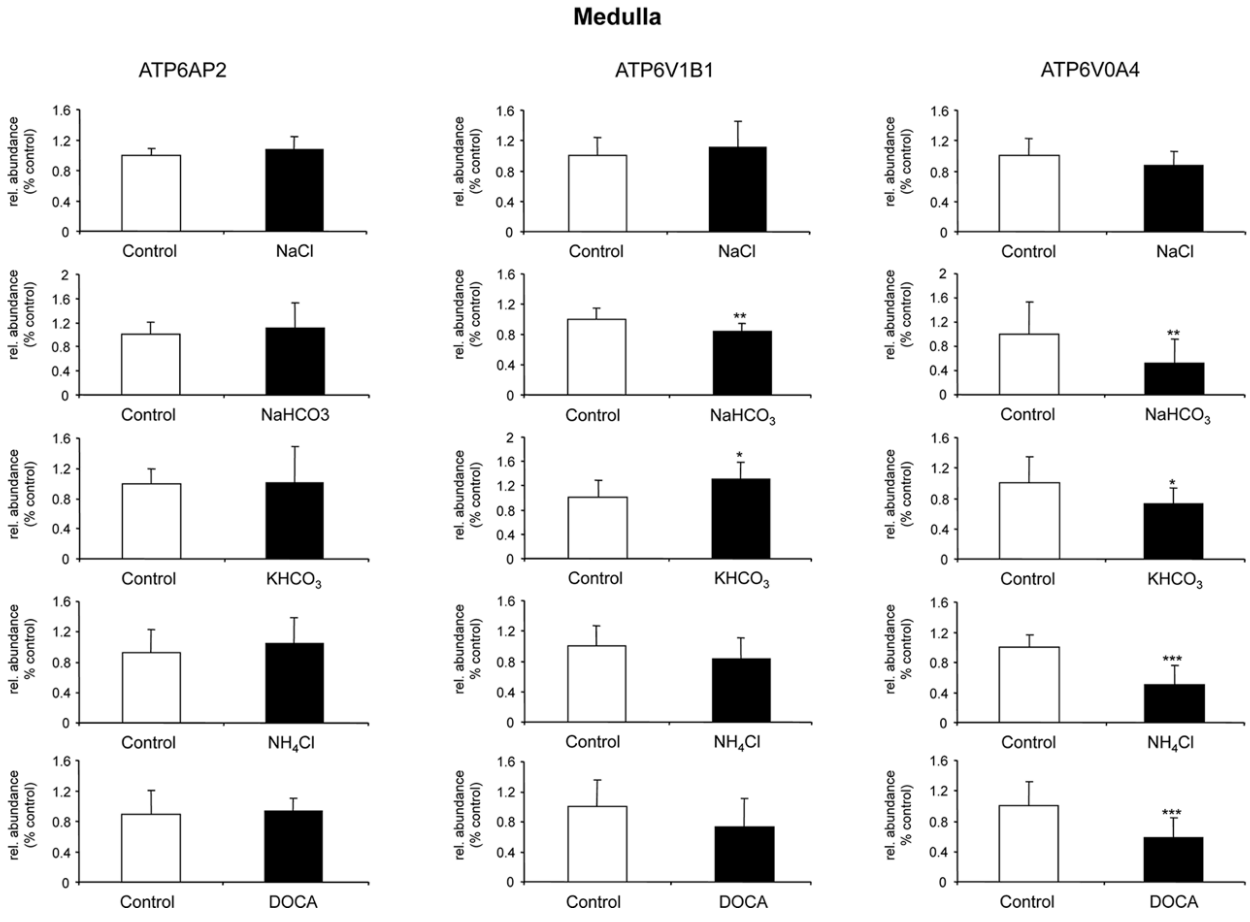
Medulla
ATP6AP2
ATP6V1B1
ATP6V0A4
rel. abundance (% control)
Control
NaCl
NaHCO3
KHCO3
NH4Cl
DOCA

FIGURE 8

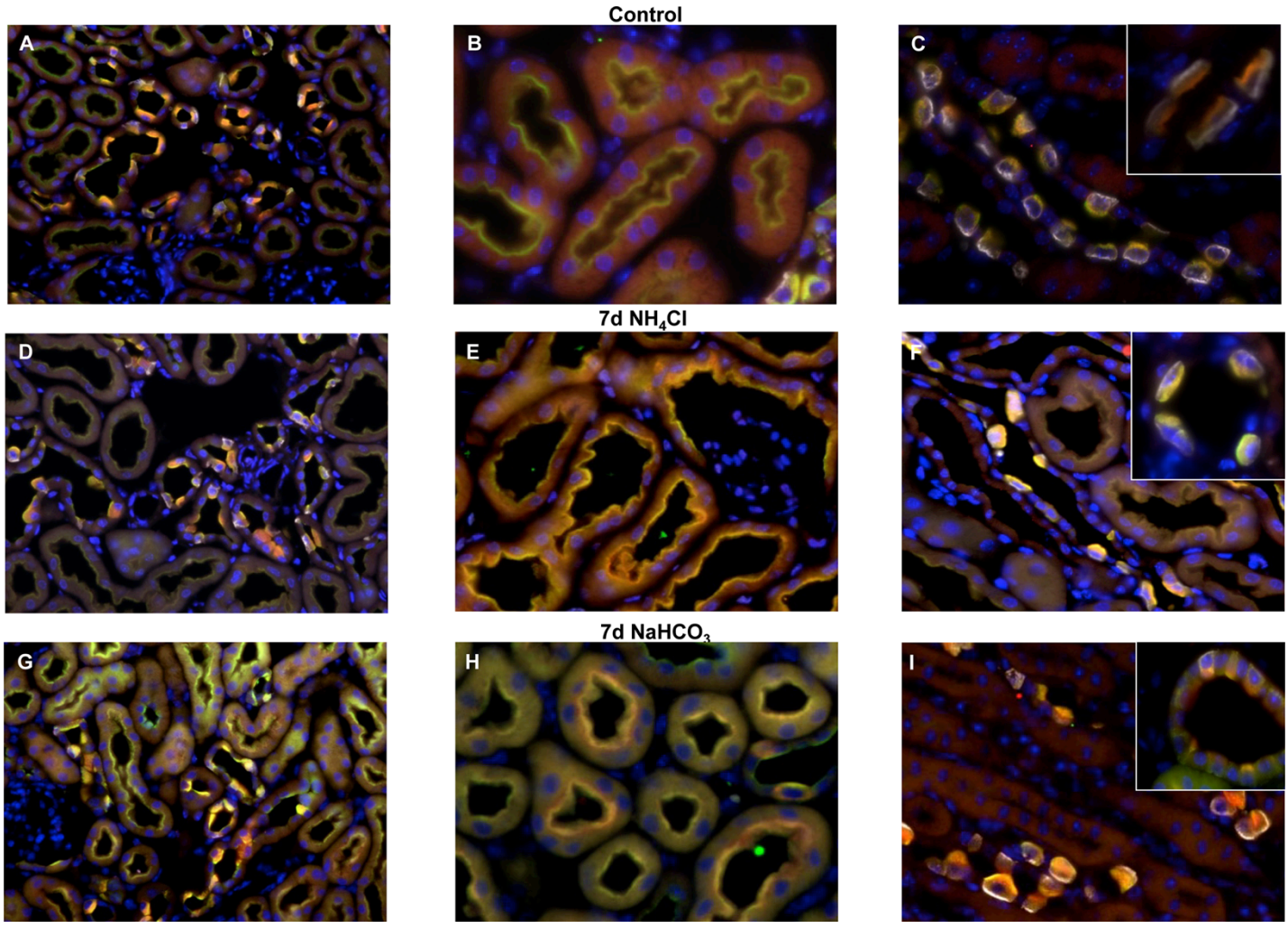

FIGURE 9

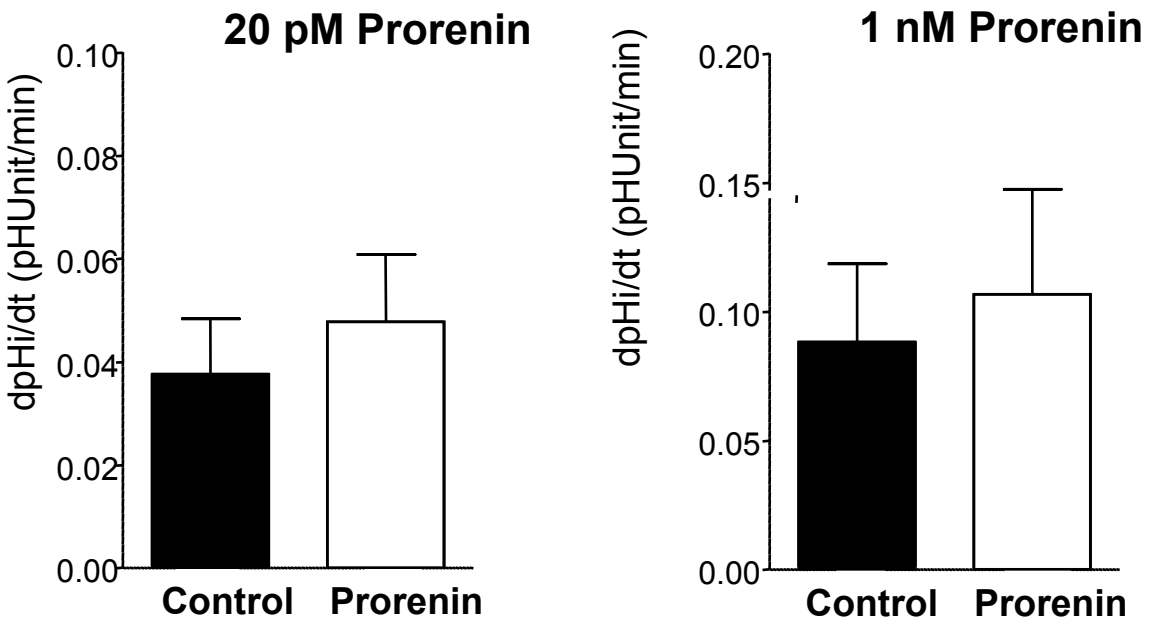
20 pM Prorenin
dpHi/dt (pHUnit/min)
0.10
0.08
0.06
0.04
0.02
0.00
Control
Prorenin
1 nM Prorenin
dpHi/dt (pHUnit/min)
0.20
0.15
0.10
0.05
0.00
Control
Prorenin

FIGURE 10

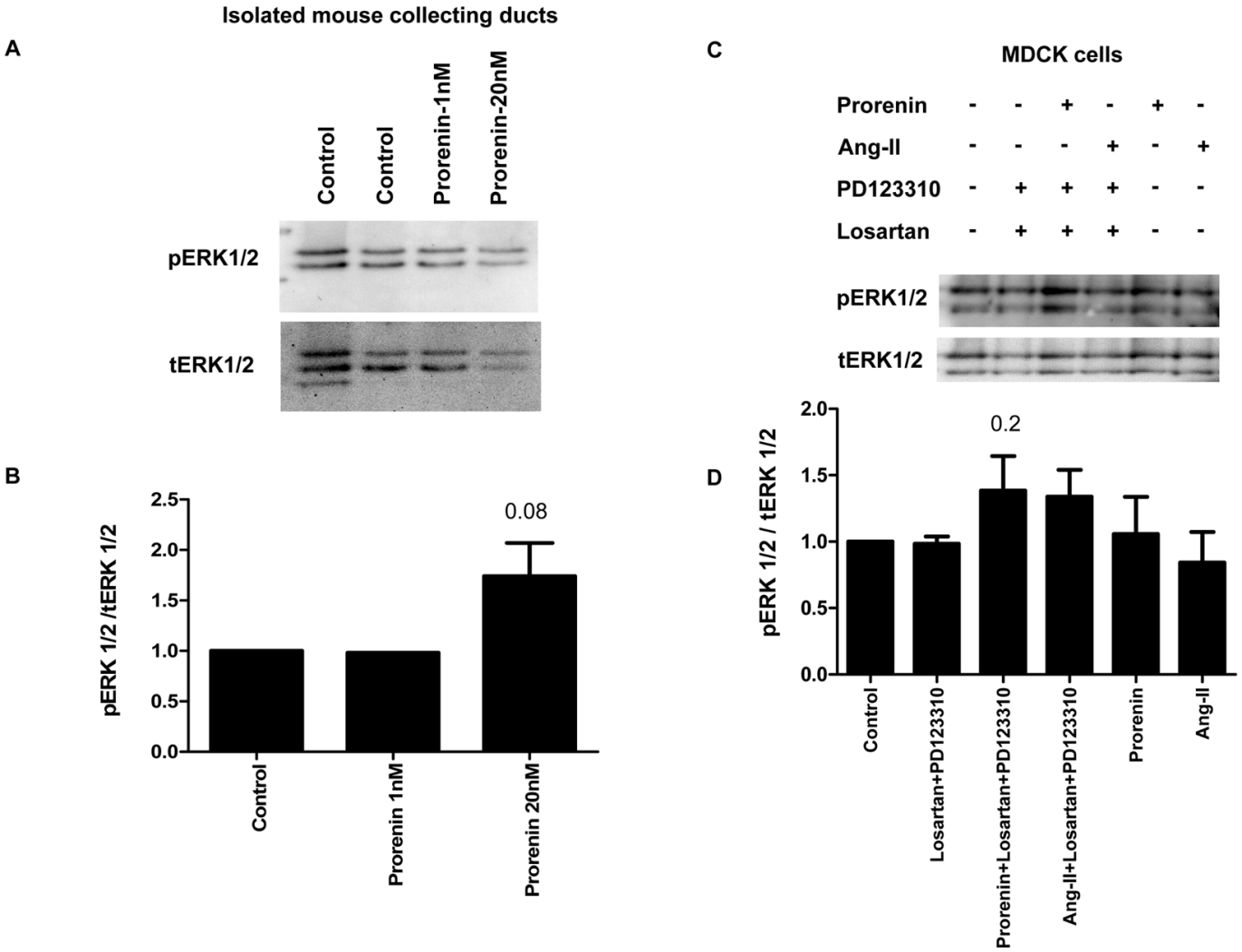
Isolated mouse collecting ducts
A
Control
Control
Prorenin-1nM
Prorenin-20nM
pERK1/2
tERK1/2
B
pERK 1/2 /tERK 1/2
2.5
2.0
1.5
1.0
0.5
0.0
0.08
Control
Prorenin 1nM
Prorenin 20nM
C
MDCK cells
Prorenin - - + - + -
Ang-II - - - + - +
PD123310 - + + + - -
Losartan - + + + - -
pERK1/2
tERK1/2
D
pERK 1/2 / tERK 1/2
2.0
1.5
1.0
0.5
0.0
0.2
Control
Losartan+PD123310
Prorenin+Losartan+PD123310
Ang-II+Losartan+PD123310
Prorenin
Ang-II

Supplementary Table 1: Primer and probe sequences

Forward and reverse primers and probes used for semi-quantitative real-time RT-PCR

	Primer	Fw / Rv	Probe
(P)RR	5' ACG CAG TGG TAG AGT TAG TGA CTG 3'	Fw	5' TCC TTG AGG CAA AAC AAG AGA ACA CCC 3'
	5' AGT TGA AAA CCA CTG AAT ACT CCA A 3'	Rv	
ATP6V1B1	5' AGG ACA GTG TGC AGC GTC AAT 3'	Fw	5' CCC AGT ATG CTG AGA TTG TCA ACT TTA CCC TCC 3'
	5' CCT GAA CAA TGG CCT TGG TC 3'	Rv	
ATP6V0A4	'5' AGC CAA GCA CCA GAA ATC TCA 3'	Fw	'5' CTG CAG TCT TTC ACG ATC CAC GAG GA 3'
	'5' GAG TGG TCA CCC TCC ACA GC 3'	Rv	
NaPi2a	5' TGA TCA CCA GCA TTG CCG 3'	Fw	'5' CCA GAC ACA ACA GAG GCT TCC ACT TCT ATG TC 3'
	5' GTG TTT GCA AGG CTG CCG 3'	Rv	
Podoplanin (Pdpn)	Mm00494716_m1 (Applied Biosystem)		
NCC	5' GGC TTT GCA GAA ACC GTA AGG 3'	Fw	'5' TAC TGC AGG AGT ATG GCA CAC CCA TCG TA 3'
	5' ACA CCG ATG ATG CGG ATG T 3'	Rv	
NKCC2	5' TCA CCA CCG TGG CCT ACA TA 3'	Fw	'5' CTA TTT GCG TAG CCG CCT GTG TGG TC 3'
	5' TTC ATG CTG CCA GTG GCA 3'	Rv	
Pendrin	5' GCC TTT GGG ATA AGC AAC GTC 3'	Fw	5' TGG ATT TTT CTC CTG TTT TGT GGC TAC CAC T 3'
	5' CAA CGA TGG CAA CCA TCA CA 3'	Rv	
AQP2	5' TGG TGC TGT GCA TCT TTG CCT 3'	Fw	5' ACC TCC TTG GGA TCT ATT TCA CCG G 3'
	5' ACT TGC CAG TGA CAA CTG CTG 3'	Rv	
HPRT	5' TTA TCA GAC TGA AGA GCT ACT GTA ATG ATC 3'	Fw	5' TGA GAG ATC ATC TCC ACC AAT AAC TTT TAT GTC CC 3'
	5' TTA CCA GTG TCA ATT ATA TCT TCA ACA ATC 3'	Rv	

Chapter 2: The (pro)renin receptor (ATP6ap2) facilitates receptor-mediated endocytosis and lysosomal function in the renal proximal tubule

Marta F.L. Figueiredo contributions: performed experiments for the figures: 1D-E-F, 2, 3, 4A-B, 5, 6, 7, 8 and supplementary figure 1 and 2 and respective data analysis. She also contributed for the design of the project, and wrote the paper.

The (pro)renin receptor (ATP6ap2) facilitates receptor-mediated endocytosis and lysosomal function in the renal proximal tubule

Marta Figueiredo[1*], Gabin Sihn [2], Dominik N. Müller[2,3],

Elena Popova[2], Anthony Rouselle[2], Genevieve Nguyen[4],

Michael Bader[2,5,6], Carsten A. Wagner[1]

[1] Institute of Physiology, University of Zurich, Switzerland, [2] Max Delbrück Center for Molecular Medicine (MDC), Berlin, Germany, [3] Experimental and Clinical Research Center, a joint cooperation between the Charité Medical Faculty and the Max Delbrück Center for Molecular Medicine, Berlin, Germany,[4] College de France, Paris, France, [5] Charite University Medicine Berlin, Germany, [6] Institute for Biology, University of Lübeck, Germany

Corresponding authors:

Carsten A. Wagner
Institute of Physiology
University of Zurich
Winterthurerstrasse 190
CH-8057 Zurich
Switzerland
Phone: +41-44-63 55023
Fax: +41-44-63 56814
Email: Wagnerca@access.uzh.ch

Michael Bader
Max-Delbrück Center for Molecular Medicine
Robert-Rössle-Str. 10
D-13125 Berlin
Germany
Phone: +49-30-94062193
Phone: +49-30-94062110
Email: mbader@mdc-berlin.de

ABSTRACT

The (Pro) renin receptor (P)RR)/ ATP6ap2 associates with H^+-ATPases which regulate organellar, cellular, and systemic acid-base homeostasis. In kidney, the (P)RR/ATP6ap2 colocalizes with H^+-ATPases in various cell types including the cells of the proximal tubule. There, H^+ ATPases are involved in receptor-mediated endocytosis of low molecular weight proteins via the megalin/cubilin receptors. To study ATP6ap2 function in the proximal tubule, we used an inducible shRNA *Atp6ap2* knockdown rat model (Kd) and an inducible kidney specific *Atp6ap2* knockout mouse model (Flox(P)RRPax8+). Both animal lines showed higher proteinuria with elevated albumin, vitamin D binding protein, and procathepsin D in urine. Endocytosis of an injected fluid phase marker (FITC- dextran, 10 kDa) was normal whereas processing of recombinant transferrin, a marker for receptor mediated endocytosis, to lysosomes was delayed. Furthermore, expression of several proteins including several subunits of the H^+-ATPase and the chloride/proton exchanger ClC-5 involved in receptor-mediated endocytosis was reduced. Expression of megalin and cubilin is not affected in both animal models. Lysosomal integrity and H^+-ATPase function is associated with mTOR signaling. In (P)RR/ATP6ap2 knockout mice the mTOR–p70S6-kinase pathway was downregulated along with increased abundance of the LC3-B subunit of the autophagosome suggesting a more generalized impairment of lysosomal function in the absence of the (P)RR/ATP6ap2. Hence, our data suggests a role for ATP6ap2 for proximal tubule function in the kidney with a defect in receptor-mediated endocytosis in mice and rats.

INTRODUCTION

The (pro)renin receptor ((P)RR) was identified as the receptor for (pro)renin and renin [1-2]. However, (P)RR expression is found also in organisms lacking a renin-angiotensin system suggesting additional functions [1, 3-5] . The (P)RR is an essential adaptor protein in the canonical Wnt signaling pathway [6] and participates also in non-canonical Wnt signaling [7-9] [10-12]. In humans, mutations in (P)RR cause epilepsy and intellectual impairment [13].

The (P)RR has been recognized to be identical to the M8-9 protein, a potential accessory subunit of H^+-ATPases and is thus also known as ATP6ap2 [14]. Additional studies confirmed protein-protein interactions between the (P)RR and H^+-ATPases [15].

H^+-ATPases, are multi-subunit complexes that mediate the transport of protons driven by hydrolysis of ATP. H^+-ATPases are composed of a membrane bound V_0 domain and a cytoplasmic V_1 domain. Its location is mainly in intracellular organelles like endosome, lysosomes, golgi membrane and secretory vesicles but it can also be found in the plasma membrane in organs like kidney, epididymis, and bone [16-17]. H^+-ATPase are fundamental for acidification of late endosomes and lysosomes allowing membrane trafficking, protein degradation, and protein maturation [16, 18-19] . The (P)RR shares H^+-ATPase location in the plasma membrane of renal and other cells [20-23] but also in intracellular organelles [24]. The importance of H^+-ATPases in endocytosis was further confirmed in studies in mice lacking the V_0 domain H^+-ATPase a4 subunit in the kidney [25-26]. These animals presented a generalized impairment of proximal tubule functions with glycosuria, phosphaturia and lysosomal defects. Similarly, humans and mice with mutations or loss of the ClC-5 chloride/proton exchanger, critical for lysosomal acidification and thought to work in tandem with endosomal and lysosomal H^+-ATPases, show impaired endocytosis and lysosomal function [27-29]. Also in

other organs, H^+-ATPase mediated acidification of lysosomes and autophagosomes is critical for their function [30].

The (P)RR/ATP6ap2 has been also linked to endocytosis in mouse and drosophila models. Conditional knockout mice for (P)RR in podocytes and cardiomyocytes exhibit accumulation of autophagic vesicles suggesting lysosomal defects [23, 31]. In addition, embryonic fibroblast and podocyte cells in which (P)RR was deleted showed a down-regulation of several V_0 H^+-ATPase subunits [22]. In drosophila, deletion of (P)RR impaired Wnt signaling by reducing endosomal recycling of frizzled-related receptors, and reduced fluid-phase endocytosis, both functions linked to reduced H^+-ATPase activity [8].

The kidney proximal tubule is among the most active endocytic tissues reabsorbing a large variety of proteins, small peptides, and peptidomimetic drugs via receptor-mediated and fluid-phase endocytosis [32]. Receptor-mediated endocytosis requires the presence and function of the endocytic receptors megalin and cubilin expressed in the brush border membrane and endocytic apparatus. Moreover, efficient acidification of the endocytic pathway is critical for recycling and processing of proteins, activation of lysosomal enzymes and transporters, and lysosomal signaling via the mammalian target of rapamycin (mTOR) pathway [33-35] . Several of these processes have been shown to be H^+-ATPase dependent [18, 36] .

To date, the role of (P)RR/ATP6ap2 in the proximal tubule has not been elucidated. Here, we investigated (P)RR/ATP6ap2 function in proximal tubule using two different animal models. A rat model with an inducible shRNA for *Atp6ap2* and an inducible kidney epithelial cell-specific knockout mouse for (P)RR/ATP6ap2. We report that (P)RR/ATP6ap2 plays a role in cargo reabsorption and processing via receptor mediated endocytosis, hence, contributing to kidney proximal tubule function.

RESULTS

Knock-down of (P)RR/Atp6ap2 in rats

Transgenic rats (Sh rats) expressing an shRNA against the (P)RR/ *Atp6ap2* were generated by inserting a transgene under the control of tetracycline repressor protein (TetR) allowing the controlled activation of the shRNA by doxycycline treatment (Figure 1A). Integration of the transgene and expression of the TetR mRNA and protein was confirmed by PCR (Figure 1B) and immunoblotting (Figure 1C). We could detect TetR protein in all organs tested. Expression of (P)RR/*Atp6ap2* protein and mRNA were studied in more detail in the kidney from animals 10 days after doxycycline treatment. RT-qPCR for *Atp6ap2* mRNA in whole kidney showed a decrease by approx. 90 % of the transcript in Sh rats when compared with control rats (Wt) (Figure 1D). Similarly, immunohistochemistry on kidney sections stained for the (P)RR/ATP6ap2 and the H^+-ATPase subunit a4 (Figure 1E) demonstrated greatly reduced or absent (P)RR/ATP6ap2 related staining in proximal tubule and intercalated cells. H^+-ATPase subunit a4 staining was used as a positive control, since both proteins share the same localization in the kidney [21]. Thus, *Atp6ap2* shRNA rats present with an efficient knock-down of *Atp6ap2*/(P)RR mRNA and protein in kidney.

At the level of light microscopy, similar overall renal morphology was seen in Wt and Sh rats (Figure 1F). However, in Sh rat kidneys, we could observe some areas containing vacuoles, suggesting degeneration of some nephrons. Such areas were less seen in Wt kidneys. The gross morphology of glomeruli was undistinguishable between Wt and Sh rats unlike in mice with podocyte specific deletion of the (P)RR/ATP6ap2 [23, 31].

Body weight, food and water intake, were not different in Wt and Sh rats 10 days after doxycycline treatment. Urine and blood analysis revealed normal electrolytes and pH. BUN and blood phosphate levels were elevated in Sh rats whereas creatinine clearance decreased consistent with a mild impairment of renal function. In urine, sodium levels were lower while

phosphate and creatinine excretion was increased in Sh rats (Supplementary table 1).

(P)RR/ATP6ap2 knock-down impairs proximal tubule receptor-mediated endocytosis

Sh rats exhibited mild albuminuria and low molecular weight proteinuria as indicated by elevated vitamin D binding protein (VDBP) in urine (Figure 2A,B). To further determine which endocytic pathway may be impaired, we coinjected in both animal groups a marker for fluid endocytosis (dextran-FITC, 10 kDa) and a marker for receptor-mediated endocytosis (human transferrin) and fixed kidneys for immunohistochemistry 10 and 40 min. after injection. Dextran-FITC was co-stained with phalloidin (marker for the brush border membrane) to allow subcellular determination of dextran localization. By immunohistochemistry, no differences were observed in FITC intensity or subcellular localization between animal groups at 10 min. In addition, the relative amount of FITC in kidney tissue at 10 min. was similar between animal groups (Figure 2D). Dextran-FITC at 40 min. was also analyzed (Supplementary figure 1) and staining intensity was weaker than at 10 min. but showed similar subcellular localization in both genotypes. Thus, fluid-phase endocytosis is not affected by (P)RR/AT6ap2 knock-down.

In contrast, endocytosis of human transferrin was altered in Sh rats compared to Wt animals. We used antibodies recognizing human but not endogenous rat or mouse transferrin and detected a weaker transferrin related staining in kidneys from Sh rats 10 min. after injection whereas 40 min. after injection more pronounced staining was found in Sh rat kidneys than in Wt kidneys (Figure 2E). At 10 min. transferrin was localized in the subapical region and presented as a punctuated pattern as expected [37]. Immunoblotting for human transferrin in urine samples collected 10 min. after transferrin injection showed abundant transferrin in urine from Sh rats but very low levels in Wt urine suggesting reduced uptake (Figure 2F). Forty min. after injection, in Wt rats transferrin staining was almost absent while in the Sh rats transferrin staining accumulated in the perinuclear region (Figure 2E).

The localization of the two major endocytic receptors megalin and cubilin was similar in both genotypes at light microscopy level (Figure 2E and supplementary figure 2). The relative amount of megalin protein was unchanged whereas cubilin was more abundant in kidneys from Sh rats (Figure 3).

(P)RR was suggested to be an accessory subunit of H^+-ATPases [1, 14, 38] therefore a loss of (P)RR/ATP6ap2 could affect H^+-ATPase regulation and/or function in the endocytic pathway. Immunoblotting showed reduced a4 H^+-ATPase (ATP6V0a4) subunit whereas B2 (ATP6V1B2) and A (ATP6V1A) subunits were unaltered (Figure 3). The ClC5 chloride/proton exchanger involved in endocytic and lysosomal acidification in the proximal tubule was upregulated [28-29, 39-40].

The abundance of NaPi-IIa, the main phosphate transporter in the proximal tubule, and NHE3 (sodium-proton exchanger 3) is directly or indirectly affected by alterations in the endocytic apparatus of the proximal tubule [41-43] NaPi-IIa showed no differences in abundance and NHE3 a slight increase in expression, however, not reaching significance due to high interindividual variability (Figure 3).

Kidney-epithelial cell specific (P)RR/ATP6ap2 KO mice

Since *Atp6ap2* shRNA rats present with a full body knock-down of the (P)RR/ATP6p2 that may impact on overall renal function and that complicates interpretation of data, we decided to examine proximal tubular endocytosis in a kidney-epithelial cell specific inducible (P)RR/ATP6ap2 knock-out (KO) mouse model using the well described doxycycline-inducible Pax8-Cre system after crossing with floxed (P)RR/ATP6ap2 mice. We used a milder induction protocol for Cre activity [44] as usual based on previous experience suggesting that higher doses of doxycyline can also produce effects in wildtype mice and with the intention to downregulate (P)RR/ATP6ap2 mostly in proximal tubules without producing the strong phenotype caused by deletion of (P)RR/ATP6ap2 in the collecting duct [45-47]. To verify kidney-specific (P)RR/ATP6ap2 deletion, we performed RT-qPCR for *Atp6ap2* in the

kidney, lung and heart (Figure 4A). *Atp6ap2* was downregulated only in kidneys from Flox/Pax8+ mice but not in other organs or kidneys from control Wt/Pax8+ mice. Western blotting using total kidney protein homogenate confirmed reduction of (P)RR/ATP6ap2 protein expression by about 75 % (Figure 4B). Residual mRNA and protein expression may be due to expression in renal cells negative for Pax8 (i.e. podocytes) or incomplete deletion in epithelial cells. Immunohistochemistry using three different antibodies against the (P)RR/ATP6ap2 demonstrated almost complete deletion of the (P)RR/ATP6ap2 from proximal tubules but widely preserved staining in intercalated cells of the connecting tubule and medullary collecting ducts (Figure 4C and supplementary figures 3 and 4).

Flox/Pax8+ mice had normal blood acid-base and electrolyte status and no evidence for reduced kidney function unlike rats. Urine analysis showed higher diuresis and mild sodium and potassium losses with reduced urinary calcium excretion consistent with the deletion of the (P)RR/ATP6ap2 mostly from proximal tubules (Supplementary table 2).

(P)RR/ATP6ap2 deletion in proximal tubule causes a defect in receptor-mediated endocytosis

Like the rat model, Flox/Pax8Cre+ mice had albuminuria and low molecular weight proteinuria loosing VDBP and procathepsin B with urine (Figure 5). Coinjection of the endocytic markers dextran-FITC (10 kDa) and human transferrin confirmed that deletion of the (P)RR/ATP6ap2 affects the receptor mediated endocytosis pathway (Figure 6). Dextran-FITC localization and intensity of staining was similar between animals groups at two time points (10 and 40 min. after injection). Human transferrin staining was similar between genotypes 10 min. after injection but showed, like in Sh rats, delayed clearance of transferrin in Flox/Pax8+ mice 40 min. after injection with perinuclear accumulation (Figure 6B). Costaining of human transferrin with Lamp1, a lysosomal marker, in kidneys 40 min. after injection (Figure 6C), revealed that in (P)RR/ATP6ap2 deficient animals human transferrin did not overlap with Lamp-1 stained lysosomes suggesting delayed transferrin processing (Figure 6C).

Western blotting demonstrated reduced expression of the a4 (ATP6V0a4) and EII (ATP6V1EII) H^+-ATPase subunits whereas the a2 (ATP6V0a2) and A (ATP6V1A) subunits showed a strong trend to be lowered. ATP6V1B2 protein abundance was unaltered. Megalin, cubilin and NHE3 abundance was not altered but ClC5 expression was strongly reduced (Figure 7).

mTOR signaling is linked to lysosomal function [36, 48-49] . Vice versa, inhibition of mTOR by rapamycin in mice caused megalin downregulation and proteinuria through a H^+-ATPase dependent mechanism [50]. In Flox/Pax8+ kidneys total mTOR amount was reduced (Figure 8) while phospho mTOR showed a trend for reduction. Importantly the down-stream effector p70 S6K showed no difference for total abundance but had reduced levels of activated phosphorylated p70 S6K consistent with reduced activity of the mTOR pathway (Figure 8).

mTOR signaling as well as (P)RR/ ATP6ap2 are linked to autophagy [23, 51-52]. Staining for the microtubule-associated protein 1A/1B-light chain 3 or LC3-B, a subunit of the autophagosome showed accumulation of LC3-B in proximal tubules from (P)RR/ATP6ap2 deficient mice but not in wild type controls (Figure 9).

DISCUSSION

In this study, we revealed that (P)RR/ATP6ap2 plays a role in receptor-mediated endocytosis and lysosomal function in the proximal tubule. Both *ATP6ap2*-Sh rats and Flox(P)RR/Pax8Cre+ mice showed excretion of albumin and low molecular weight proteins in urine, delayed processing of substrates of the receptor-mediated endocytosis pathway, reduced expression of other key molecules involved in this process as well as downregulation of the mTOR pathway and accumulation of the LC3-B subunit of the autophagosome. All these changes are consistent with impaired lysosome function and reduced activity of the receptor-mediated endocytosis pathway.

We used two rodent models to demonstrate a role of the (P)RR/ATP6ap2 in proximal tubule endocytosis of low molecular weight proteins and lysosomal function. Both models yield similar results as discussed below in more detail. The mouse model used is similar to previously published models with a more severe renal defect including an urinary concentration defect, salt loss, and distal renal tubular acidosis [45-47]. A major difference between these models our model is that we used a milder protocol [44] to induce Cre activity and deletion of the (P)RR/ATP6ap2 which resulted only in an almost complete deletion in the proximal tubule but with well preserved expression in the collecting duct thereby circumventing a more severe renal damage and phenotype allowing to focus on proximal tubule functions.

(P)RR/ATP6ap2 associates with H^+-ATPases [6, 14-15, 53]. We and others had shown that the (P)RR/ATP6ap2 is expressed in the renal proximal tubule and colocalizes with H^+-ATPases in this nephron segments and others [21, 54-55]. H^+-ATPases contribute to several functions of the proximal tubule such as reabsorption of bicarbonate, trafficking and recycling of membrane proteins, or endocytosis of proteins from urine, acidification of vesicles along the endocytic pathway and lysosomes processing or degrading absorbed substrates.

Several lines of evidence suggest that the (P)RR/ATP6ap2 modulates H^+-ATPase function in the proximal tubule and thereby contributes to receptor-mediated endocytosis and lysosomal function. However, our data do not support a role of the (P)RR/ATP6ap2 in fluid–phase mediated endocytosis as suggested by data from Drosophila [8] or other generalized functions of the proximal tubule. Urine analysis and immunoblotting showed no generalized Fanconi-syndrome like loss of function as indicated by the absence of glucosuria, massive proteinuria or changes in urine and blood pH. Both, Sh rats with reduced (P)RR/ATP6ap2 as well as (P)RR/ATP6ap2 KO mice, showed albuminuria in combination with the presence of low molecular weight proteins such as the vitamin D binding protein (VDBP) or procathepsin in urine indicative of reduced proximal tubular protein absorption. In case of the Sh rats, we cannot exclude also increased filtration of albumin as in these animals (P)RR/ATP6ap2 expression in podocytes may be reduced and podocyte specific deletion of (P)RR/ATP6ap2 causes massive proteinuria and glomerular damage [23, 31]. Therefore, we created mice with deletion of the (P)RR/ATP6ap2 in the epithelial cells along the nephron with intact expression of the protein in podocytes and found similar urinary excretion of albumin, VDBP and procathepsin. Absorption of these proteins depends on the initial recognition by and binding to the multispecific receptors megalin and cubilin present in the brush border membrane [32]. Deletion of the (P)RR/ATP6ap2 did not alter overall abundance of these receptors and affected also not their localization at the level of light microscopy. Proteins bound to these receptors are then internalized in a receptor-ligand complex and further processed through early endosomes to late endosomes and lysosomes. In our experiments, four different ligands of these receptors were further investigated: albumin and VDBP which are internalized by both megalin and cubilin, procathepsin B which is preferentially absorbed by megalin and transferrin a preferred substrate for cubilin [32]. All four proteins were found at elevated levels in urine suggesting a defect common to both receptors. More detailed analysis of transferrin internalization showed that transferrin is taken up from urine, albeit at somewhat lower rates (as indicated by higher urinary excretion after injection of transferrin) and that processing of transferrin to lysosomes is delayed as suggested by accumulation of

transferrin 40 min. after injection and much reduced colocalization of injected transferrin with a lysosomal marker at this later time point.

The delayed processing of endocytic substrates is most likely due to a reduced capacity of endocytic and lysosomal vesicles to acidify. A role of the (P)RR/ATP6ap2 in endosomal acidification has been described in Xenopus frog embryos and linked to reduced H^+-ATPase activity [6]. Consistently, we found decreased expression of several H^+-ATPase subunits including the a4 subunit (ATP6V0a4) in Sh rats and KO mice as well as the EII (ATP6V1EII) subunit in the KO mice. Similarly, ablation of the (P)RR/ATP6ap2 in embryonic cardiomyocytes reduced expression of several subunits of the V_0 domain of the H^+-ATPase and impaired lysosomal acidification [22]. In mice, deletion of ATP6V0a4 causes proximal tubular dysfunction and reduced receptor-mediated endocytosis with impaired lysosomal function consistent with an important role of H^+-ATPases in these processes [26]. Whether the lower expression of the a4 subunit in the (P)RR/ATP6ap2 deficient rodent models is the consequence of absent (P)RR/ATP6ap2 function and/or directly causes the endocytic and lysosomal defect remains unclear at this point. Moreover, reduced levels of the chloride/proton exchanger ClC-5 were found in (P)RR/ATP6ap2 KO mice. ClC-5 mutations cause Dent's disease which features also reduced receptor-mediated endocytosis and lysosomal defects in the proximal tubule due to a reduced capacity to acidify endosomes and lysosomes and reduced expression of the endocytic receptors megalin and cubilin [28-29, 56-59]. In contrast, in the Sh rat model ClC-5 expression was upregulated. Thus, the endocytic defect exists also in the presence of elevated ClC-5 levels suggesting that the reduction of ClC-5 expression is rather the consequence of the defect than the cause. The reasons for the difference in ClC-5 expression between the two rodent models may be due to species differences or due to deletion of (P)RR/ATP6ap2 from podocytes and a mild glomerular phenotype in the Sh rats.

Defects in lysosomal acidification due to reduced or absent H^+-ATPase function can cause altered mTOR signaling and activation of the autophagosome as in X-linked autophagic myopathy due to mutations in the

VMA21 protein required for lysosomal H^+-ATPase assembly [60] or in podocytes with specific deletion of the (P)RR/ATP6ap2 and impaired lysosomal function [23, 31]. Fusion of lysosomes and autophagosomes occurs independently from lysosomal acidification but requires H^+-ATPases [61]. Lysosomes act as signaling platforms associating with the mTOR complex 1 and H^+-ATPase function is required for mTORC1 signaling whereas in turn mTOR signaling regulates H^+-ATPase expression [62-63]. mTOR is also a regulator of autophagosome function and autophagosome-lysosomal fusion and reduced mTOR signaling impairs autophagosome-lysosome fusion [64-65]. Thus, deletion of the (P)RR/ATP6ap2 may impair H^+-ATPase assembly and function, thereby decreasing endosomal and lysosomal acidification as well as mTOR signaling. Consequently, lysosome-autophagosome fusion may be decreased due to H^+-ATPase dependent but acidification independent as well as mTOR dependent mechanisms. Of note, increased levels of the (P)RR/ATP6ap2 in a podocyte cell line enhance mTOR signaling and reduce autophagosome expression and activity [66].

In summary, genetic deletion of the (P)RR/ATP6ap2 from the proximal tubule in rats and mice causes albuminuria and low molecular weight proteinuria paralleled by reduced expression of several H^+-ATPase subunits and delayed processing of substrates of receptor mediated endocytosis to lysosomes. Lysosomal dysfunction is suggested by altered mTOR signaling and accumulation of the LC3-B subunit of the autophagosome. Thus, the (P)RR/ATPap2 facilitates receptor-mediated endocytosis in the proximal tubule possibly by modulating H^+-ATPases.

METHODS

Animals

Generation and breeding of transgenic Atp6ap2 shRNA rats

Transgenic rats were generated as described previously [67]. Briefly, complementary sense and antisense oligonucleotides (r*Atp6ap2*sh3: 5'- TCC CCC TAC AAC CTT GCG TAT AAT TCA AGA GAT TAT ACG CAA GGT TGT AGG TTT TTT A -3' and r*Atp6ap2*sh4: 5'- CGC GTA AAA AAC CTA CAA CCT TGC GTA TAA TCT CTT GAA TTA TAC GCA AGG TTG TAG G -3') specifically targeting a sequence in the exon 9 of the rat (P)RR/*Atp6ap2* mRNA, were annealed and cloned into the bimodal pINV7 vector (Taconic) using the BbsI and MluI restriction sites.

To generate transgenic rats, a 4 kb DNA fragment containing pTet-shAtp6ap2 (Figure 1A) was cut out with the PacI and KpnI restriction enzymes, purified from the gel using a Wizard® SV Gel and PCR Clean-Up System (Promega), dissolved at 3 ng/µl with microinjection buffer (8 mM Tris-HCl, pH 7.4 and 0.15 mM EDTA) and microinjected into fertilized oocytes of Sprague-Dawley (SD) rats according to established techniques [68]. Integration of the transgene was detected by PCR in genomic DNA isolated from tail biopsies with the primers TetOfw: 5' -TGC ATG TCG CTA TGT GTT CT -3' and CAGGSrv: 5′- TGG CGT TAC TAT GGG AAC AT -3′. Using one positive newborn, the transgenic line Sh*Atp6ap2* was then established on the SD background. Negative littermates were used as wild type (Wt) controls.

Rats were maintained in individually ventilated cages under standardized, pathogen-free conditions (at a temperature of 21 ± 2°C, humidity of 65 ± 5% and with an artificial 12 h light/dark cycle) with free access to standard chow (0.25% sodium; SSNIFF) and drinking water *ad libitum*. All animal care and experiments were performed in accordance with the institutional guidelines of German Federal Law and local authorities of Berlin (LaGeSo).

Doxycycline treatment of rats in vivo

To induce expression of shRNA against (P)RR/ATP6ap2, animals were treated with 0.5 g/l doxycycline (Sigma) in the drinking water for 8 days. The doxycycline water was freshly prepared each day and kept dark due to the light sensitivity. To confirm the functionality of the system, (P)RR/ATP6ap2 protein and RNA levels were analyzed in organs by western blot and real time PCR, respectively.

Western blotting to confirm shAtp6ap2 rats

Rats were anaesthetized with isofluorane followed by exsanguination. Tissues were collected, snap frozen in liquid nitrogen, coarsely ground using a mortar and pestle, and further homogenized in RIPA buffer (Cell Signaling) for protein extraction, using a FastPrep™-24 (MP Biomedicals) according to the manufacturers' instructions. Total proteins were added to 4x Roti®-load buffer (Carl Roth) and separated by 12% SDS/PAGE. Proteins were then blotted on a PVDF membrane (Amersham Biosciences), which was subsequently blocked with Odyssey® Blocking Buffer and incubated with the following primary antibodies: mouse anti-TetR (1:8000, MoBiTec) and rabbit anti-GAPDH (1:1000, Cell Signaling). Protein revelation was performed with an Odyssey® Infrared imaging system (LI-COR Biosciences) using IRdye® 800-coupled secondary antibodies (1:10000, LI-COR Biosciences).

Kidney-epithelial cell specific (P)RR/ATP6ap2 KO mice generation

The generation and genotype of (P)RR/ATP6ap2$^{flox/y}$ has been already described [23]. Heterozygous (P)RR/ATP6ap2 $^{flox/x}$ females were crossed with males both positive for Pax8-rtTA and Cre [44, 69]. Expression of Cre-recombinase was induced in male (P)RR/ATP6ap2$^{flox/y,Pax8Cre+}$ and (P)RR/ATP6ap2$^{+/+,Pax8Cre+}$ transgenic mice by 0.5 mg/ml of doxycycline (Sigma) in drinking water containing 2% of Sucrose (Sigma) for 5 days followed by 5 days induction with 0.25 mg/ml Doxycycline in 2% sucrose drinking water and 4 days without doxycycline [44]. Animals used for experiments were 2 to 3 months old male mice bred in a C57BL/6 background. All animal studies were performed according to Swiss welfare laws and with approval of the local veterinary authorities.

Plasma and urine analysis

Blood was collected from the tail vein of anesthetized rats and vena cava from anesthetized mice. Heparinized blood was centrifuged at 7000 rpm for 7 min., plasma collected, and rapidly frozen. Measurements of blood pH, and blood electrolyte concentrations (Na^+, K^+, Cl^-, Ca^{2+}) were analyzed using an ABL80 FLEX CO-OX (Radiometer, Copenhagen) and performed on heparinized tail vein blood. Urine was collected under mineral oil for 24 hours in metabolic cages (Tecniplast®, Italy) and aliquots were rapidly frozen and stored at -80°C until measurement. Urine and plasma laboratory analyses were performed in the Zurich Integrative Rodent Physiology (ZIRP) core facility.

RNA extraction and RT-qPCR

Harvested organs were snap frozen in liquid nitrogen. Total RNA was extracted using the Qiagen RNeasy Mini Kit (Qiagen, Hombrechtikon, Switzerland). Snap-frozen tissue slices were homogenized in a pestle homogenizer (Potter-Elvehjem type) together with 1 ml precooled RLT-Buffer supplemented with β-mercaptoethanol at a final concentration of 1 %. Subsequently, 350 µl of the homogenate were used for RNA preparation carried out according to the manufacturer's instructions. DNAse digestion was performed using the RNase-free DNAase Set (Qiagen; Hilden, Germany). Total RNA extractions were analysed for quality, purity, and concentration using the NanoDrop ND-1000 spectrophotometer (Wilmington, DE, USA). RNA samples were diluted to a final concentration of 100 ng/µl and cDNA was prepared using the TaqMan Reverse Transcriptase Reagent Kit (Applied Biosystems, Roche; Forster City, CA, USA). In brief, in a reaction volume of 40 µl, 300 ng of RNA was used as template and mixed with the following final concentrations of RT buffer (1x), $MgCl_2$ (5.5 mM), random hexamers (2.5 µM), dNTP mix (500 µM each), RNase inhibitor (0.4 U/µl), multiscribe reverse transcriptase (1.25 U/µl) and RNAse-free water. Reverse transcription was performed with thermocycling conditions set at 25°C for 10 min., 48°C for 30 min., and 95°C for 5 min. on a thermocyler (Biometra, Goettingen, Germany).

Semi-quantitative real-time PCR (RT-qPCR) was performed on the ABI PRISM 7700 Sequence Detection System (Applied Biosystems). Primers for Atp6ap2 were designed using Primer Express software from Applied Biosystems and purchased from Microsynth, Switzerland. Probes were labelled with the reporter dye FAM at the 5'-end and the quencher dye TAMRA at the 3'-end (Microsynth, Balgach, Switzerland).

For *mus musculus* RT-qPCR, the following pair of primers for *Atp6ap2* were used forward 5'-GTGCTGGTCGTTCTCCTGTTC- 3'; reverse 5'-GGGATTCGATCTCCTGGTATAG- 3' together with a probe 5'GTGGCGGGTGCTTTAGGGAATGAAT- 3' which target only *Atp6ap2* exon 2. For *rattus norvegicus Atp6ap2* RT-qPCR we used: forward 5'-TCGGATCCTTGTTGATGCTCTC -3'; reverse 5'-CTCACCAGGGATGTGTCGAA- 3' primers and 5'-TGGGAATGCAGTGGTAGAGTTGGTGA -3' as probe. Real-Time PCR reactions were performed using TaqMan Universal PCR Master Mix (Applied Biosystems) as described in the manufacturer's user manual.

Protein extraction and immunoblotting

Crude membrane and cytosolic proteins were extracted from half a kidney. Briefly, organs were homogenized in 200 μl of ice cold resuspension buffer (200 mM Mannitol, 80 mM HEPES, 41 mM KOH, pH 7.5 supplemented with 1 tablet/10 ml Complete Mini Protease Inhibitor Cocktail, Roche) using a Polytron homogenizer (0.5 mm diameter at 20'000 rpm for 1 minute at 4°C). The homogenate centrifuged at 2'000 rpm for 20 min. at 4°C. The resulting supernatant was further centrifuged at 41'000 rpm for 1 hour at 4°C. Brush border membrane protein preparation was performed according to the Mg^{2+} precipitation procedure [70].

Tissue and urine samples were normalized for protein or creatinine levels, respectively, diluted in Laemmli buffer, heated at 95° for 5 min. and separated by SDS-polyacrylamide gels electrophoresis on 8-12 % gels. For immunoblotting, proteins were transferred to polyvinylidene fluoride membranes (Immobilon-P, Millipore, Bedford, MA, USA). After blocking with 5 % milk powder in Tris-buffered saline/0.1 % Tween-20 for 30 min., blots were

incubated with the primary antibodies: rabbit anti-ATP6V0a4 serum (1:1000) [71], rabbit anti-ATP6V0a2 (a kind gift of Dr. X. S. Xie, Dallas, TX, USA) [72-73], rabbit anti-ATP6V1B2 serum (1:5000 raised against the sequence EFYPRDSAKH, Pineda Berlin, Germany), mouse monoclonal anti-ATP6V1E2 (1:1000, a kind gift of Dr. S. L Gluck, University of California, San Francisco, CA,USA) [74], rabbit anti-ClC-5 serum (1:1000, a kind gift from Dr. Olivier Devuyst, University of Zurich) [75], rabbit polyclonal anti-NaPi-IIa (1:5000) [76], sheep anti-Megalin (1:10.000, a kind gift from Dr. Olivier Devuyst, University of Zurich, Switzerland) [29], rabbit anti-cubilin (1:1000, a kind gift from Dr. Erik Ilsø Christensen, Aarhus University, Denmark), rabbit anti-VDBP (1:2500, Dako, A0021), rabbit-human transferrin (1:2000, Dako, A0061), rabbit anti-NHE3 (1:1000,StressMarq,SPC-400D), rabbit anti-(P)RR (1:500,Sigma, HPA003156), rabbit anti-mTOR (1:1000, #2972, Cell Signaling Technology, Boston, MA, USA), rabbit anti-phospho-mTOR (1:1000, #2974, Cell Signaling Technology, Boston, MA, USA), rabbit anti-p70 S6K (1:1000, #2708, Cell Signaling Technology, Boston, MA, USA), mouse anti-phospho-p70 S6K (1:1000, #9206, Cell Signaling Technology, Boston, MA, USA), and mouse monoclonal anti-β-actin antibody (1:5000, A5441, Sigma,), either for 2h at room temperature or overnight at 4°C. Membranes were then incubated for 1h at room temperature with secondary anti-rabbit or ant-mouse antibodies linked to alkaline phosphatase (1:10'000, S373B, S372B, Promega, USA), or anti-sheep-antibodies coupled to HRP (1:20'000, Dako, P0163), or anti-mouse-HRP (1:20'000, W402B, Promega, USA). The protein signal was detected with the appropriate substrates using the LAS 4000 (Fujifilm) detection system. All images were analyzed using the software Quantity One 4.6.1 (Biorad) to calculate the protein of interest/β-actin ratio.

Immunofluorescence staining

Mouse and rat kidneys were perfused in situ through the left heart ventricle with a solution containing 10'000 IU Heparin-Na Solution (B. Braun Medical AG, Sempach, Switzerland), 2 ml Lidocain 1 % (Streuli Pharma AG, Uznach, Switzerland), 2 ml $CaCl_2$, 16 %, 2 ml 0.9 % NaCl, and 2 ml distilled

water. Subsequently, animals were perfused with 3 % paraformaldehyde in phosphate buffered saline (PBS). Fixed kidneys were cryoprotected with 2.3 M sucrose (Sigma), embedded in TissueTec OCT compound 4583 (Sakura Finetek USA, Torrance, CA), and frozen in liquid nitrogen and stored at -80°C. Kidney cryosections were cut with 5 µm thickness on a Leica CM3050S cryostat (Leica Microsystems, Bannockburn, IL). Slides were rehydrated in PBS and treated either with 10 mM Tris (Trizma Base,Sigma), pH 10 at 100° for 20 min. in a pressure cooker (HistoPro, Millestone) or 10 mM Citric acid (Sigma), pH 6.0 at 98°C for 20 min or 1 % Sodium dodecyl sulfate (SDS) in PBS. In the case of Lamp1 staining, slides were quenched with 50 mM of NH_4Cl in PBS, three times for 10 min. Unspecific sites were blocked with a solution containing 1X PBS/ 5% donkey serum (Sigma)/ 0.3% Triton X-100 (Sigma) for 20 min. at room temperature. Primary antibodies were diluted in 1X PBS/ 1% BSA/ 0.3% TritonX-100: goat polyclonal anti-(P)RR/ATP6AP2 (1:100, Novus Biologicals, NB100-1318, used with SDS pretreatment); rabbit polyclonal anti-ATP6IP2 antibody (1:200, ABCAM ab40790, used with microwaving in citric acid), goat polyclonal anti-(P)RR antibody (1:100, R&D Systems, #AF5716, used with SDS pretreatment), rabbit anti- ATP6V0a4 serum (1:2000) [71], goat anti-megalin (1:600, Santa Cruz, sc-16478), rabbit anti-human transferrin (1:600, Dako, A006), rabbit anti-cubilin (1:700, kindly provided by Dr. Erik Ilsø Christensen, Aarhus University, Denmark), rat anti-Lamp1 (1.1000, 1D4B was deposited to the DSHB by August, J.T. (DSHB Hybridoma Product 1D4B)), anti-rabbit LC3B (1:250, Cell Signaling Technology, # 2775), goat anti-AQP2 (1:400, Santa Cruz) or rabbit anti-AQP2 (1:1000, kindly provided by Dr. J. Loffing, University of Zurich) and kidney sections were incubated with the primary antibodies overnight at 4°C. Sections were washed twice with hypertonic PBS (18 g/l NaCl/PBS) and once with 1X PBS. Afterwards sections were incubated with corresponding secondary antibodies (1:1000) (anti-goat Alexa594 and anti-goat Alexa488, anti-rat Alexa 647,anti-rabbit Alexa 488 and anti-rabbit Alexa594 (Invitrogen, Switzerland), phalloidin-Texas Red® (1:100, Molecular Probes), phalloidin-A647 (1:1'000, Abcam, ab176759), and DAPI (1:1000, Invitrogen) for 1h at room temperature. Slides were washed twice with hypertonic PBS and then once with 1X PBS before being mounted with Dako glycergel mounting

medium. Semi-thin section (200 nm thickness) were cut with an ultramicrotome (Leica Microsystems Leica EM FCS) and stained with Toluidine Blue O (T3260 Sigma-Aldrich). Semi-thin sections were visualized with slide-scanner Axio Scan.Z1 Zeiss, Objective Plan Apochromat 40x, NA 0.95 air (Zeiss Germany). Immunofluorescence sections were either visualized with a confocal laser scanning microscope (Zeiss LSM 700, Carl Zeiss) or a Leica DFC490 charged coupled device camera attached to a Leica DM 6000 fluorescence microscope (Leica, Wetzlar, Germany). The confocal microscope pinhole was set at 1 Airy unit and pixel size at 90 nm and a 40×/1.3 oil DIC M27 objective was used. Images were processed (overlays) using Adobe Photoshop and ImageJ software (http://rsb.info.nih.gov/ij/).

Endocytic marker injection and tissue fluorescence measurement

Dextran-FITC 10 kDa (D1821, Molecular Probes) was used as fluid phase endocytosis marker and human recombinant transferrin (T3795, Sigma) was used as receptor-mediator endocytosis marker [32]. Dextran-FITC and human transferrin were diluted in the same isotonic saline solution (6.25 mg/mL for dextran-FITC and 50 mg/mL for transferrin) and injected into the tail vein. Cytoplasmic fractions for kidney protein extraction were used for measuring FITC in the tissue with Nanodrop 3300 Fluorospectrometer (ThermoScientific). Samples were normalized for protein content and blanked with a sample from an animal that was not injected.

Statistical analysis

Statistical significances were calculated by student's t-test. $P < 0.05$ was considered significant. Results are presented as mean ± SEM.

Disclosure

The authors declare to have nothing to disclose.

Acknowledgements

This study was supported by grants from the Swiss National Science Foundation (31003A_138143 and 31003A_155959) to C. A. Wagner. Dr. O. Devuyst, University of Zurich, kindly provided urine from a Clnc5 KO mouse and antibodies against ClC-5 and megalin, Dr. J. Loffing, University of Zurich kindly provided rabbit anti-AQP2 antibodies. Dr. X.S. Xie, University of Texas, Dallas, TX, and Dr. E. I. Christensen, University of Aarhus, kindly provided antibodies against ATP6V0a2 and cubilin, respectively.

Table 1

Parameters	Wt	Sh
Body weight (g)	303.8 ± 10.7	268.1 ± 18.7
H_2O intake (g/g BW)	0.13 ± 0.01	0.13 ± 0.01
Food intake (g/g BW)	0.09 ± 0.01	0.09 ± 0.01
Plasma		
pH	7.47 ± 0.01	7.51 ± 0.02
Glucose (mg/dL)	225.8 ± 22.2	206.8 ± 16.6
Na^+ (mM)	136.5 ± 1.0	136.2 ± 0.3
K^+ (mM)	4.37 ± 0.15	3.62 ± 0.22
Ionized Ca^{2+} (mM)	0.84 ± 0.14	0.80 ± 0.05
Cl^- (mM)	97.8 ± 0.8	95.7 ± 0.6
Phosphate (mg/dL)	8.6 ± 0.4	9.8 ± 0.3 *
Prealbumin (mg/dL)	1.72 ± 0.31	1.53 ± 0.22
Creatinine (mg/dL)	0.30 ± 0.02	0.40 ± 0.01
BUN (mg/dL)	35.2 ± 1.0	48.3 ± 2.6 ***
Urine		
Urine (g/g BW)	0.04 ± 0.01	0.03 ± 0.01
Creatinine (mg/dL)	72.2 ± 10.3	111.9 ± 13.2 *
Creatinine Clearance (g/min)	1.9 ± 0.2	1.5 ± 0.2
Na^+ (mM)/Crea (mg/dL)	95.0 ± 8.3	71.2 ± 22.8 **
K^+ (mM)/Crea (mg/dL)	2.60 ± 0.11	2.73 ± 0.14
Ca^{2+} (mM)/Crea (mg/dL)	0.020 ± 0.003	Not detectable
Mg^{2+} (mg/dL)/Crea (mg/dL)	0.57 ± 0.10	0.32 ± 0.15
Phosphate (mg/dL)/Crea(mg/dL)	0.08 ± 0.08	1.71 ± 0.20 ***
Cl^- (mM)/Crea (mg/dL)	2.2 ± 0.1	2.1 ± 0.1

Table 2

Parameters	Wt/Pax8+	Flox/Pax8+
Body weight (g)	25.2 ± 1.0	23.6 ± 18.7 *
H_2O intake (g/g BW)	0.19 ± 0.02	0.26 ± 0.01 *
Food intake (g/g BW)	0.16 ± 0.02	0.19 ± 0.01
Plasma		
pH	7.26 ± 0.03	7.27 ± 0.05
Glucose (mg/dL)	250.5 ± 8.9	238.9 ± 15.3
Na^+ (mM)	144.7 ± 1.1	146.0 ± 1.1
K^+ (mM)	3.9 ± 0.4	3.2 ± 0.1 *
Ionized Ca^{2+} (mM)	0.96 ± 0.23	1.11 ± 0.05
Cl^- (mM)	108.2 ± 1.5	109.2 ± 0.1
Phosphate (mg/dL)	5.9 ± 0.1	6.2 ± 0.3
Prealbumin (mg/dL)	1.76± 0.42	1.88± 0.15
Creatinine (mg/dL)	0.05 ± 0.01	0.07 ± 0.01
BUN (mg/dL)	40.6 ± 5.9	40.7 ± 3.3
Urine		
Urine (g/g BW)	0.051 ± 0.009	0.083 ± 0.008 *
Creatinine (mg/dL)	63.0 ± 4.2	42.8 ± 2.9 **
Creatinine clearance (mL/min)	1.09 ± 0.35	0.98 ± 0.23
Na^+ (mM)/Crea (mg/dL)	1.7 ± 0.2	5.8 ± 1.1 **
K^+ (mM)/Crea (mg/dL)	6.0 ± 0.3	7.1 ± 0.3*
Ca^{2+} (mM)/Crea (mg/dL)	0.03 ± 0.01	0.01 ± 0.21*
Mg^{2+} (mg/dL)/Crea (mg/dL)	1.65 ± 0.10	1.70 ± 6.25
Phosphate (mg/dL)/Crea(mg/dL)	6.7 ± 0.4	7.1 ± 0.6
Cl^- (mM)/Crea (mg/dL)	4.0 ± 0.2	5.0 ± 0.3

FIGURE LEGENDS

Figure 1. Generation of the *Atp6ap2* shRNA rat model and efficiency of *Atp6ap2* / (P)RR) knock-down

(A) Structure of the transgene construct, pTet-sh, made of two expression cassettes. A first one carries a tetracycline operator (tetO) sequence and expresses an shRNA against *Atp6ap2* under the control of the human H1 promoter. A second cassette consists of a tetracycline repressor (tetR) cDNA followed by a polyadenylation site (pA), and is driven by the CAGGS promoter. Primers TetOfw and CAGGSrv (arrows) were used for genotyping of rats. **(B)** Genotyping by PCR performed on newborn rat tails with a 195-bp PCR product characteristic of the transgenic animals (Sh). **(C)** Comparative expression of tetracycline repressor (TetR) protein between transgenic (Sh) and control (Wt) rats, as studied in various tissues by western blot. GAPDH was used as loading control. **(D)** RT-qPCR analysis of total mRNA of kidneys from rat Wt and Sh demonstrates successful knock-down of (P)RR/*Atp6ap2* mRNA (n = 6/genotype). **(E)** Immunohistochemistry for the H^+ATPase a4 subunit (green) and (P)RR (red) in kidney sections from Wt and Sh rats. Original magnification 400x. **(F)** Renal morphology of Sh and control animals**.** Semi-thin section (200 nm thick) were stained with Toluidine Blue (original magnification 40X)

Figure 2. Preserved fluid-phase endocytosis but impaired receptor-mediated endocytosis in (P)RR/ATP6ap2 deficient rats

(A) Albuminuria in Sh rats detected by coomassie blue staining of SDS-Page gels loaded with urine samples normalized to creatinine (7 mg/ml) BSA (7 mg /ml) was loaded as positive control. Bar graph summarizing data (n=4 in each animal group). Student's *t*-test * $p < 0.05$. **(B)** Elevated vitamin D binding protein (VDBP) in urine of Sh rats detected by immunoblotting of urine samples normalized to creatinine (7 mg/ml). Urine from a Clcn5 KO mouse (C+) was loaded as positive control. Bar graph summarizing data from n = 4/genotype. **(C)** Immunohistochemistry for dextran-FITC (10 kDa, green) and phalloidin (red) in kidney slices from Wt and shRNA rat 10 min. after injection (original magnification 400x). **(D)** Quantification of dextran-FITC in the

cytoplasmic fraction of the control and Sh rats kidney homogenate. FITC-dextran was normalized to total protein content. **(E)** Immunohistochemistry for human transferrin (red) and megalin (green) in Wt and Sh rats kidney 10 min and 40 min. after injection showed strong residual staining of transferrin after 40 min in Sh rat kidneys (see insert) (original magnification 400x). **(F)** Western blotting for human transferrin in Wt and Sh rat urine 10 min. after injection. Urine samples were normalized to creatinine (7 mg/ml). Bar graph summarizing data from n = 4/genotype. **(G)** Western blotting of kidney total homogenate for human transferrin 10 and 40 min after injection. Statistical analyses were performed using Student's *t*-test ** $p < 0.01$.

Figure 3. Altered expression of proteins involved in receptor-mediated endocytosis

(A) Brush border membrane preparations of control and Sh rats kidneys were used for blotting for H^+ATPase a4 (ATP6Voa4), B2 (ATP6V1B2), and A (ATP6V1A) subunits as well as for NaPiIIa, NHE3, megalin, and cubilin. Total membrane protein kidney preparations were used for blotting of ClC-5. **(B)** Densitometries were adjusted to β-Actin (loading control). Statistical analysis using Student`s *t*-test (n = 6/genotype or n = 4/genotype for NaPiIIa). * $p < 0.05$ *** $p \leq 0.001$.

Figure 4. Generation of kidney epithelial cell specific (P)RR/ATP6ap2 ablation in mouse.

(A) RT-qPCR analysis of total mRNA of kidneys, lungs and hearts from Wt and Flox /Pax8+ mice. *Atp6ap2* mRNA abundance was normalized to *HPRT*. Statistical analysis was performed using Student's *t*-test (Wt/Pax8+: n = 4 and Flox /Pax8+: n=5) *** $p < 0.001$. **(B)** Western blotting for (P)RR/ATP6ap2 in total membrane preparations from kidney of Wt and Flox/Pax8+ mice and summary of data as bar graph. Statistical analysis was performed using Student's *t*-test (Wt/Pax8+: n = 4 and Flox/Pax8+: n = 5) * $p < 0.05$. **(C)** Immunohistochemistry for (P)RR/ATP6ap2 (red), AQP2 (green) and DAPI (blue) in kidney sections from Wt/Pax8 and Flox/Pax8+ mice with proximal

tubules (upper panels) and medullary collecting ducts (lower panels). Original magnification 400x.

Figure 5. Albuminuria and low molecular weight proteinuria in the absence of the (P)RR/ATP6ap2

Urine samples were normalized to creatinine. Bovine serum albumin (BSA, 7 mg/ml) or urine from a Clcn-5 KO mouse was loaded as positive control. **(A)** Albumin was detected by coomassie blue staining whereas **(B)** vitamin D binding protein (VDBP) or **(C)** (Pro)cathepsin B were revealed by immunoblotting. Data were summarized as bar graphs (n = 4/genotype. Student's *t*-test ** $p < 0.01$, *** $p < 0.001$.

Figure 6. Delayed receptor-mediated endocytosis in (P)RR/ATP6ap2 deleted mice

WT/Pax8+ and Flox/Pax8+ mice were coinjected with dextran-FITC (10 kDa) and human recombinant transferrin and kidneys collected 10 and 40 min. after injection. **(A)** Immunohistochemistry for dextran-FITC,10 kDa (green) and phalloidin (red) in kidney slices from Wt and Flox/Pax8+ mice 10 and 40 min. after injection. **(B)** Immunohistochemistry for human transferrin (red) and megalin (green) in kidneys from Wt and Flox/Pax8+ mice 10 and 40 min. after injection. **(C)** Immunohistochemistry for Lamp-1 (green) and human transferrin (red) 40 min. after injection. Original magnification 400x.

Figure 7. Deletion of the (P)RR/ATP6ap2 alters expression of major proteins in the endocytic pathway.

(A) Brush border membrane preparations from kidneys of Wt/Pax8+ and Flox/Pax8+ mice were blotted for the H^+ATPase a4 (ATP6V0a4), a2 (ATP6V0a2), EII (ATP6V1EII), B2 (ATP6V1B2) and A (ATP6V1A) subunits as well as for NHE3, megalin and cubilin. Total membrane protein kidney preparations were used for the western blot of ClC-5. **(B)** Densitometries were normalized to β-Actin (loading control). Student`s *t*-test (n = 4 per group), * $p \leq 0.05$, ** $p \leq 0.01$, *** $p \leq 0.001$

Figure 8. Down-regulation of the mTOR pathway in (P)RR/ATP6ap2 deficient mice and accumulation of autophagosomes

(A, B) Western blotting for total and phosphorylated mammalian target of rapamycin (mTOR) and S6 kinase (S6K) and (B) densitometry summarizing results. Student`s *t*-test (n = 4 per group), * $p \leq 0.05$. **(C)** Immunohistochemistry for Microtubule-associated proteins 1A/1B light chain 3B (LC3-B) (red) in kidneys from Wt and Flox/Pax8+ mice. Original magnification 400x.

Supplementary figure legends

Table 1. Metabolic and urine parameters from Wt and Sh rats.

Water and food intake and also urine volume were monitored in metabolic cages under baseline conditions. After adaptation, 24-hrs urine and blood was collected for analysis. Statistical analysis were performed using Student's *t*-test (n=6/ genotype) * $p < 0.05$, ** $p < 0.01$, *** $p < 0.001$.

Table 2. Metabolic and urine parameters of Wt and Flox/Pax8+ mice.

Water and food intake were monitored in metabolic cages under baseline conditions. 24-hrs urine and blood was collected for analysis. Statistical analysis were performed using Student's *t*-test (n=8 in both groups) * $p < 0.05$, ** $p < 0.01$, *** $p < 0.001$.

Supplementary figure 1. Dextran-FITC staining intensity and localization is similar in both animal groups at 10 min. and 40 min. time points.

Immunohistochemistry for dextran-FITC, 10 kDa (green) and phalloidin (red) in kidney slices from Wt and shRNA rats 10 and 40 min. after injection. Original magnification 400x.

Supplementary figure 2. Cubilin localization in control and shRNA rat kidneys.

Immunohistochemistry for cubilin (green) in kidney slices from Wt and shRNA rats. Original magnification 400 x.

Supplementary figure 3. Detection of (P)RR/ATP6ap2 in mouse kidneys with antibodies from Novus Biologicals.

Kidneys from wildtype (Wt/ Pax8+)**(A-C)** and Flox/Pax8+ **(D-F)** mice were stained with antibodies from Novus Biologicals against the (P)RR/ATP6ap2 (green), AQP2 (red), and with DAPI (blue) to detect nuclei. In wildtype kidney, strong staining with antibodies against the (P)RR/ATP6ap2 was detected in proximal tubules and in collecting ducts, in Flox/Pax8+ kidney, staining was weaker in the proximal tubule but preserved in collecting ducts. Of note, all cell types in the collecting duct were stained. Original magnification 400-630 x.

Supplementary figure 4. Detection of (P)RR/ATP6ap2 in mouse kidneys with antibodies from R&D Systems.

Kidneys from wildtype (Wt/ Pax8+)**(A-B)** and Flox/Pax8+ **(C-D)** mice were stained with antibodies from R&D Systems against the (P)RR/ATP6ap2 (green), AQP2 (red), and with DAPI (blue) to detect nuclei. In wildtype kidney, strong staining with antibodies against the (P)RR/ATP6ap2 was detected in proximal tubules and in collecting ducts, in Flox/Pax8+ kidney, staining in the proximal tubule and collecting ducts remained unchanged. In contrast to staining with other antiobodies, staining with R&D Systems antibodies was mostly intracellular. Original magnification 400-630 x.

REFERENCES

1. Sihn G, Rousselle A, Vilianovitch L*, et al.* Physiology of the (pro)renin receptor: Wnt of change? *Kidney Int* 2010; **78:** 246-256.

2. Nguyen G, Delarue F, Burckle C*, et al.* Pivotal role of the renin/prorenin receptor in angiotensin II production and cellular responses to renin. *J Clin Invest* 2002; **109:** 1417-1427.

3. Seva Pessoa B, van der Lubbe N, Verdonk K*, et al.* Key developments in renin-angiotensin-aldosterone system inhibition. *Nat Rev Nephrol* 2013; **9:** 26-36.

4. Krop M, Lu X, Danser AH*, et al.* The (pro)renin receptor. A decade of research: what have we learned? *Pflugers Arch* 2013; **465:** 87-97.

5. Nguyen G, Muller DN. The biology of the (pro)renin receptor. *J Am Soc Nephrol* 2010; **21:** 18-23.

6. Cruciat CM, Ohkawara B, Acebron SP*, et al.* Requirement of prorenin receptor and vacuolar H+-ATPase-mediated acidification for Wnt signaling. *Science* 2010; **327:** 459-463.

7. Hermle T, Guida MC, Beck S*, et al.* Drosophila ATP6AP2/VhaPRR functions both as a novel planar cell polarity core protein and a regulator of endosomal trafficking. *EMBO J* 2013; **32:** 245-259.

8. Hermle T, Saltukoglu D, Grunewald J*, et al.* Regulation of Frizzled-dependent planar polarity signaling by a V-ATPase subunit. *Curr Biol* 2010; **20:** 1269-1276.

9. Buechling T, Bartscherer K, Ohkawara B*, et al.* Wnt/Frizzled signaling requires dPRR, the Drosophila homolog of the prorenin receptor. *Curr Biol* 2010; **20:** 1263-1268.

10. Hermle T, Saltukoglu D, Grünewald J*, et al.* Regulation of Frizzled-Dependent Planar Polarity Signaling by a V-ATPase Subunit. *Current Biology* 2010; **20:** 1269-1276.

11. Buechling T, Bartscherer K, Ohkawara B*, et al.* Wnt/Frizzled signaling requires dPRR, the Drosophila homolog of the prorenin receptor. *Current biology : CB* 2010; **20:** 1263-1268.

12. Hermle T, Guida MC, Beck S*, et al.* Drosophila ATP6AP2/VhaPRR functions both as a novel p... [EMBO J. 2013] - PubMed - NCBI. *The EMBO journal* 2013; **32:** 245-259.

13. Ramser J, Abidi FE, Burckle CA*, et al.* A unique exonic splice enhancer mutation in a family with X-linked mental retardation and epilepsy

points to a novel role of the renin receptor. *Hum Mol Genet* 2005; **14:** 1019-1027.

14. Ludwig J, Kerscher, S, Brandt, U, Pfeiffer, K, Getlawi, F, Apps, D K, Schagger, H. Identification and characterization of a novel 9.2-kDa membrane sector-associated protein of vacuolar proton-ATPase from chromaffin granules. *J Biol Chem* 1998; **273:** 10939-10947.

15. Merkulova M, Paunescu TG, Azroyan A*, et al.* Mapping the H(+) (V)-ATPase interactome: identification of proteins involved in trafficking, folding, assembly and phosphorylation. *Sci Rep* 2015; **5:** 14827.

16. Wagner CA, Finberg, K E, Breton, S, Marshansky, V, Brown, D, Geibel, J P. Renal vacuolar H^+-ATPase. *Physiol Rev* 2004; **84:** 1263-1314.

17. Breton S, Brown D. Regulation of luminal acidification by the V-ATPase. *Physiology (Bethesda)* 2013; **28:** 318-329.

18. Marshansky V, Ausiello, D A, Brown, D. Physiological importance of endosomal acidification: potential role in proximal tubulopathies. *Curr Opin Nephrol Hypertens* 2002; **11:** 527-537.

19. Forgac M. Vacuolar ATPases: rotary proton pumps in physiology and pathophysiology. *Nat Rev Mol Cell Biol* 2007; **8:** 917-929.

20. Advani A, Kelly DJ, Cox AJ*, et al.* The (Pro)renin receptor: site-specific and functional linkage to the vacuolar H+-ATPase in the kidney. *Hypertension* 2009; **54:** 261-269.

21. Daryadel A, Bourgeois S, Figueiredo MF*, et al.* Colocalization of the (Pro)renin Receptor/Atp6ap2 with H+-ATPases in Mouse Kidney but Prorenin Does Not Acutely Regulate Intercalated Cell H+-ATPase Activity. *PLoS One* 2016; **11:** e0147831.

22. Kinouchi K, Ichihara A, Sano M*, et al.* The (pro)renin receptor/ATP6AP2 is essential for vacuolar H+-ATPase assembly in murine cardiomyocytes. *Circ Res* 2010; **107:** 30-34.

23. Riediger F, Quack I, Qadri F*, et al.* Prorenin receptor is essential for podocyte autophagy and survival. *J Am Soc Nephrol* 2011; **22:** 2193-2202.

24. Schefe JH, Menk M, Reinemund J*, et al.* A novel signal transduction cascade involving direct physical interaction of the renin/prorenin receptor with the transcription factor promyelocytic zinc finger protein. *Circ Res* 2006; **99:** 1355-1366.

25. Norgett EE, Golder ZJ, Lorente-Canovas B*, et al.* Atp6v0a4 knockout mouse is a model of distal renal tubular acidosis with hearing loss, with

additional extrarenal phenotype. *Proc Natl Acad Sci U S A* 2012; **109:** 13775-13780.

26. Hennings JC, Picard N, Huebner AK*, et al.* A mouse model for distal renal tubular acidosis reveals a previously unrecognized role of the V-ATPase a4 subunit in the proximal tubule. *EMBO Mol Med* 2012; **4:** 1057-1071.

27. Wang SS, Devuyst O, Courtoy PJ*, et al.* Mice lacking renal chloride channel, CLC-5, are a model for Dent's disease, a nephrolithiasis disorder associated with defective receptor-mediated endocytosis. *Hum Mol Genet* 2000; **9:** 2937-2945.

28. Piwon N, Gunther, W, Schwake, M, Bosl, M R, Jentsch, T J. ClC-5 Cl^- -channel disruption impairs endocytosis in a mouse model for Dent's disease. *Nature* 2000; **408:** 369-373.

29. Christensen EI, Devuyst, O, Dom, G, Nielsen, R, Van Der Smissen, P, Verroust, P, Leruth, M, Guggino, W B, Courtoy, P J. Loss of chloride channel ClC-5 impairs endocytosis by defective trafficking of megalin and cubilin in kidney proximal tubules. *Proc Natl Acad Sci U S A* 2003; **100:** 8472-8477.

30. Frattini A, Orchard, P J, Sobacchi, C, Giliani, S, Abinun, M, Mattsson, J P, Keeling, D J, Andersson, A K, Wallbrandt, P, Zecca, L, Notarangelo, L D, Vezzoni, P, Villa, A. Defects in TCIRG1 subunit of the vacuolar proton pump are responsible for a subset of human autosomal recessive osteopetrosis. *Nat Genet* 2000; **25:** 343-346.

31. Oshima Y, Kinouchi K, Ichihara A*, et al.* Prorenin receptor is essential for normal podocyte structure and function. *J Am Soc Nephrol* 2011; **22:** 2203-2212.

32. Nielsen R, Christensen EI, Birn H. Megalin and cubilin in proximal tubule protein reabsorption: from experimental models to human disease. *Kidney Int* 2016; **89:** 58-67.

33. Maxson ME, Grinstein S. The vacuolar-type H(+)-ATPase at a glance - more than a proton pump. *J Cell Sci* 2014; **127:** 4987-4993.

34. Sun-Wada GH, Wada Y. Vacuolar-type proton pump ATPases: acidification and pathological relationships. *Histol Histopathol* 2013; **28:** 805-815.

35. Schwake M, Schroder B, Saftig P. Lysosomal membrane proteins and their central role in physiology. *Traffic* 2013; **14:** 739-748.

36. Laplante M, Sabatini DM. mTOR signaling in growth control and disease. *Cell* 2012; **149:** 274-293.

37. Christensen EI, Birn H. Megalin and cubilin: multifunctional endocytic receptors. *Nat Rev Mol Cell Biol* 2002; **3:** 256-266.

38. Kinouchi K, Ichihara A, Sano M*, et al.* The role of individual domains and the significance of shedding of ATP6AP2/(pro)renin receptor in vacuolar H(+)-ATPase biogenesis. *PLoS One* 2013; **8:** e78603.

39. Rickheit G, Wartosch L, Schaffer S*, et al.* Role of ClC-5 in renal endocytosis is unique among ClC exchangers and does not require PY-motif-dependent ubiquitylation. *J Biol Chem* 2010; **285:** 17595-17603.

40. Devuyst O, Luciani A. Chloride transporters and receptor-mediated endocytosis in the renal proximal tubule. *J Physiol* 2015; **593:** 4151-4164.

41. de Seigneux S, Courbebaisse M, Rutkowski JM*, et al.* Proteinuria Increases Plasma Phosphate by Altering Its Tubular Handling. *J Am Soc Nephrol* 2015; **26:** 1608-1618.

42. Bachmann S, Schlichting U, Geist B*, et al.* Kidney-specific inactivation of the megalin gene impairs trafficking of renal inorganic sodium phosphate cotransporter (NaPi-IIa). *J Am Soc Nephrol* 2004; **15:** 892-900.

43. Bacic D, Capuano, P, Gisler, SM, Pribanic, S, Christensen, EI, Biber, J, Loffing, J, Kaissling, B, Wagner, CA, Murer, H. Impaired PTH-induced endocytotic down-regulation of the renal type IIa Na^+/P_i-cotransporter in RAP deficient mice with reduced megalin expression. *Pflügers Arch* 2003; **446:** 475-484.

44. Myakala K, Motta S, Murer H*, et al.* Renal-specific and inducible depletion of NaPi-IIc/Slc34a3, the cotransporter mutated in HHRH, does not affect phosphate or calcium homeostasis in mice. *Am J Physiol Renal Physiol* 2014; **306:** F833-843.

45. Trepiccione F, Gerber SD, Grahammer F*, et al.* Renal Atp6ap2/(Pro)renin Receptor Is Required for Normal Vacuolar H+-ATPase Function but Not for the Renin-Angiotensin System. *J Am Soc Nephrol* 2016.

46. Ramkumar N, Stuart D, Calquin M*, et al.* Nephron-specific deletion of the prorenin receptor causes a urine concentration defect. *Am J Physiol Renal Physiol* 2015; **309:** F48-56.

47. Ramkumar N, Stuart D, Mironova E*, et al.* Renal tubular epithelial cell prorenin receptor regulates blood pressure and sodium transport. *Am J Physiol Renal Physiol* 2016**:** ajprenal 00088 02016.

48. Xu H, Ren D. Lysosomal physiology. *Annu Rev Physiol* 2015; **77:** 57-80.

49. Betz C, Hall MN. Where is mTOR and what is it doing there? *J Cell Biol* 2013; **203:** 563-574.

50. Gleixner EM, Canaud G, Hermle T*, et al.* V-ATPase/mTOR signaling regulates megalin-mediated apical endocytosis. *Cell Rep* 2014; **8:** 10-19.

51. Kim YC, Guan KL. mTOR: a pharmacologic target for autophagy regulation. *J Clin Invest* 2015; **125:** 25-32.

52. Mrschtik M, Ryan KM. Lysosomal proteins in cell death and autophagy. *FEBS J* 2015; **282:** 1858-1870.

53. Rousselle A, Sihn G, Rotteveel M*, et al.* (Pro)renin receptor and V-ATPase: from Drosophila to humans. *Clin Sci (Lond)* 2014; **126:** 529-536.

54. Rong R, Ito O, Mori N*, et al.* Expression of (pro)renin receptor and its upregulation by high salt intake in the rat nephron. *Peptides* 2015; **63:** 156-162.

55. Huang J, Ledford KJ, Pitkin WB*, et al.* Targeted deletion of murine CEACAM 1 activates PI3K-Akt signaling and contributes to the expression of (Pro)renin receptor via CREB family and NF-kappaB transcription factors. *Hypertension* 2013; **62:** 317-323.

56. Gorvin CM, Wilmer MJ, Piret SE*, et al.* Receptor-mediated endocytosis and endosomal acidification is impaired in proximal tubule epithelial cells of Dent disease patients. *Proc Natl Acad Sci U S A* 2013; **110:** 7014-7019.

57. Gunther W, Piwon N, Jentsch TJ. The ClC-5 chloride channel knock-out mouse - an animal model for Dent's disease. *Pflugers Arch* 2003; **445:** 456-462.

58. Wang SS, Devuyst, O, Courtoy, P J, Wang, X T, Wang, H, Wang, Y, Thakker, R V, Guggino, S, Guggino, W B. Mice lacking renal chloride channel, CLC-5, are a model for Dent's disease, a nephrolithiasis disorder associated with defective receptor-mediated endocytosis. *Hum Mol Genet* 2000; **9:** 2937-2945.

59. Novarino G, Weinert S, Rickheit G*, et al.* Endosomal chloride-proton exchange rather than chloride conductance is crucial for renal endocytosis. *Science* 2010; **328:** 1398-1401.

60. Ramachandran N, Munteanu I, Wang P*, et al.* VMA21 deficiency prevents vacuolar ATPase assembly and causes autophagic vacuolar myopathy. *Acta Neuropathol* 2013; **125:** 439-457.

61. Mauvezin C, Nagy P, Juhasz G*, et al.* Autophagosome-lysosome fusion is independent of V-ATPase-mediated acidification. *Nat Commun* 2015; **6:** 7007.

62. Pena-Llopis S, Vega-Rubin-de-Celis S, Schwartz JC*, et al.* Regulation of TFEB and V-ATPases by mTORC1. *EMBO J* 2011; **30:** 3242-3258.

63. Zoncu R, Bar-Peled L, Efeyan A*, et al.* mTORC1 senses lysosomal amino acids through an inside-out mechanism that requires the vacuolar H(+)-ATPase. *Science* 2011; **334:** 678-683.

64. Hosokawa N, Hara T, Kaizuka T*, et al.* Nutrient-dependent mTORC1 association with the ULK1-Atg13-FIP200 complex required for autophagy. *Mol Biol Cell* 2009; **20:** 1981-1991.

65. Mavrakis M, Lippincott-Schwartz J, Stratakis CA*, et al.* Depletion of type IA regulatory subunit (RIalpha) of protein kinase A (PKA) in mammalian cells and tissues activates mTOR and causes autophagic deficiency. *Hum Mol Genet* 2006; **15:** 2962-2971.

66. Li C, Siragy HM. (Pro)renin receptor regulates autophagy and apoptosis in podocytes exposed to high glucose. *Am J Physiol Endocrinol Metab* 2015; **309:** E302-310.

67. Kotnik K, Popova E, Todiras M*, et al.* Inducible transgenic rat model for diabetes mellitus based on shRNA-mediated gene knockdown. *PLoS One* 2009; **4:** e5124.

68. Popova E, Bader M, Krivokharchenko A. Strain differences in superovulatory response, embryo development and efficiency of transgenic rat production. *Transgenic Res* 2005; **14:** 729-738.

69. Traykova-Brauch M, Schonig K, Greiner O*, et al.* An efficient and versatile system for acute and chronic modulation of renal tubular function in transgenic mice. *Nat Med* 2008; **14:** 979-984.

70. Biber J, Stieger B, Stange G*, et al.* Isolation of renal proximal tubular brush-border membranes. *Nat Protoc* 2007; **2:** 1356-1359.

71. Wagner CA, Lukewille, U, Valles, P, Breton, S, Brown, D, Giebisch, G H, Geibel, J P. A rapid enzymatic method for the isolation of defined kidney tubule fragments from mouse. *Pflugers Arch* 2003; **446:** 623-632.

72. Peng SB, Li, X, Crider, B P, Zhou, Z, Andersen, P, Tsai, S J, Xie, X S, Stone, D K. Identification and reconstitution of an isoform of the 116-

kDa subunit of the vacuolar proton translocating ATPase. *J Biol Chem* 1999; **274:** 2549-2555.

73. Schulz N, Dave MH, Stehberger PA*, et al.* Differential localization of vacuolar H+-ATPases containing a1, a2, a3, or a4 (ATP6V0A1-4) subunit isoforms along the nephron. *Cell Physiol Biochem* 2007; **20:** 109-120.

74. Bastani B, Purcell, H, Hemken, P, Trigg, D, Gluck, S. Expression and distribution of renal vacuolar proton-translocating adenosine triphosphatase in response to chronic acid and alkali loads in the rat. *J Clin Invest* 1991; **88:** 126-136.

75. Luyckx VA, Goda, F O, Mount, D B, Nishio, T, Hall, A, Hebert, S C, Hammond, T G, Yu, A S. Intrarenal and subcellular localization of rat CLC5. *Am J Physiol* 1998; **275:** F761-769.

76. Custer M, Lötscher, M, Biber, J, Murer, H, Kaissling, B. Expression of Na-P_i cotransport in rat kidney: localization by RT-PCR and immunohistochemistry. *Am J Physiol* 1994; **266:** F767-774.

FIGURE 1

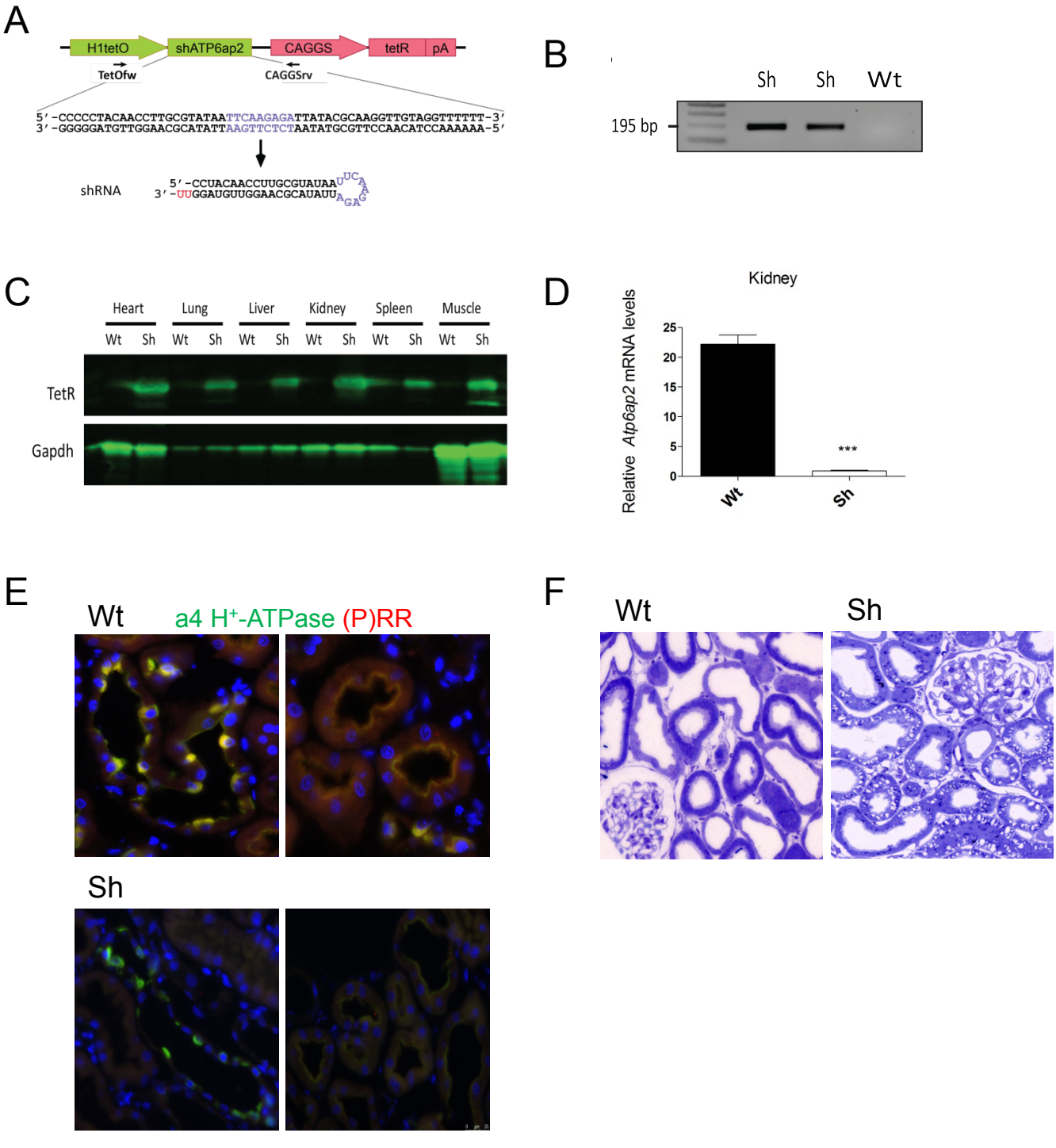
A
H1tetO
shATP6ap2
CAGGS
tetR
pA
TetOfw
CAGGSrv
5′-CCCCCTACAACCTTGCGTATAATTCAAGAGATTATACGCAAGGTTGTAGGTTTTTT-3′
3′-GGGGGATGTTGGAACGCATATTAAGTTCTCTAATATGCGTTCCAACATCCAAAAAA-5′
shRNA
5′-CCUACAACCUUGCGUAUAA
3′-UUGGAUGUUGGAACGCAUAUU
B
Sh
Sh
Wt
195 bp
C
Heart
Lung
Liver
Kidney
Spleen
Muscle
Wt Sh Wt Sh Wt Sh Wt Sh Wt Sh Wt Sh
TetR
Gapdh
D
Kidney
Relative Atp6ap2 mRNA levels
25
20
15
10
5
0
***
Wt
Sh
E
Wt
a4 H+-ATPase (P)RR
Sh
F
Wt
Sh

FIGURE 2

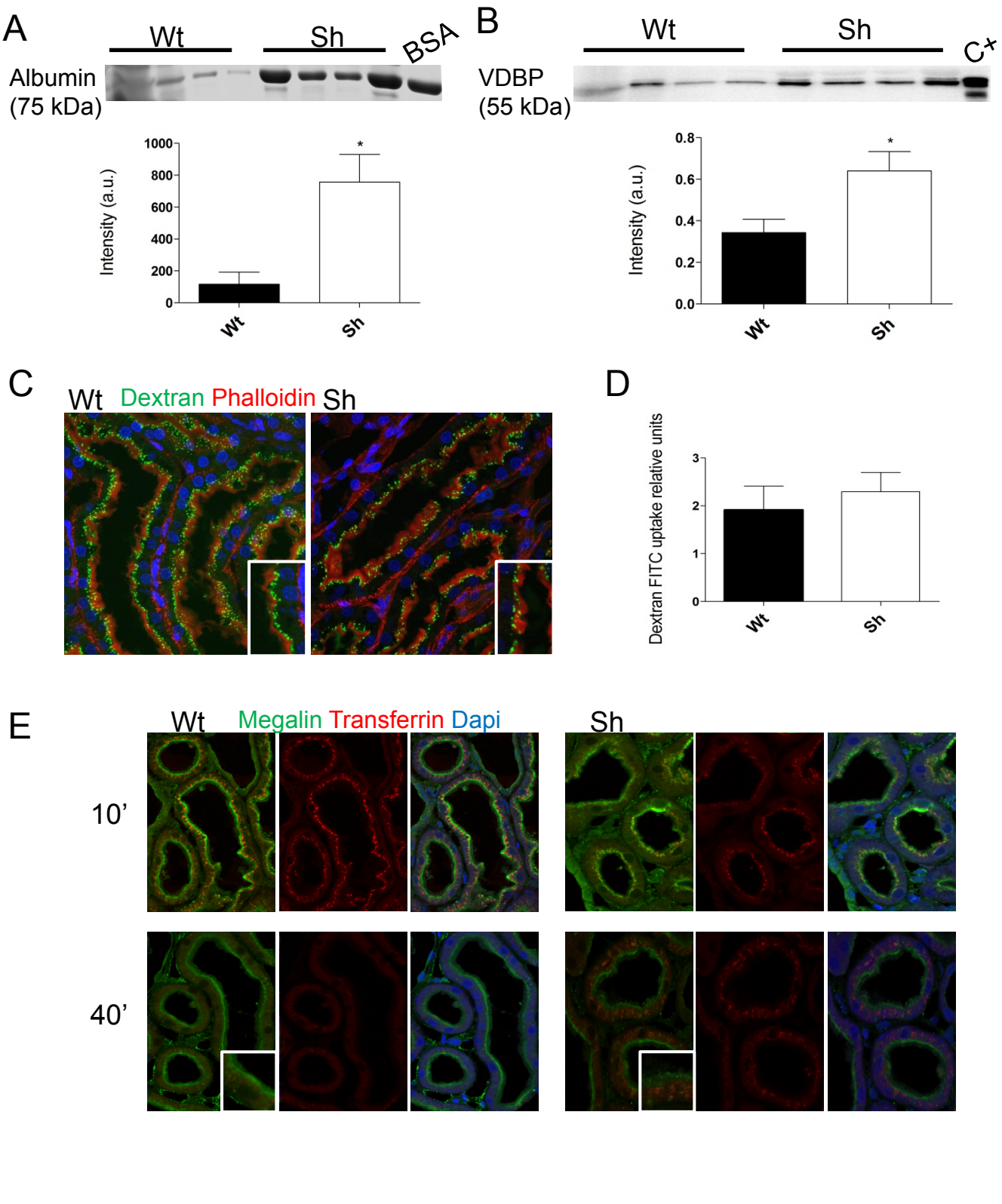
A
Wt
Sh
BSA
Albumin
(75 kDa)
Intensity (a.u.)
1000
800
600
400
200
0
*
Wt
Sh
B
Wt
Sh
C+
VDBP
(55 kDa)
Intensity (a.u.)
0.8
0.6
0.4
0.2
0.0
*
Wt
Sh
C
Wt
Dextran Phalloidin
Sh
D
Dextran FITC uptake relative units
3
2
1
0
Wt
Sh
E
Wt
Megalin Transferrin Dapi
Sh
10’
40’

FIGURE 2

F

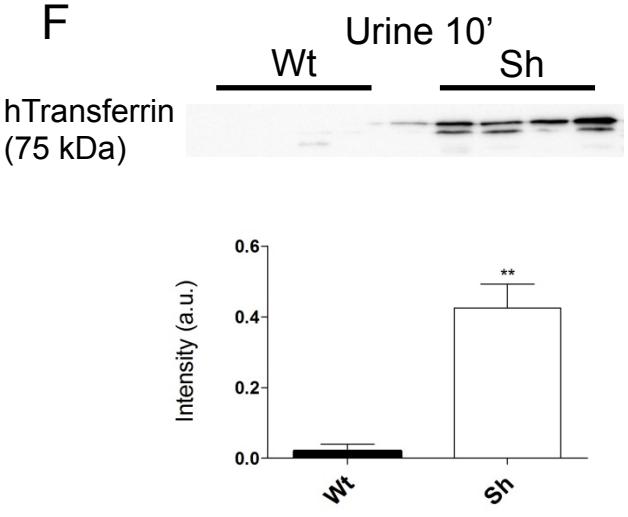
Urine 10’
Wt
Sh
hTransferrin
(75 kDa)
Intensity (a.u.)
0.6
0.4
0.2
0.0
**
Wt
Sh

FIGURE 3

A

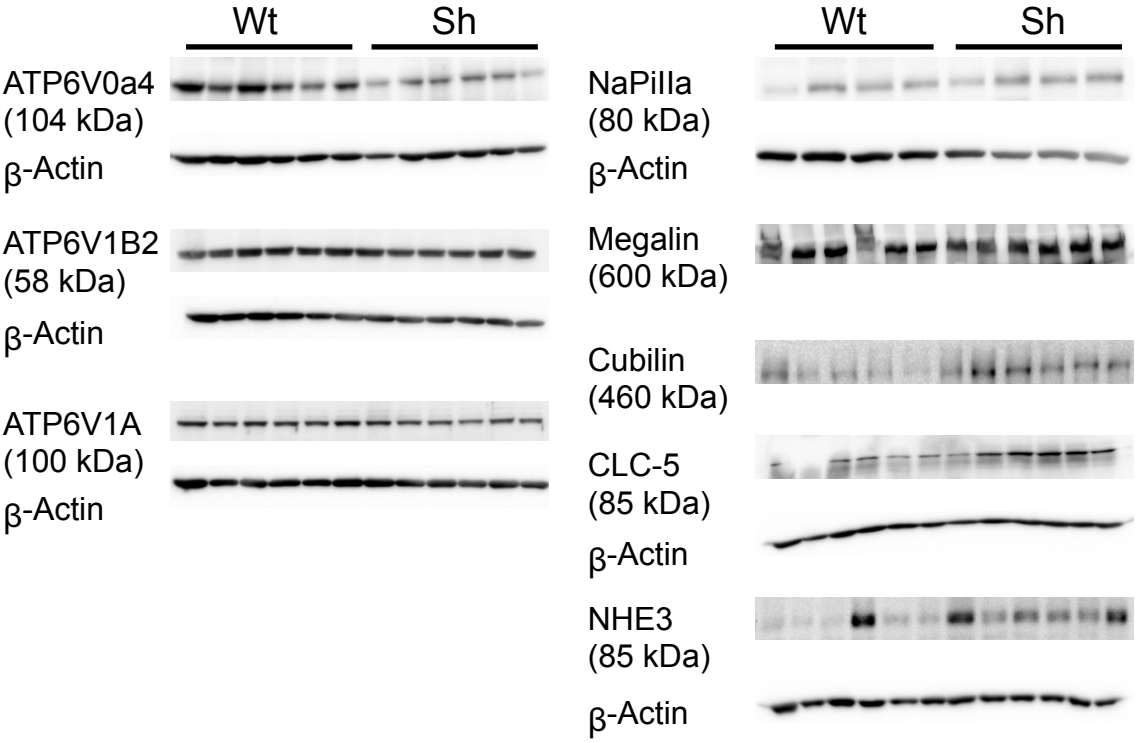
Wt
Sh
ATP6V0a4
(104 kDa)
β-Actin
ATP6V1B2
(58 kDa)
β-Actin
ATP6V1A
(100 kDa)
β-Actin
Wt
Sh
NaPiIIa
(80 kDa)
β-Actin
Megalin
(600 kDa)
Cubilin
(460 kDa)
CLC-5
(85 kDa)
β-Actin
NHE3
(85 kDa)
β-Actin

B

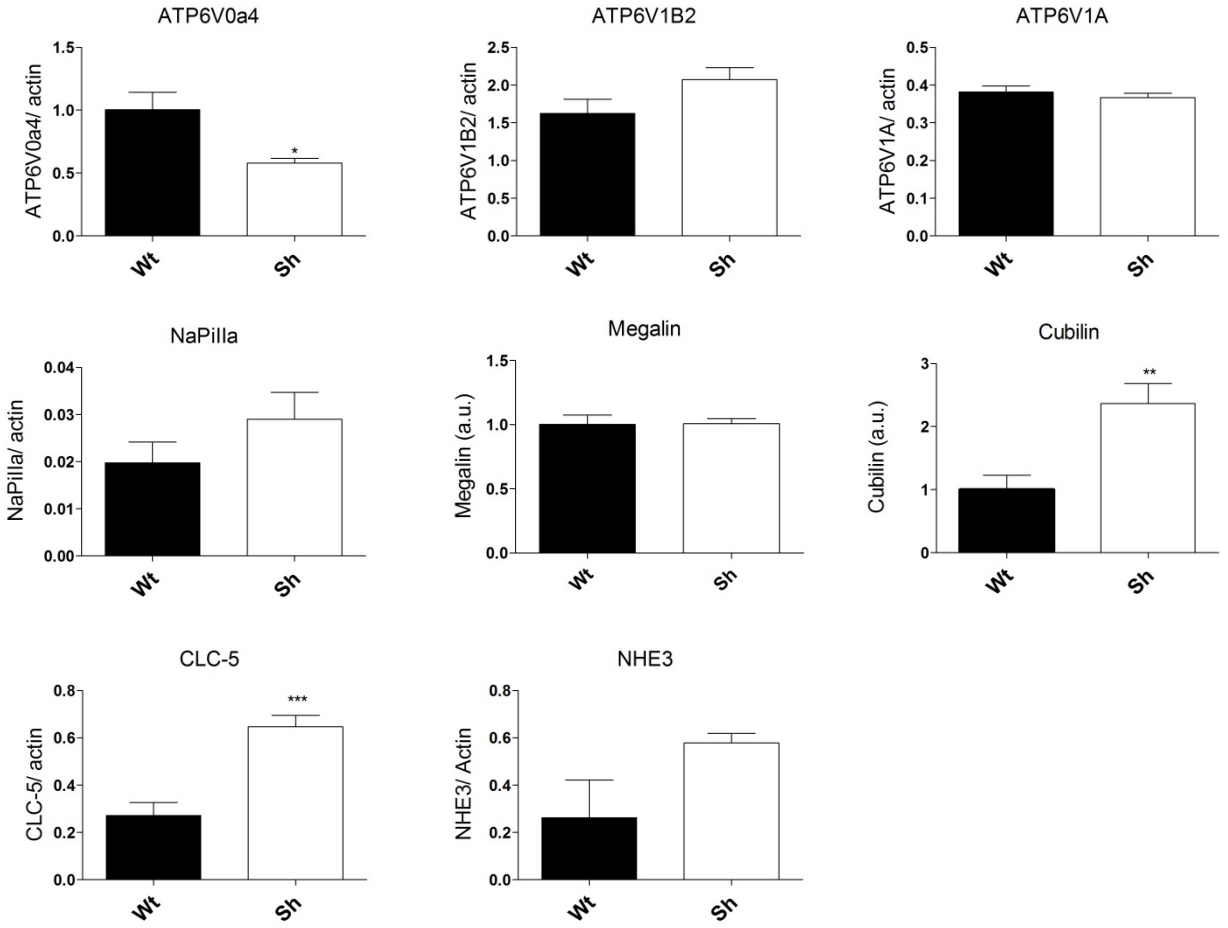
ATP6V0a4
ATP6V0a4/ actin
ATP6V1B2
ATP6V1B2/ actin
ATP6V1A
ATP6V1A/ actin
NaPiIIa
NaPiIIa/ actin
Megalin
Megalin (a.u.)
Cubilin
Cubilin (a.u.)
CLC-5
CLC-5/ actin
NHE3
NHE3/ Actin
Wt
Sh

FIGURE 4

A

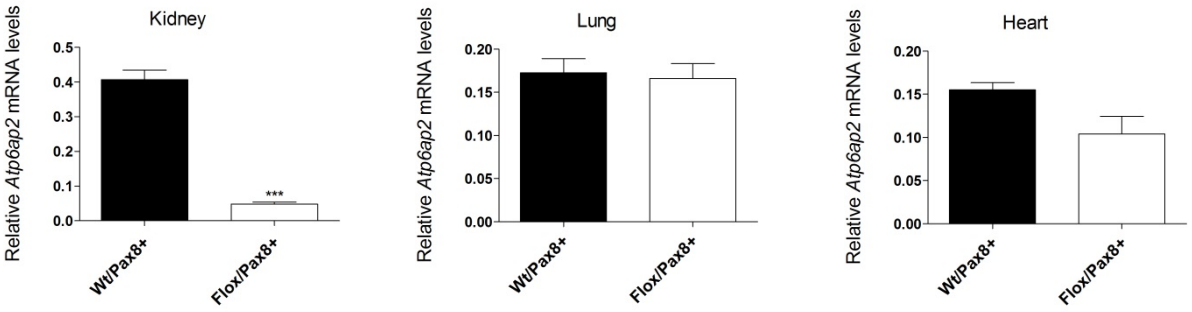
Kidney
Relative Atp6ap2 mRNA levels
0.5
0.4
0.3
0.2
0.1
0.0
***
Wt/Pax8+
Flox/Pax8+
Lung
Relative Atp6ap2 mRNA levels
0.20
0.15
0.10
0.05
0.00
Wt/Pax8+
Flox/Pax8+
Heart
Relative Atp6ap2 mRNA levels
0.20
0.15
0.10
0.05
0.00
Wt/Pax8+
Flox/Pax8+

B

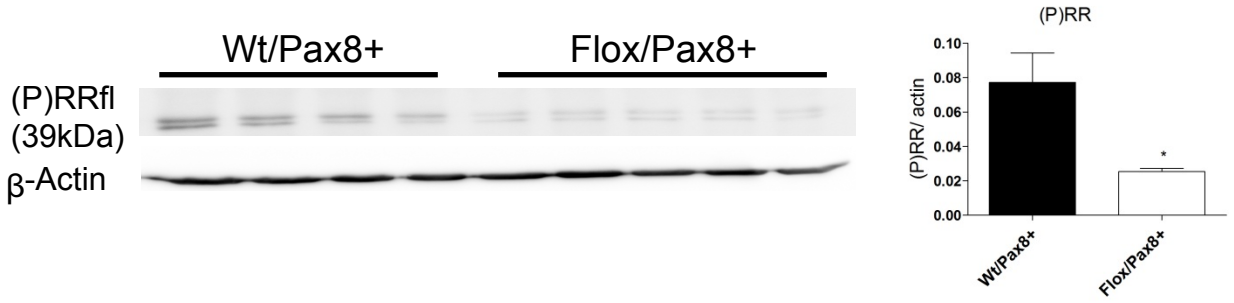
Wt/Pax8+
Flox/Pax8+
(P)RRfl
(39kDa)
β-Actin
(P)RR
(P)RR/ actin
0.10
0.08
0.06
0.04
0.02
0.00
*
Wt/Pax8+
Flox/Pax8+

C

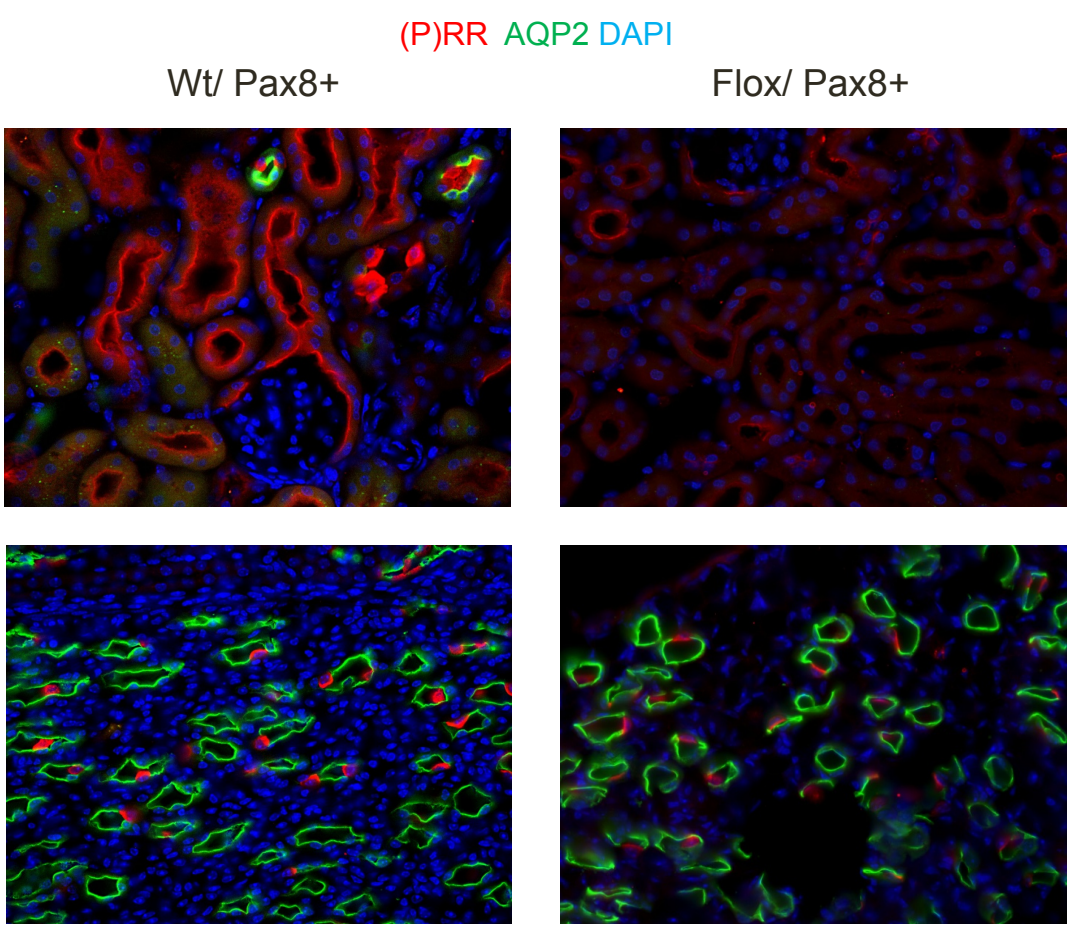
(P)RR AQP2 DAPI
Wt/ Pax8+
Flox/ Pax8+

FIGURE 5

A

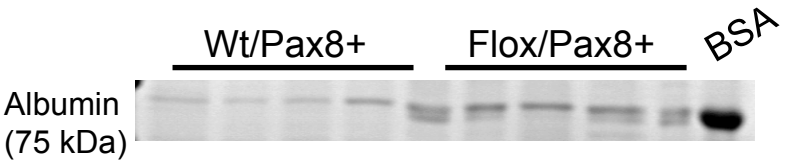
Wt/Pax8+
Flox/Pax8+
BSA
Albumin
(75 kDa)

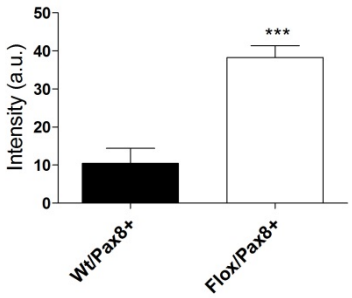
Intensity (a.u.)
50
40
30
20
10
0
***
Wt/Pax8+
Flox/Pax8+

B

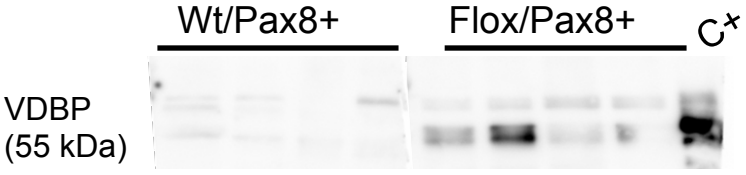
Wt/Pax8+
Flox/Pax8+
C+
VDBP
(55 kDa)

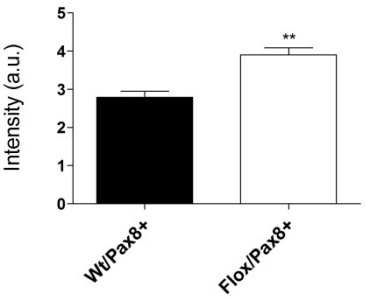
Intensity (a.u.)
5
4
3
2
1
0
**
Wt/Pax8+
Flox/Pax8+

C

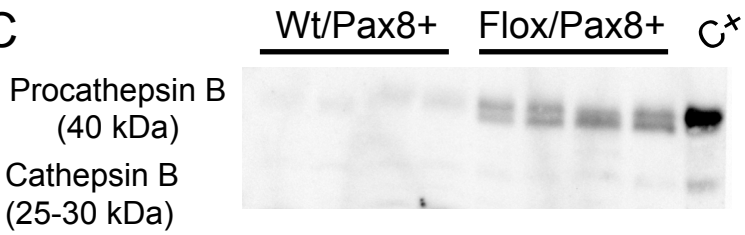
Wt/Pax8+
Flox/Pax8+
C+
Procathepsin B
(40 kDa)
Cathepsin B
(25-30 kDa)

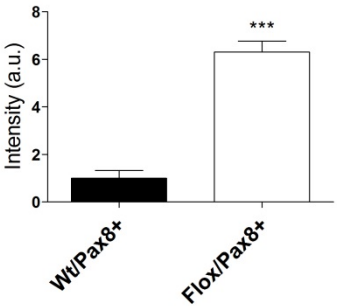
Intensity (a.u.)
8
6
4
2
0
***
Wt/Pax8+
Flox/Pax8+

FIGURE 6

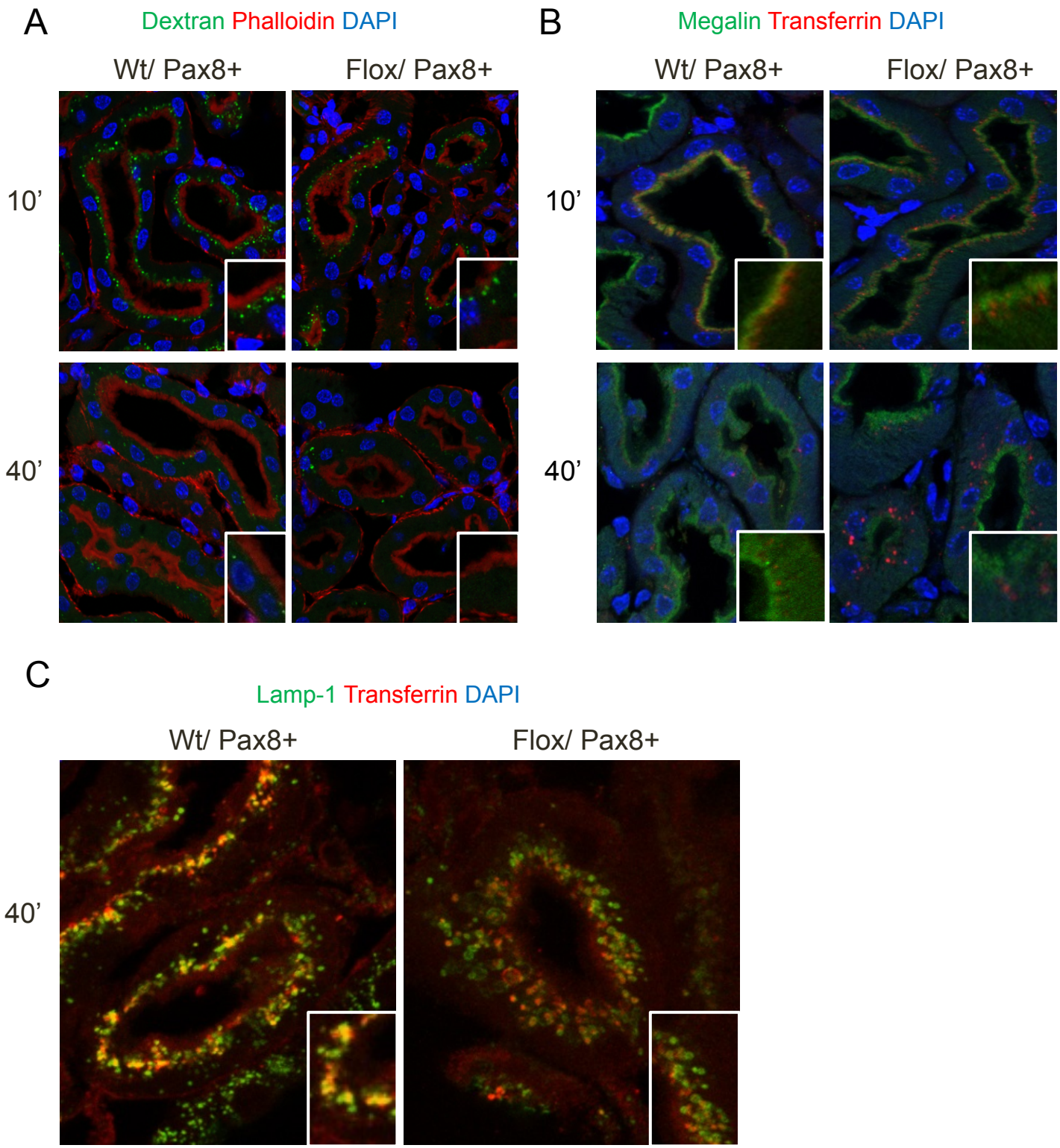
A
Dextran Phalloidin DAPI
Wt/ Pax8+
Flox/ Pax8+
10'
40'
B
Megalin Transferrin DAPI
Wt/ Pax8+
Flox/ Pax8+
10'
40'
C
Lamp-1 Transferrin DAPI
Wt/ Pax8+
Flox/ Pax8+
40'

FIGURE 7

A

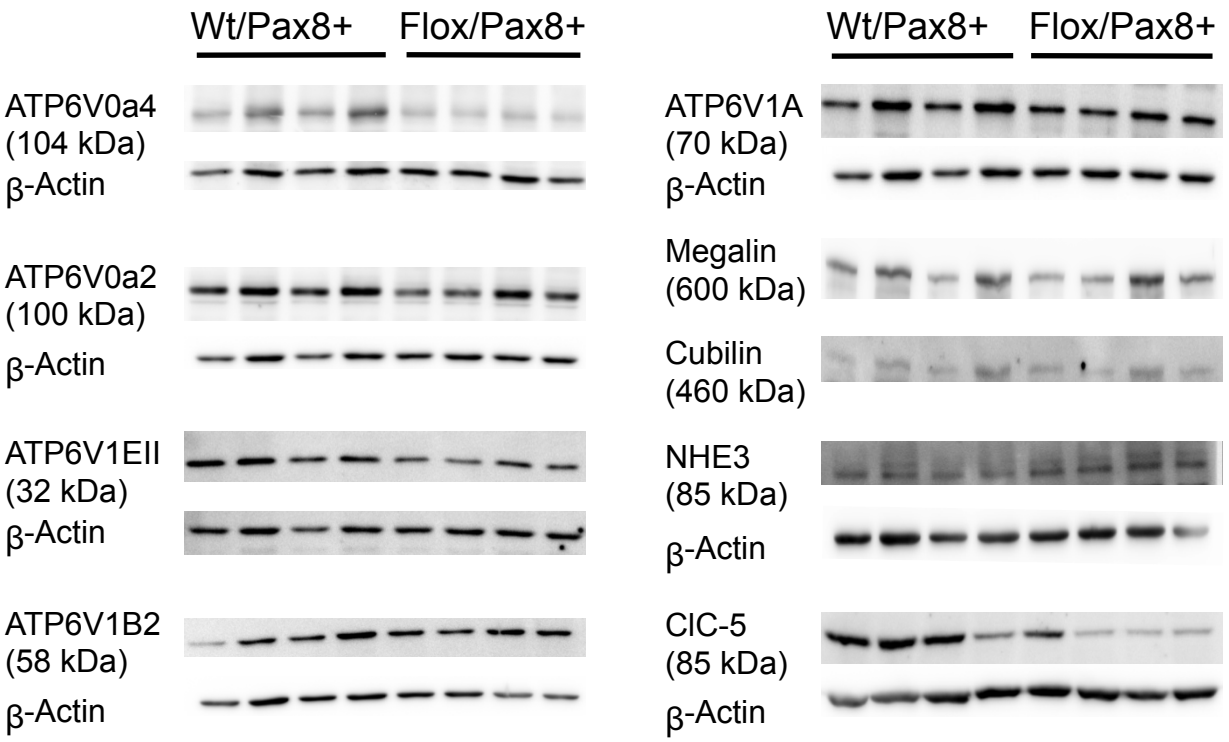
Wt/Pax8+
Flox/Pax8+
ATP6V0a4
(104 kDa)
β-Actin
ATP6V0a2
(100 kDa)
β-Actin
ATP6V1EII
(32 kDa)
β-Actin
ATP6V1B2
(58 kDa)
β-Actin
Wt/Pax8+
Flox/Pax8+
ATP6V1A
(70 kDa)
β-Actin
Megalin
(600 kDa)
Cubilin
(460 kDa)
NHE3
(85 kDa)
β-Actin
ClC-5
(85 kDa)
β-Actin

B

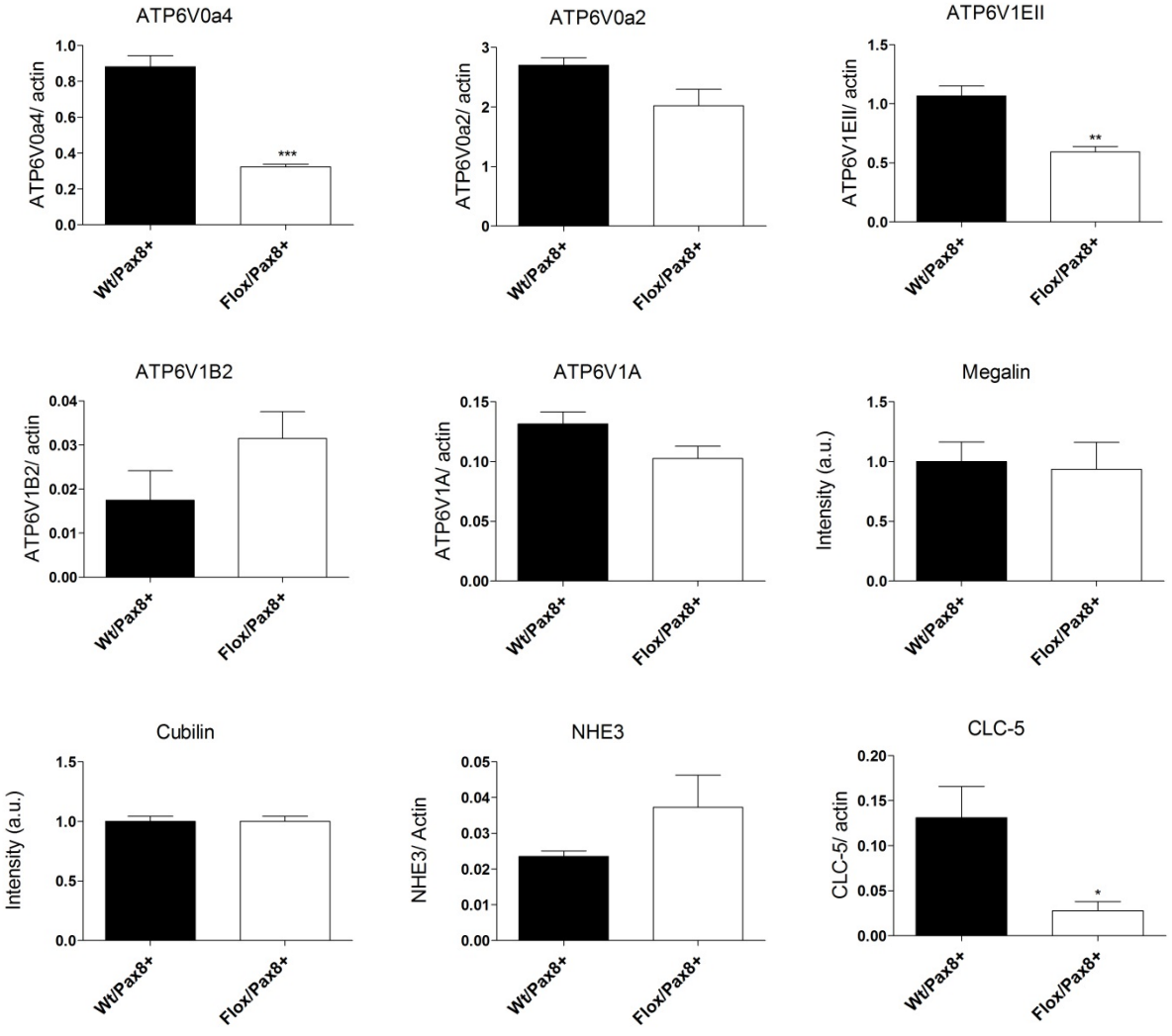
ATP6V0a4
ATP6V0a4/ actin
***
ATP6V0a2
ATP6V0a2/ actin
ATP6V1EII
ATP6V1EII/ actin
**
ATP6V1B2
ATP6V1B2/ actin
ATP6V1A
ATP6V1A/ actin
Megalin
Intensity (a.u.)
Cubilin
Intensity (a.u.)
NHE3
NHE3/ Actin
CLC-5
CLC-5/ actin
*
Wt/Pax8+
Flox/Pax8+

FIGURE 8

A

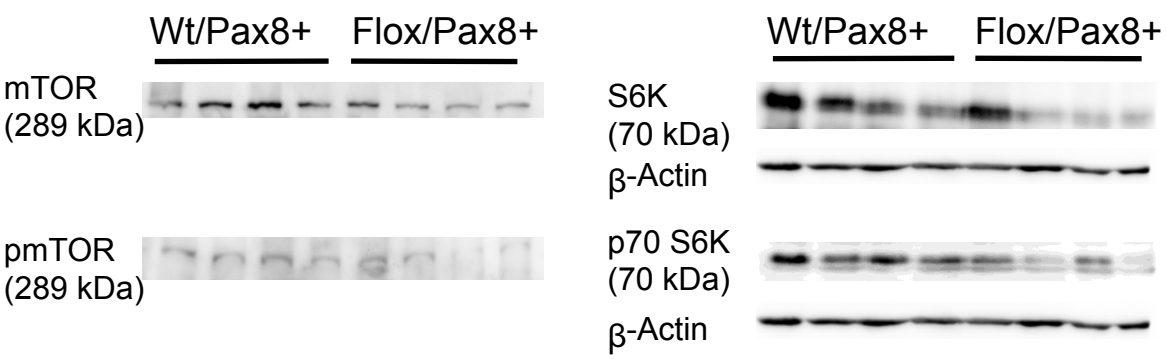
Wt/Pax8+
Flox/Pax8+
mTOR
(289 kDa)
pmTOR
(289 kDa)
Wt/Pax8+
Flox/Pax8+
S6K
(70 kDa)
β-Actin
p70 S6K
(70 kDa)
β-Actin

B

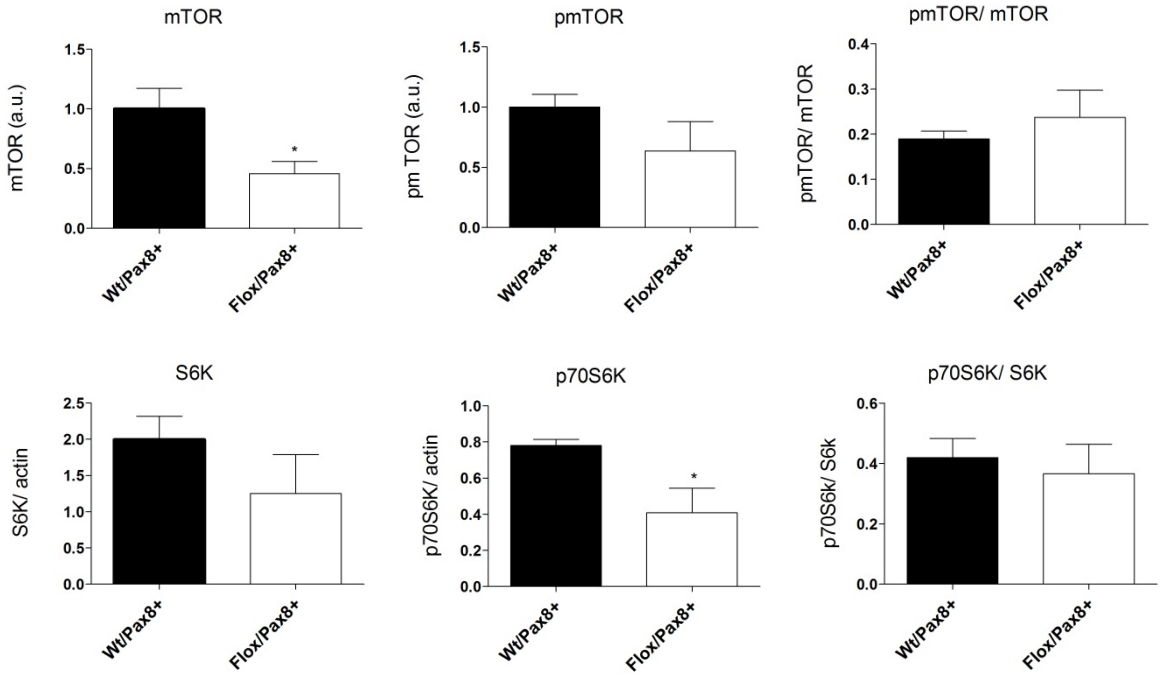
mTOR
mTOR (a.u.)
pmTOR
pm TOR (a.u.)
pmTOR/ mTOR
pmTOR/ mTOR
S6K
S6K/ actin
p70S6K
p70S6K/ actin
p70S6K/ S6K
p70S6k/ S6k
Wt/Pax8+
Flox/Pax8+

C

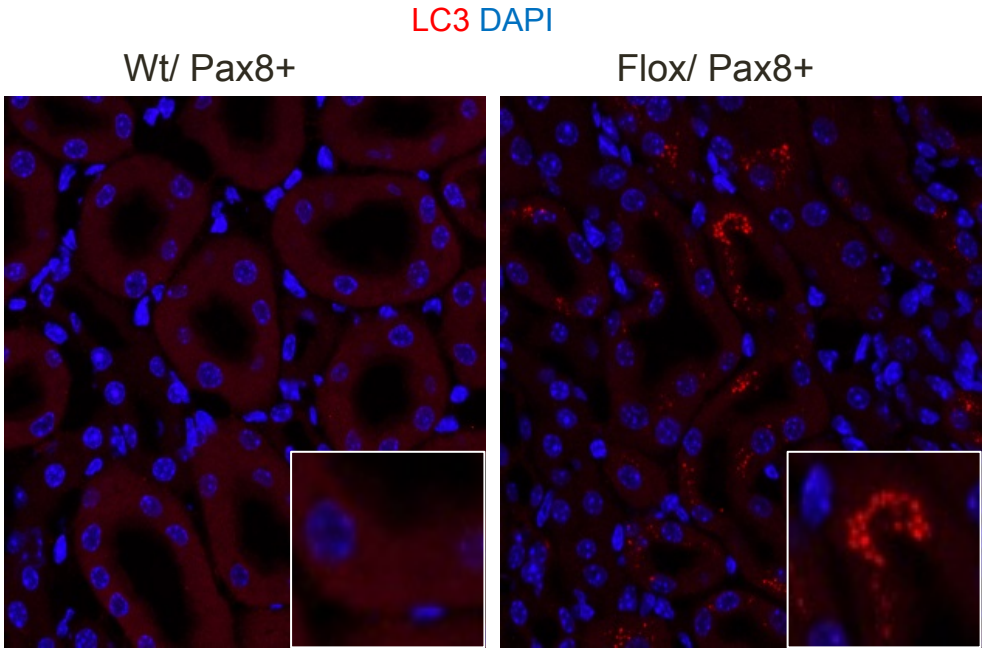
LC3 DAPI
Wt/ Pax8+
Flox/ Pax8+

SUPPLEMENTARY FIGURE 1

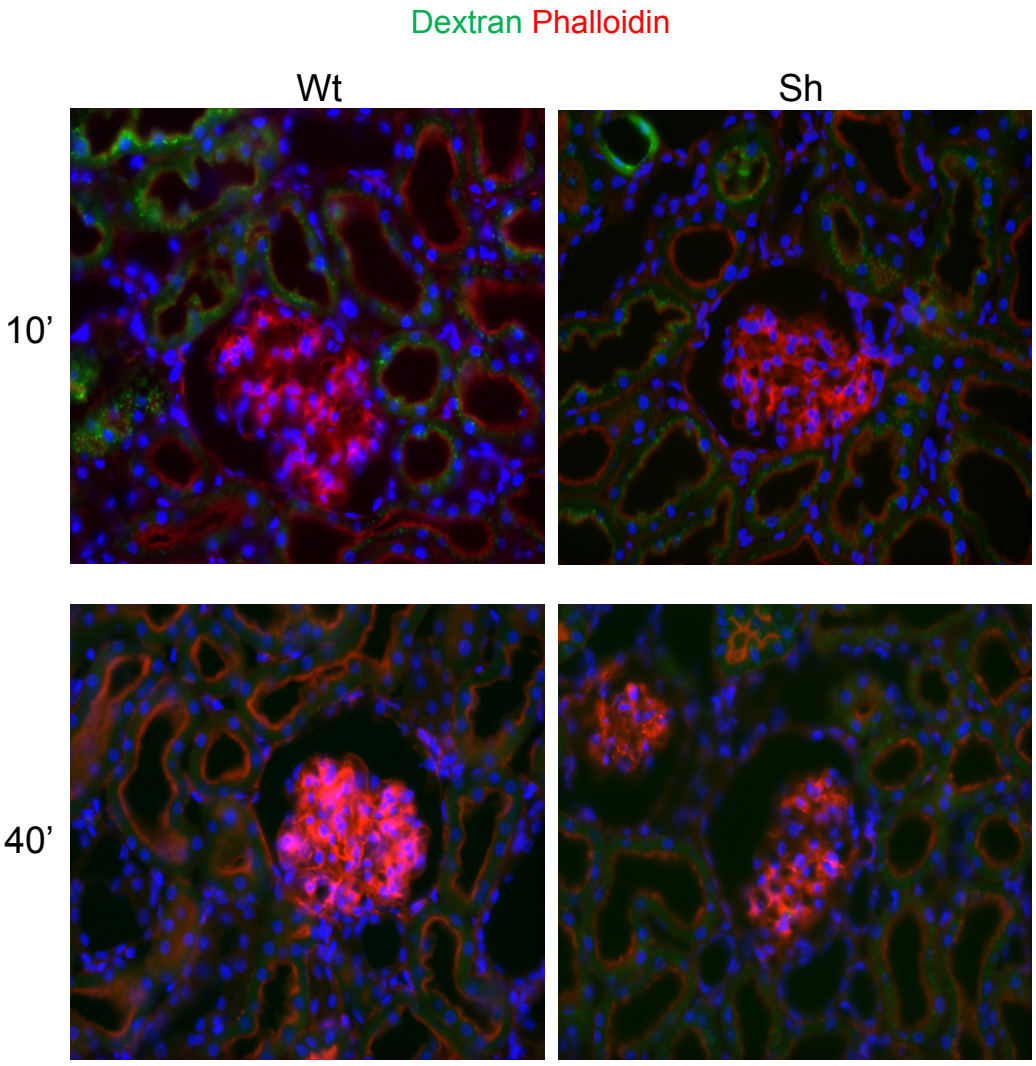

SUPPLEMENTARY FIGURE 2

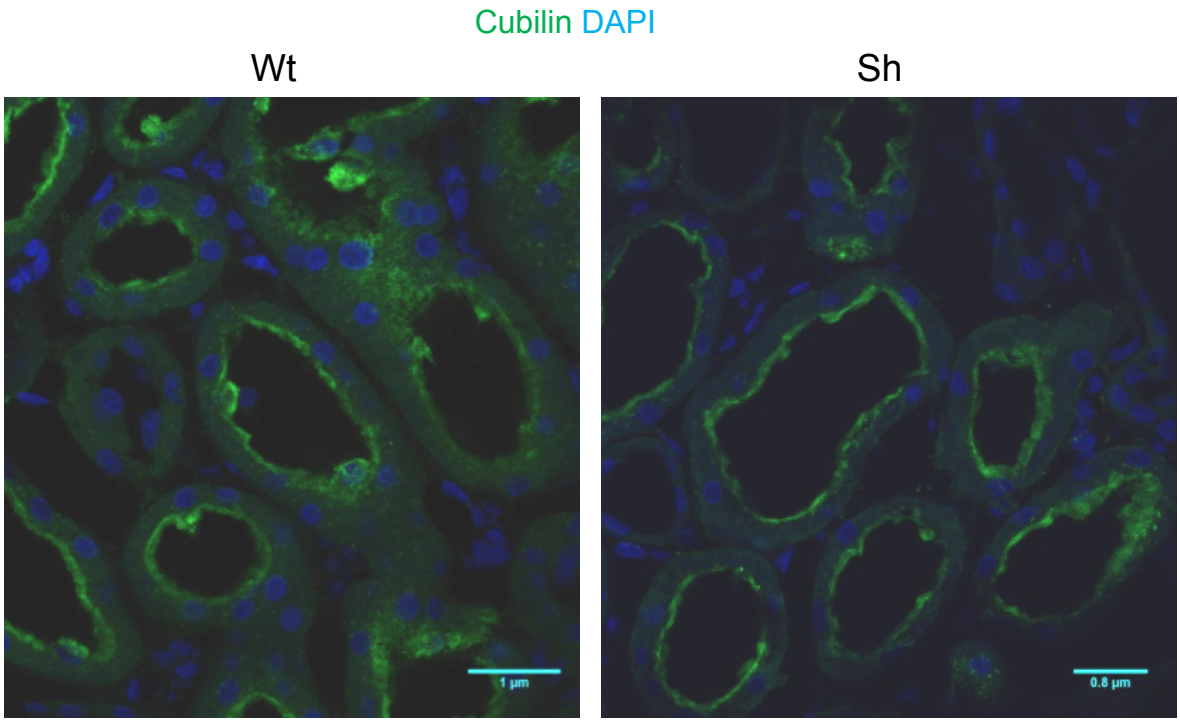

SUPPLEMENTARY FIGURE 3

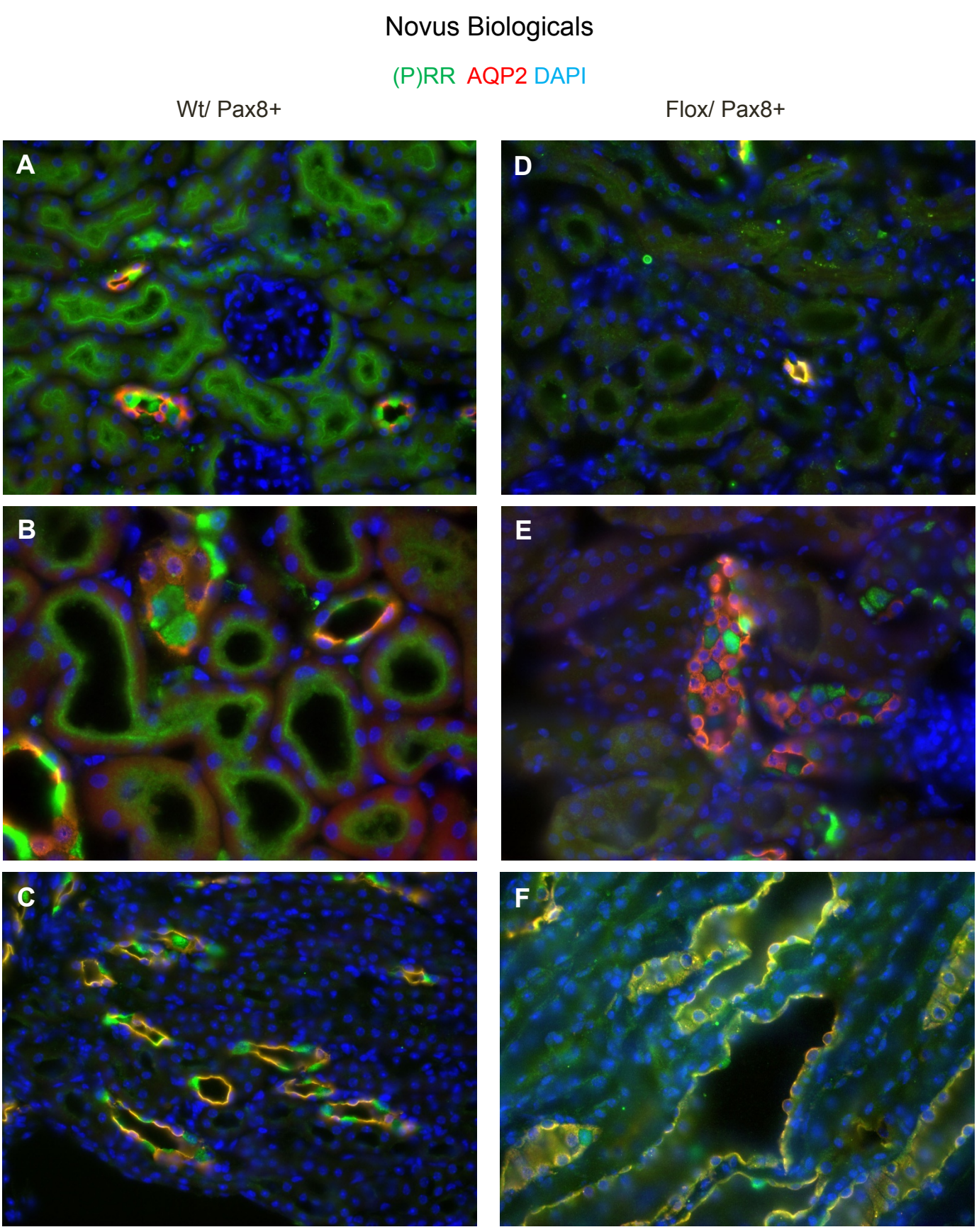

SUPPLEMENTARY FIGURE 4

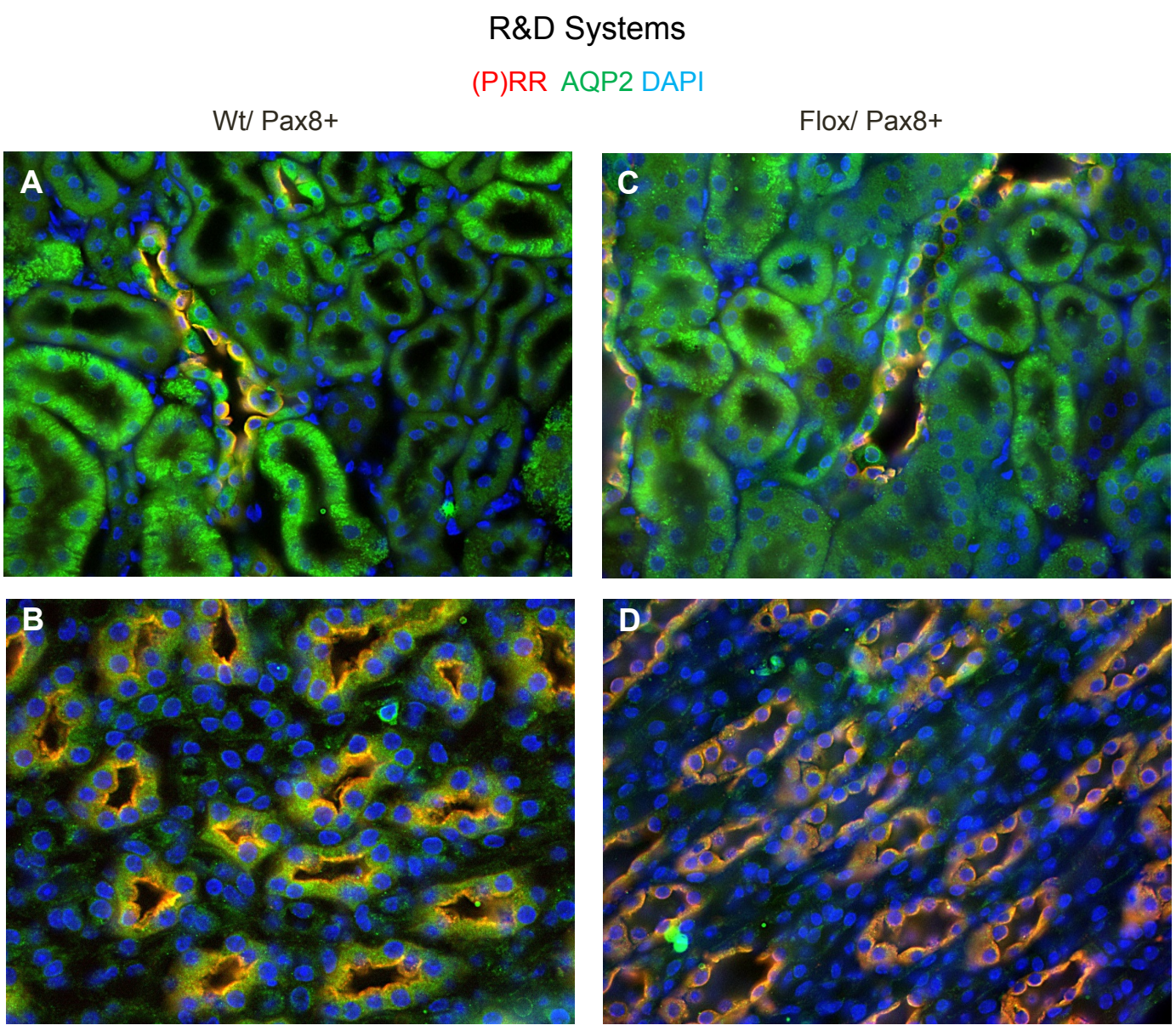

5. Discussion and outlook

The renin-angiotensin system (RAS) is a hormonal system that regulates blood pressure by controlling fluid volume and vascular tone. The RAS system is activated when there is a drop in blood pressure or a drop in extracellular body fluid volume. This system is a pharmacological target for the most common drugs used for hypertension and cardiovascular diseases. Drugs like renin inhibitors (aliskiren), angiotensin-converting enzyme (ACE) inhibitors (captopril), angiotensin II receptor type 1 (AT1) antagonist (losartan) or mineralocorticoid receptor blockers (spironolactone**)** are widely prescribed [125]. The RAS is activated by the conversion of prorenin by proteolytical removal of its pro-segment into its active form renin. Renin then converts angiotensinogen into angiotensin I (AngI), representing the rate limiting step in the RAS system. Subsequently, AngI is further cleaved by the angiotensin-converting enzyme (ACE) to give origin to angiotensin II (AngII) [125]. This system was considered the classic RAS or systemic RAS in which prorenin was viewed as an inactive precursor. This concept was challenged by evidence pointing to a local RAS in several organs that seemed to work independently from the systemic RAS. Furthermore, upon blocking of several RAS components it was observed that plasma renin but also prorenin increased [125]. Hypertension and diabetes also cause a rise of plasma levels of both renin and prorenin [126,127]. Furthermore, in another study using transgenic mice, it was shown that prorenin was activated in pituitary glands in a non proteolytic fashion [128].

In the sequence of these events, the (Pro)renin receptor or (P)RR was discovered in 2002 by Nguyen et al. as a membrane protein that could bind both renin and prorenin [62]. They found that prorenin could also become activated through a conformational change leading to initiation of the RAS system. In addition to the activation of RAS and Ang II production, binding of renin/prorenin to (P)RR stimulates signaling pathways like ERK1/2 or MAP kinase independent from AngII production [75,129,130]. Importantly, the affinity for

renin and prorenin to the (P)RR is in the nanomolar range for both while under physiological conditions their concentration is in the picomolar range (≅ 0.5 pmol/L for renin and ≅ 5pmol/L for prorenin) [131,132]. Also, attempts to generate (P)RR full knockout mouse failed while knockouts models for other RAS members were generated successfully [133,134]. These discordant data together with evidence that (P)RR is expressed in animals lacking a functional RAS system such as Drosophila and Zebra fish suggests that (P)RR has more fundamental functions not related to the RAS. Furthermore, (P)RR was found to be identical to a protein M8-9 that was co-purified together with H^+-ATPases from chromaffin cells [62,69]. Hence, in the last 6 years the (P)RR field is moving towards understanding the fundamental functions of the (P)RR/ATP6ap2. Since then, the (P)RR was found to be important in Wnt signaling [81,117], for podocyte [118,120,135] and cardiomyocyte [116] function but also for lysosomal and autophagy function [117,119,136]. These studies together with immunoprecipitation and immunohistochemistry studies indicate that (P)RR/ATP6ap2 is physically coupled to H^+-ATPases [64,81,115]. In this context, this thesis addresses a timely question in the research focus of (P)RR/ATP6ap2 functions related to H^+-ATPases. We were particularly interested in studying this potential partnership in the kidney where H^+-ATPases are highly expressed.

In chapter 1, our study expands earlier observations on (P)RR/ATP6ap2 expression in the murine kidney. Our results demonstrate that (P)RR/ATP6ap2 has higher expression in the collecting duct, specifically in IC. Furthermore, with regard to (P)RR/ATP6ap2 localization in IC subtypes, (P)RR/ATP6ap2 follows H^+-ATPase plasma membrane localization. The same applies for PT localization. By placing mice on different diets known to affect H^+-ATPase abundance and subcellular localization we looked whether H^+-ATPase expression and trafficking also has a parallel effect on (P)RR/ATP6ap2. Using a combination of mRNA and protein expression studies we found no evidence for coordinated regulation of mRNA/ protein of (P)RR/ATP6ap2 and H^+-ATPase subunits a4 and B1. On the other side, immunohistochemistry showed that (P)RR/ATP6ap2 co-localizes with the V-ATPase subunit a4 to a high degree in IC-type A (basolateral staining for

Ae1) and IC- type B or non-A non-B (negative staining for Ae1) following H^+-ATPase trafficking upon different diets/treatments. In a last set of experiments we addressed the question whether prorenin would acutely affect basal H^+-ATPase function in type A intercalated cells. We address this question by performing microperfusion experiments in murine isolated cortical collecting ducts exposed to different prorenin concentrations and examined H^+-ATPase activity (measured as pHi recovery rates after intracellular acidification with a NH_4Cl prepulse). We also checked for (P)RR/ATP6ap2 signaling output by looking at phosphorylation of ERK1/2 in MDCK cell and in freshly isolated collecting ducts. Prorenin had no effect on basal H^+-ATPase activity and ERK1/2 phosphorylation indicating that prorenin is not directly regulating H^+-ATPase activity. Therefore, we could rule out a relevance of acute prorenin for the regulation of H^+-ATPase activity which seems to be independent of the role of (P)RR/ATP6ap2 in the RAS. Also, our work suggests that H^+-ATPase trafficking does seem to be paralleled by (P)RR/ATP6ap2 trafficking. We have to consider that we only look at a4 and B1 H^+-ATPase subunits. Therefore, our observations can be due to this H^+-ATPase subunits composition. This work does not address the potential functional relevance of (P)RR/ATP6ap2 for PT or IC function.

In chapter 2, we investigated the function of the (P)RR/ATP6ap2 in the PT using two different animal models. A rat model with an inducible shRNA for *Atp6ap2* and an inducible kidney epithelial cell-specific knockout mouse for (P)RR/ATP6ap2. The rat model was a full knockdown of (P)RR/ATP6ap2 which means that (P)RR/ATP6ap2 expression was also abrogated in the podocytes. The inducible kidney epithelial cell-specific knockout mouse model bypassed the problems of a full knockdown of (P)RR/ATP6ap2 and in particular in the podocytes, resulting in a better model to study PT. Furthermore, our mild induction protocol for the mouse model led to a successful knockout for (P)RR/ATP6ap2 in the PT but only partial knockout in the IC. With a milder induction we circumvented doxycycline kidney side effects and also avoided IC cells phenotype already described in previous studies [72,73,137]. In this manner, we could better focus on study (P)RR/ATP6ap2 function in the PT. In this study, we revealed that

(P)RR/ATP6ap2 plays a role in receptor-mediated endocytosis and lysosomal function in the proximal tubule. Both *Atp6ap2*-Sh rats and Flox(P)RR/Pax8Cre+ mice showed excretion of albumin and low molecular weight proteins in urine, delayed processing of substrates of the receptor-mediated endocytosis pathway, reduced expression of other key molecules involved in this process as well as downregulation of the mTOR pathway and accumulation of the LC3B subunit of the autophagosome.

Furthermore we observed reduced expression of several H^+-ATPase subunits including the a4 subunit (ATP6V0a4) in *Atp6ap2*-Sh rats and knockout mice. The chloride/proton exchanger ClC-5 had reduced expression in knockout mice while in the *Atp6ap2*-Sh rats was increased. Both H^+-ATPase and ClC-5 are known to be important for endosomal pathway acidification, suggesting impairment in the acidification of endosomes and lysosomes. Lysosomal dysfunction is also suggested by altered mTOR signaling and accumulation of LC3B, a marker for autophagy. It still remains unclear, whether the observed effects are caused by (P)RR/ATP6ap2 deletion and/or are a direct consequence of endosome/ lysosome defects.

This study confirms the role of the (P)RR/ATP6ap2 in autophagy already observed in podocytes [118,120] and cardiomyocytes [116], by showing it in a different cell type, in PT epithelial cells. In fact, this was the first study assessing the role of the (P)RR/ATP6ap2 role in PT function. Although we described a specific defect in receptor-mediated endocytosis and suggested that this defect may be due to acidification problems. It would be interesting to actually measure lysosomal pH in (P)RR/ATP6ap2 transgenic models. This could be done by performing a functional study by measuring lysosome activity (by using DQ-albumin for example) and lysosome acidification (by using Lysotracker) in isolated PT or primary cells by microperfusion.

We could not explain why there is no defect in the expression or localization of megalin and cubulin, the multispecific receptors involved in receptor-mediated endocytosis. Megalin and cubilin are responsible for reabsorbing transferrin, albumin, vitamin D binding protein and procathepsin B, ligands that were found in the urine of (P)RR/ATP6ap2 transgenic animals.

Furthermore, both megalin and cubulin, after releasing their respective ligands in the early endosome, are recycled back to the plasma membrane. In the case of an impairment of endocytic acidification, the release of ligands from their receptors is also delayed. Accordingly, CLC-5 KO mice, had an impaired endocytic uptake due to a decreased expression of megalin and cubilin in PT BBM [53]. Also, rapamycin chronically treated mice (inhibition of mTORC1) showed LMW proteinuria consistent with lower expression of megalin in the PT [102]. Similarly, animal models of cystinosis displayed LMW proteinuria related to a reduced expression of megalin and cubilin in the PT [58,138].

It is important to note that (P)RR/ATP6ap2 knockdown or knockout leads to a mild defect which could be due to residual expression of (P)RR/ATP6ap2 in both animal models. In the case of flox(P)RR/Pax8Cre+ mice although most of the (P)RR/ATP6ap2 is deleted in the PT, it was still expressed in the IC..

As mentioned above, upon (P)RR/ATP6ap2 downregulation or deletion, only a few H^+-ATPase subunit isoforms were affected. It is also important to note, that the (P)RR/ATP6ap2 does not have a homolog in unicellular organisms like yeast where H^+-ATPase is functional and well characterized. This suggests that the (P)RR/ATP6ap2 is not essential for all types of H^+-ATPases [116,139]. It may be that the (P)RR/ATP6ap2 does not participate in all H^+-ATPase functions and that plasma membrane function and intracellular membrane function should be addressed separately. One should also keep in mind an important observation from our studies in Chapter 1 where we demonstrate that (P)RR/ATP6ap2 and H^+-ATPase do not seem to be regulated in parallel in all situations. When we used *Atp6ap2*-Sh Rats and Flox(P)RR/Pax8Cre+ mice, we see only a defect in receptor-mediated endocytosis but not in fluid phase endocytosis. Also, we cannot discard the idea that lysosomal and autophagy defects resulting from (P)RR/ATP6ap2 knockdown or knockout could be a consequence of cellular defects, instead of a direct effect of impaired H^+-ATPase expression or function. Another open question that remains to be addressed is what is the

mechanism through which (P)RR/ATP6ap2 is important for H^+-ATPase function.

The body of work covered in the current thesis sheds new light on the role of the (P)RR/ATP6ap2 in intracellular organelles in PT. However, further experiments are required to fill the knowledge gap in the field. The mechanistic basis for (P)RR/ATP6ap2 would be an essential first step towards understanding its role in the regulation of H^+-ATPase function.

In the (P)RR/ATP6ap2 field it is becoming clear that (P)RR functions go beyond the RAS regulation. The (P)RR/ATP6ap2 is important for cellular homeostasis by regulating H^+-ATPase activity. With our work we build on the work already done in kidney to understand the role of the (P)RR/ATP6ap2 in this organ [64,118,120] and also extend the knowledge on the role of the (P)RR/ ATP6ap2 in intracellular trafficking. Our data also suggests that this role of (P)RR/ATP6ap2 could be via H^+-ATPase regulation. The identity of the H^+-ATPase subtypes and the mechanism(s) underlying (P)RR/ATP6ap2 effects on H^+-ATPase function needs to be determined.

References

1. Hall, J. E. *Guyton and Hall Textbook of Medical Physiology*. (Elsevier Health Sciences, 2015).
2. Haraldsson, B., Nyström, J. & Deen, W. M. Properties of the glomerular barrier and mechanisms of proteinuria. *Physiol. Rev.* **88,** 451–487 (2008).
3. Scott, R. P. & Quaggin, S. E. The cell biology of renal filtration. *J. Cell Biol.* **209,** 199–210 (2015).
4. D'Amico, G. & Bazzi, C. Pathophysiology of proteinuria. *Kidney International* **63,** 809–825 (2003).
5. Christensen, E. I., Wagner, C. A. & Kaissling, B. *Uriniferous Tubule: Structural and Functional Organization*. (John Wiley & Sons, Inc., 2011). doi:10.1002/cphy.c100073
6. Maunsbach, A. B. & Christensen, E. I. *Functional Ultrastructure of the Proximal Tubule*. (John Wiley & Sons, Inc., 1992). doi:10.1002/cphy.cp080102
7. Christensen, E. I. & Birn, H. Megalin and cubilin: multifunctional endocytic receptors. *Nat. Rev. Mol. Cell Biol.* **3,** 256–266 (2002).
8. Dickson, L. E., Wagner, M. C., Sandoval, R. M. & Molitoris, B. A. The proximal tubule and albuminuria: really! *J. Am. Soc. Nephrol.* **25,** 443–453 (2014).
9. Christensen, E. I., Verroust, P. J. & Nielsen, R. Receptor-mediated endocytosis in renal proximal tubule. *Pflugers Arch.* **458,** 1039–1048 (2009).
10. Maack, T. *Renal Handling of Proteins and Polypeptides*. (John Wiley & Sons, Inc., 2010). doi:10.1002/cphy.cp080244
11. Huotari, J. & Helenius, A. Endosome maturation. *EMBO J.* **30,** 3481–3500 (2011).
12. Doherty, G. J. & McMahon, H. T. Mechanisms of endocytosis. *Annu. Rev. Biochem.* **78,** 857–902 (2009).
13. Scott, C. C., Vacca, F. & Gruenberg, J. Endosome maturation, transport and functions. *Seminars in Cell and Developmental Biology* **31,** 2–10 (2014).
14. Dobrowolski, R. & De Robertis, E. M. Endocytic control of growth factor signalling: multivesicular bodies as signalling organelles. *Nat. Rev. Mol. Cell Biol.* **13,** 53–60 (2011).
15. Mattila, P. E., Raghavan, V., Rbaibi, Y., Baty, C. J. & Weisz, O. A. Rab11a-positive compartments in proximal tubule cells sort fluid-phase and membrane cargo. *Am. J. Physiol., Cell Physiol.* **306,** C441–9 (2014).
16. Nielsen, R. *et al.* Characterization of a kidney proximal tubule cell line, LLC-PK1, expressing endocytotic active megalin. *Journal of the American Society of Nephrology* **9,** 1767–1776 (1998).
17. Ryan, M. J. *et al.* HK-2: An immortalized proximal tubule epithelial cell line from normal adult human kidney. *Nat Rev Nephrol* **45,** 48–57

(1994).
18. Wohlfarth, V., Drumm, K., Mildenberger, S., Freudinger, R. & Gekle, M. Protein uptake disturbs collagen homeostasis in proximal tubule-derived cells. *Kidney International* **63,** S103–S109 (2003).
19. Rodman, J. S., Kerjaschki, D., Merisko, E. & Farquhar, M. G. Presence of an extensive clathrin coat on the apical plasmalemma of the rat kidney proximal tubule cell. *J. Cell Biol.* **98,** 1630–1636 (1984).
20. Nielsen, S. Endocytosis in proximal tubule cells involves a two-phase membrane-recycling pathway. *Am. J. Physiol.* **264,** C823–35 (1993).
21. Rodman, J. S., Seidman, L. & Farquhar, M. G. The membrane composition of coated pits, microvilli, endosomes, and lysosomes is distinctive in the rat kidney proximal tubule cell. *J. Cell Biol.* **102,** 77–87 (1986).
22. Birn, H., Christensen, E. I. & Nielsen, S. Kinetics of endocytosis in renal proximal tubule studied with ruthenium red as membrane marker. *Am. J. Physiol.* **264,** F239–50 (1993).
23. Hatae, T., Ichimura, T., Ishida, T. & Sakurai, T. Apical tubular network in the rat kidney proximal tubule cells studied by thick-section and scanning electron microscopy. *Cell Tissue Res* **288,** 317–325 (1997).
24. Kerjaschki, D. & Farquhar, M. G. The pathogenic antigen of Heymann nephritis is a membrane glycoprotein of the renal proximal tubule brush border. *Proc. Natl. Acad. Sci. U.S.A.* **79,** 5557–5561 (1982).
25. Sahali, D. *et al.* Characterization of a 280-kD protein restricted to the coated pits of the renal brush border and the epithelial cells of the yolk sac. Teratogenic effect of the specific monoclonal antibodies. *J. Exp. Med.* **167,** 213–218 (1988).
26. Christensen, E. I., Birn, H., Storm, T., Weyer, K. & Nielsen, R. Endocytic receptors in the renal proximal tubule. *Physiology (Bethesda)* **27,** 223–236 (2012).
27. Nielsen, R., Christensen, E. I. & Birn, H. Megalin and cubilin in proximal tubule protein reabsorption: from experimental models to human disease. *Nat Rev Nephrol* **89,** 58–67 (2016).
28. Marzolo, M.-P. & Farfán, P. New insights into the roles of megalin/LRP2 and the regulation of its functional expression. *Biol. Res.* **44,** 89–105 (2011).
29. Takeda, T., Yamazaki, H. & Farquhar, M. G. Identification of an apical sorting determinant in the cytoplasmic tail of megalin. *AJP: Cell Physiology* **284,** C1105–C1113 (2003).
30. Yuseff, M. I., Farfán, P., Bu, G. & Marzolo, M.-P. A Cytoplasmic PPPSP Motif Determines Megalin‘s Phosphorylation and Regulates Receptor’s Recycling and Surface Expression. *Traffic* **8,** 1215–1230 (2007).
31. Bachinsky, D. R. *et al.* Detection of two forms of GP330. Their role in Heymann nephritis. *Am. J. Pathol.* **143,** 598–611 (1993).
32. Zou, Z. *et al.* Linking Receptor-mediated Endocytosis and Cell Signaling: EVIDENCE FOR REGULATED INTRAMEMBRANE PROTEOLYSIS OF MEGALIN IN PROXIMAL TUBULE. *J. Biol. Chem.* **279,** 34302–34310 (2004).
33. Li, Y., Cong, R. & Biemesderfer, D. The COOH terminus of megalin regulates gene expression in opossum kidney proximal tubule cells.

AJP: Cell Physiology **295,** C529–C537 (2008).
34. Seetharam, B., Christensen, E. I., Moestrup, S. K., Hammond, T. G. & Verroust, P. J. Identification of rat yolk sac target protein of teratogenic antibodies, gp280, as intrinsic factor-cobalamin receptor. *J. Clin. Invest.* **99,** 2317–2322 (1997).
35. Seetharam, B., Levine, J. S., Ramasamy, M. & Alpers, D. H. Purification, properties, and immunochemical localization of a receptor for intrinsic factor-cobalamin complex in the rat kidney. *J. Biol. Chem.* **263,** 4443–4449 (1988).
36. Kozyraki, R. *et al.* Megalin-dependent cubilin-mediated endocytosis is a major pathway for the apical uptake of transferrin in polarized epithelia. *Proc. Natl. Acad. Sci. U.S.A.* **98,** 12491–12496 (2001).
37. Moestrup, S. K. *et al.* The Intrinsic Factor-Vitamin B12 Receptor and Target of Teratogenic Antibodies Is a Megalin-binding Peripheral Membrane Protein with Homology to Developmental Proteins. *J. Biol. Chem.* **273,** 5235–5242 (1998).
38. Ahuja, R. *et al.* Interactions of cubilin with megalin and the product of the amnionless gene (AMN): effect on its stability. *Biochem. J.* **410,** 301–308 (2008).
39. He, Q. Amnionless function is required for cubilin brush-border expression and intrinsic factor-cobalamin (vitamin B12) absorption in vivo. *Blood* **106,** 1447–1453 (2005).
40. Nykjaer, A. *et al.* An endocytic pathway essential for renal uptake and activation of the steroid 25-(OH) vitamin D3. *Cell* **96,** 507–515 (1999).
41. Nielsen, R. *et al.* Endocytosis provides a major alternative pathway for lysosomal biogenesis in kidney proximal tubular cells. *Proc. Natl. Acad. Sci. U.S.A.* **104,** 5407–5412 (2007).
42. Willnow, T. E. *et al.* Defective forebrain development in mice lacking gp330/megalin. *Proc. Natl. Acad. Sci. U.S.A.* **93,** 8460–8464 (1996).
43. Leheste, J. R. *et al.* Megalin knockout mice as an animal model of low molecular weight proteinuria. *Am. J. Pathol.* **155,** 1361–1370 (1999).
44. Leheste, J. R. Hypocalcemia and osteopathy in mice with kidney-specific megalin gene defect. *The FASEB Journal* 1–22 (2002). doi:10.1096/fj.02-0578fje
45. Bachmann, S. *et al.* Kidney-specific inactivation of the megalin gene impairs trafficking of renal inorganic sodium phosphate cotransporter (NaPi-IIa). *Journal of the American Society of Nephrology* **15,** 892–900 (2004).
46. Nykjaer, A. *et al.* An endocytic pathway essential for renal uptake and activation of the steroid 25-(OH) vitamin D3. *Cell* **96,** 507–515 (1999).
47. Kur, E. *et al.* Loss of Lrp2 in zebrafish disrupts pronephric tubular clearance but not forebrain development. *Dev. Dyn.* **240,** 1567–1577 (2011).
48. Amsellem, S. *et al.* Cubilin is essential for albumin reabsorption in the renal proximal tubule. *J. Am. Soc. Nephrol.* **21,** 1859–1867 (2010).
49. Devuyst, O. & Thakker, R. V. Dent's disease. *Orphanet Journal of Rare Diseases* **5,** 28 (2010).
50. Devuyst, O., Jouret, F., Auzanneau, C. & Courtoy, P. J. Chloride channels and endocytosis: new insights from Dent's disease and ClC-5 knockout mice. *Nephron Physiol* **99,** p69–73 (2005).

51. YAMAMOTO, K. *et al.* Characterization of Renal Chloride Channel (CLCN5) Mutations in Dent's Disease. *Journal of the American Society of Nephrology* **11,** 1460–1468 (2000).
52. Devuyst, O. & Luciani, A. Chloride transporters and receptor-mediated endocytosis in the renal proximal tubule. *J Physiol* **593,** 4151–4164 (2015).
53. Christensen, E. I. *et al.* Loss of chloride channel ClC-5 impairs endocytosis by defective trafficking of megalin and cubilin in kidney proximal tubules. *Proc. Natl. Acad. Sci. U.S.A.* **100,** 8472–8477 (2003).
54. Piwon, N., Günther, W., Schwake, M., Bösl, M. R. & Jentsch, T. J. ClC-5 Cl- -channel disruption impairs endocytosis in a mouse model for Dent's disease. *Nature* **408,** 369–373 (2000).
55. Gorvin, C. M. *et al.* Receptor-mediated endocytosis and endosomal acidification is impaired in proximal tubule epithelial cells of Dent disease patients. *Proc. Natl. Acad. Sci. U.S.A.* **110,** 7014–7019 (2013).
56. Wright, J. *et al.* Transcriptional adaptation to Clcn5 knockout in proximal tubules of mouse kidney. *Physiol. Genomics* **33,** 341–354 (2008).
57. Sharma, S., Skowronek, A. & Erdmann, K. S. The role of the Lowe syndrome protein OCRL in the endocytic pathway. *Biological Chemistry* **396,** 1–8 (2015).
58. Ivanova, E. A. *et al.* Endo-Lysosomal Dysfunction in Human Proximal Tubular Epithelial Cells Deficient for Lysosomal Cystine Transporter Cystinosin. *PLoS ONE* **10,** e0120998–18 (2015).
59. de Gasparo, M., Catt, K. J., Inagami, T., Wright, J. W. & Unger, T. International union of pharmacology. XXIII. The angiotensin II receptors. *Pharmacol. Rev.* **52,** 415–472 (2000).
60. Krop, M. & Danser, A. H. J. Circulating versus tissue renin-angiotensin system: on the origin of (pro)renin. *Curr. Hypertens. Rep.* **10,** 112–118 (2008).
61. Krop, M., de Bruyn, J. H. B., Derkx, F. H. M. & Danser, A. H. J. Renin and prorenin disappearance in humans post-nephrectomy: evidence for binding? *Front. Biosci.* **13,** 3931–3939 (2008).
62. Nguyen, G. *et al.* Pivotal role of the renin/prorenin receptor in angiotensin II production and cellular responses to renin. *J. Clin. Invest.* **109,** 1417–1427 (2002).
63. Ichihara, A., Kaneshiro, Y., Takemitsu, T., Sakoda, M. & Itoh, H. The (pro)renin receptor and the kidney. *Semin. Nephrol.* **27,** 524–528 (2007).
64. Advani, A. *et al.* The (Pro)renin receptor: site-specific and functional linkage to the vacuolar H+-ATPase in the kidney. *Hypertension* **54,** 261–269 (2009).
65. Sihn, G., Burcklé, C., Rousselle, A., Reimer, T. & Bader, M. (Pro)renin receptor: subcellular localizations and functions. *Front Biosci (Elite Ed)* **5,** 500–508 (2013).
66. Nguyen, G. & Muller, D. N. The Biology of the (Pro)Renin Receptor. *Journal of the American Society of Nephrology* **21,** 18–23 (2010).
67. Cousin, C. *et al.* Soluble form of the (pro)renin receptor generated by

intracellular cleavage by furin is secreted in plasma. *Hypertension* **53,** 1077–1082 (2009).
68. Yoshikawa, A. *et al.* The (pro)renin receptor is cleaved by ADAM19 in the Golgi leading to its secretion into extracellular space. *Hypertens. Res.* **34,** 599–605 (2011).
69. Ludwig, J. *et al.* Identification and Characterization of a Novel 9.2-kDa Membrane Sector-associated Protein of Vacuolar Proton-ATPase from Chromaffin Granules. *jbc.org*
70. Matavelli, L. C., Huang, J. & Siragy, H. M. IN VIVO REGULATION OF RENAL EXPRESSION OF (PRO)RENIN RECEPTOR BY LOW SODIUM DIET. *Am. J. Physiol. Renal Physiol.* (2012). doi:10.1152/ajprenal.00204.2012
71. Gonzalez, A. A., Womack, J. P., Liu, L., Prieto, M. C. & Seth, D. M. Angiotensin II Increases the Expression of (Pro)Renin Receptor During Low-Salt Conditions. *The American Journal of the Medical Sciences* **348,** 416–422 (2014).
72. Ramkumar, N. *et al.* Nephron-specific deletion of the prorenin receptor causes a urine concentration defect. *Am. J. Physiol. Renal Physiol.* **309,** F48–F56 (2015).
73. Trepiccione, F. *et al.* Renal Atp6ap2/(Pro)renin Receptor Is Required for Normal Vacuolar H+-ATPase Function but Not for the Renin-Angiotensin System. *Journal of the American Society of Nephrology* 1–11 (2016). doi:10.1681/ASN.2015080915
74. Sakoda, M. *et al.* (Pro)renin receptor-mediated activation of mitogen-activated protein kinases in human vascular smooth muscle cells. *Hypertens. Res.* **30,** 1139–1146 (2007).
75. Huang, J., Matavelli, L. C. & Siragy, H. M. Renal (pro)renin receptor contributes to development of diabetic kidney disease through transforming growth factor-β1-connective tissue growth factor signalling cascade. *Clin. Exp. Pharmacol. Physiol.* **38,** 215–221 (2011).
76. Zhang, J. *et al.* Receptor-mediated nonproteolytic activation of prorenin and induction of TGF-β1 and PAI-1 expression in renal mesangial cells. *Am. J. Physiol. Renal Physiol.* **303,** F11–20 (2012).
77. Kaneshiro, Y. *et al.* Increased expression of cyclooxygenase-2 in the renal cortex of human prorenin receptor gene-transgenic rats. *Kidney International* **70,** 641–646 (2006).
78. Huang, J. & Siragy, H. M. Glucose promotes the production of interleukine-1beta and cyclooxygenase-2 in mesangial cells via enhanced (Pro)renin receptor expression. *Endocrinology* **150,** 5557–5565 (2009).
79. Lu, X., Garrelds, I. M., Wagner, C. A., Danser, A. H. J. & Meima, M. E. (Pro)renin receptor is required for prorenin-dependent and -independent regulation of vacuolar H+-ATPase activity in MDCK.C11 collecting duct cells. *Am. J. Physiol. Renal Physiol.* **305,** F417–F425 (2013).
80. Krop, M., Lu, X., Danser, A. H. J. & Meima, M. E. The (pro)renin receptor. A decade of research: what have we learned? *Pflugers Arch.* (2012). doi:10.1007/s00424-012-1105-z
81. Cruciat, C.-M. *et al.* Requirement of prorenin receptor and vacuolar

H+-ATPase-mediated acidification for Wnt signaling. *Science* **327,** 459–463 (2010).
82. Buechling, T. *et al.* Wnt/Frizzled signaling requires dPRR, the Drosophila homolog of the prorenin receptor. *Curr. Biol.* **20,** 1263–1268 (2010).
83. Hermle, T., Saltukoglu, D., Grünewald, J., Walz, G. & Simons, M. Regulation of Frizzled-Dependent Planar Polarity Signaling by a V-ATPase Subunit. *Current Biology* **20,** 1269–1276 (2010).
84. Song, R., Preston, G., Ichihara, A. & Yosypiv, I. V. Deletion of the Prorenin Receptor from the Ureteric Bud Causes Renal Hypodysplasia. *PLoS ONE* **8,** e63835–12 (2013).
85. Song, R. *et al.* Prorenin receptor is critical for nephron progenitors. *Developmental Biology* **409,** 382–391 (2016).
86. Nishi, T. & Forgac, M. The vacuolar (H+)-ATPases--nature's most versatile proton pumps. *Nat. Rev. Mol. Cell Biol.* **3,** 94–103 (2002).
87. Wagner, C. A. *et al.* Renal vacuolar H+-ATPase. *Physiol. Rev.* **84,** 1263–1314 (2004).
88. Forgac, M. Vacuolar ATPases: rotary proton pumps in physiology and pathophysiology. *Nat. Rev. Mol. Cell Biol.* **8,** 917–929 (2007).
89. Toei, M., Saum, R. & Forgac, M. Regulation and isoform function of the V-ATPases. *Biochemistry* **49,** 4715–4723 (2010).
90. Hinton, A., Bond, S. & Forgac, M. V-ATPase functions in normal and disease processes. *Pflugers Arch.* **457,** 589–598 (2009).
91. Breton, S. & Brown, D. Regulation of luminal acidification by the V-ATPase. *Physiology (Bethesda)* **28,** 318–329 (2013).
92. Casey, J. R., Grinstein, S. & Orlowski, J. Sensors and regulators of intracellular pH. *Nat. Rev. Mol. Cell Biol.* **11,** 50–61 (2010).
93. Hurtado-Lorenzo, A. *et al.* V-ATPase interacts with ARNO and Arf6 in early endosomes and regulates the protein degradative pathway. *Nature cell biology* **8,** 124–136 (2006).
94. Marshansky, V., Rubinstein, J. L. & Grüber, G. Eukaryotic V-ATPase: Novel structural findings and functional insights. *BBA - Bioenergetics* **1837,** 857–879 (2014).
95. Marshansky, V., Ausiello, D. A. & Brown, D. Physiological importance of endosomal acidification: potential role in proximal tubulopathies. *Curr. Opin. Nephrol. Hypertens.* **11,** 527–537 (2002).
96. Hosokawa, H. *et al.* The N termini of a-subunit isoforms are involved in signaling between vacuolar H+-ATPase (V-ATPase) and cytohesin-2. *Journal of Biological Chemistry* **288,** 5896–5913 (2013).
97. Marshansky, V. The V-ATPase a2-subunit as a putative endosomal pH-sensor. *Biochem. Soc. Trans.* **35,** 1092–1099 (2007).
98. Cotter, K., Stransky, L., McGuire, C. & Forgac, M. Recent Insights into the Structure, Regulation, and Function of the V-ATPases. *Trends in Biochemical Sciences* **40,** 611–622 (2015).
99. Zoncu, R. *et al.* mTORC1 senses lysosomal amino acids through an inside-out mechanism that requires the vacuolar H(+)-ATPase. *Science* **334,** 678–683 (2011).
100. Zhang, C.-S. *et al.* The Lysosomal v-ATPase-Ragulator Complex Is a Common Activator for AMPK and mTORC1, Acting as a Switch between Catabolism and Anabolism. *Cell Metabolism* **20,** 526–540

(2014).
101. Efeyan, A., Zoncu, R. & Sabatini, D. M. Amino acids and mTORC1: from lysosomes to disease. *Trends Mol Med* **18,** 524–533 (2012).
102. Gleixner, E. M. *et al.* V-ATPase/mTOR Signaling Regulates Megalin-Mediated Apical Endocytosis. *CellReports* **8,** 10–19 (2014).
103. Susani, L. *et al.* TCIRG1-dependent recessive osteopetrosis: Mutation analysis, functional identification of the splicing defects, andin vitro rescue by U1 snRNA. *Hum. Mutat.* **24,** 225–235 (2004).
104. Capecci, J. & Forgac, M. The Function of Vacuolar ATPase (V-ATPase) a Subunit Isoforms in Invasiveness of MCF10a and MCF10CA1a Human Breast Cancer Cells. *J. Biol. Chem.* **288,** 32731–32741 (2013).
105. Brown, D., Paunescu, T. G., Breton, S. & Marshansky, V. Regulation of the V-ATPase in kidney epithelial cells: dual role in acid-base homeostasis and vesicle trafficking. *J. Exp. Biol.* **212,** 1762–1772 (2009).
106. Wall, S. M. Recent advances in our understanding of intercalated cells. *Curr. Opin. Nephrol. Hypertens.* **14,** 480–484 (2005).
107. Brown, D., Hirsch, S. & Gluck, S. An H+-ATPase in opposite plasma membrane domains in kidney epithelial cell subpopulations. *Nature* **331,** 622–624 (1988).
108. Hennings, J. C. *et al.* A mouse model for distal renal tubular acidosis reveals a previously unrecognized role of the V-ATPase a4 subunit in the proximal tubule. *EMBO Mol Med* n/a–n/a (2012). doi:10.1002/emmm.201201527
109. Smith, A. N., Skaug, J., Choate, K. A., Nayir, A. & Bakkaloglu, A. Mutations in ATP6N1B, encoding a new kidney vacuolar proton pump 116-kD subunit, cause recessive distal renal tubular acidosis with preserved hearing. *Nature* **26,** 71–75 (2000).
110. Karet, F. E. *et al.* Mutations in ATP6N1B, encoding a new kidney vacuolar proton pump 116-kD subunit, cause recessive distal renal tubular acidosis with preserved hearing - Nature Genetics. *Nat. Genet.* **26,** 71–75 (2000).
111. Finberg, K. E. *et al.* The B1-subunit of the H(+) ATPase is required for maximal urinary acidification. *Proc. Natl. Acad. Sci. U.S.A.* **102,** 13616–13621 (2005).
112. Paunescu, T. G. *et al.* Compensatory membrane expression of the V-ATPase B2 subunit isoform in renal medullary intercalated cells of B1-deficient mice. *AJP: Renal Physiology* **293,** F1915–F1926 (2007).
113. Vedovelli, L. *et al.* Altered V-ATPase expression in renal intercalated cells isolated from B1 subunit-deficient mice by fluorescence-activated cell sorting. *Am. J. Physiol. Renal Physiol.* **304,** F522–F532 (2013).
114. Connelly, K. A. *et al.* The cardiac (pro)renin receptor is primarily expressed in myocyte transverse tubules and is increased in experimental diabetic cardiomyopathy. *Journal of Hypertension* **29,** 1175–1184 (2011).
115. Merkulova, M. *et al.* Mapping the H+ (V)-ATPase interactome: identification of proteins involved in trafficking, folding, assembly and phosphorylation. *Nature Publishing Group* 1–15 (2015). doi:10.1038/srep14827

116. Kinouchi, K. *et al.* The (pro)renin receptor/ATP6AP2 is essential for vacuolar H+-ATPase assembly in murine cardiomyocytes. *Circ. Res.* **107,** 30–34 (2010).
117. Hermle, T., Guida, M. C., Beck, S., Helmstädter, S. & Simons, M. Drosophila ATP6AP2/VhaPRR functions both as a novel p... [EMBO J. 2013] - PubMed - NCBI. *EMBO J.* **32,** 245–259 (2013).
118. Riediger, F. *et al.* Prorenin Receptor Is Essential for Podocyte Autophagy and Survival. *jasn.asnjournals.org*
119. Rousselle, A., Sihn, G., Rotteveel, M. & Bader, M. (Pro)renin receptor and V-ATPase: from Drosophila to humans. *Clin. Sci.* **126,** 529–536 (2014).
120. Oshima, Y. *et al.* Prorenin receptor is essential for normal podocyte structure and function. *Journal of the American Society of Nephrology* **22,** 2203–2212 (2011).
121. Winter, C. *et al.* Aldosterone stimulates vacuolar H(+)-ATPase activity in renal acid-secretory intercalated cells mainly via a protein kinase C-dependent pathway. *Am. J. Physiol., Cell Physiol.* **301,** C1251–61 (2011).
122. Bastani, B., Purcell, H., Hemken, P., Trigg, D. & Gluck, S. Expression and distribution of renal vacuolar proton-translocating adenosine triphosphatase in response to chronic acid and alkali loads in the rat. *J. Clin. Invest.* **88,** 126–136 (1991).
123. Kotnik, K. *et al.* Inducible transgenic rat model for diabetes mellitus based on shRNA-mediated gene knockdown. *PLoS ONE* **4,** e5124 (2009).
124. Traykova-Brauch, M. *et al.* An efficient and versatile system for acute and chronic modulation of renal tubular function in transgenic mice. *Nat. Med.* **14,** 979–984 (2008).
125. Bader, M. Tissue renin-angiotensin-aldosterone systems: Targets for pharmacological therapy. *Annu. Rev. Pharmacol. Toxicol.* **50,** 439–465 (2010).
126. Véniant, M. *et al.* Vascular damage without hypertension in transgenic rats expressing prorenin exclusively in the liver. *J. Clin. Invest.* **98,** 1966–1970 (1996).
127. Deinum, J. *et al.* Increase in serum prorenin precedes onset of microalbuminuria in patients with insulin-dependent diabetes mellitus. *Diabetologia* **42,** 1006–1010 (1999).
128. Methot, D., Silversides, D. W. & Reudelhuber, T. L. In vivo enzymatic assay reveals catalytic activity of the human renin precursor in tissues. *Circ. Res.* **84,** 1067–1072 (1999).
129. Feldt, S. *et al.* Prorenin and renin-induced extracellular signal-regulated kinase 1/2 activation in monocytes is not blocked by aliskiren or the handle-region peptide. *Hypertension* **51,** 682–688 (2008).
130. Huang, Y., Noble, N. A., Zhang, J., Xu, C. & Border, W. A. Renin-stimulated TGF-beta1 expression is regulated by a mitogen-activated protein kinase in mesangial cells. *Kidney International* **72,** 45–52 (2007).
131. Jan Danser, A. H. *et al.* Determinants of interindividual variation of renin and prorenin concentrations: evidence for a sexual dimorphism

of (pro)renin levels in humans. *Journal of Hypertension* **16,** (1998).
132. Batenburg, W. W. & Danser, A. H. J. (Pro)renin and its receptors: pathophysiological implications. *Clin. Sci.* **123,** 121–133 (2012).
133. Burckle, C. & Bader, M. Prorenin and Its Ancient Receptor. *Hypertension* **48,** 549–551 (2006).
134. Sihn, G., Rousselle, A., Vilianovitch, L., Burcklé, C. & Bader, M. Physiology of the (pro)renin receptor: Wnt of change&quest. *Kidney International* **78,** 246–256 (2010).
135. Li, C. & Siragy, H. M. (Pro)renin receptor regulates autophagy and apoptosis in podocytes exposed to high glucose. *Am. J. Physiol. Endocrinol. Metab.* **309,** E302–10 (2015).
136. Binger, K. J. & Müller, D. N. Autophagy and the (Pro)renin Receptor. *Cellular Endocrinology* **4,** (2013).
137. Ramkumar, N. *et al.* Renal tubular epithelial cell prorenin receptor regulates blood pressure and sodium transport. *Am. J. Physiol. Renal Physiol.* ajprenal.00088.2016 (2016). doi:10.1152/ajprenal.00088.2016
138. Raggi, C. *et al.* Dedifferentiation and aberrations of the endolysosomal compartment characterize the early stage of nephropathic cystinosis. *Human Molecular Genetics* **23,** 2266–2278 (2014).
139. Binger, K. J. & Müller, D. N. Autophagy and the (Pro)renin Receptor. *Front Endocrinol (Lausanne)* **4,** 155 (2013).

Acknowledgements

First, I would like to thank my supervisor, Prof. Carsten Wagner for giving me the opportunity to do my Ph.D in his lab.

Next, I would like to thank my thesis committee members, Dr. Nati Hernando and Prof. Loffing for their feedback and suggestions for my project. In particular, I would like to thank Dr. Nati for helping me troubleshoot complicated experiments and for cheering me up when I had negative results.

I would also like to thank my external member, Prof. Christensen for carefully reviewing this thesis.

I would like to thank old and present member of the Wagner group in particular: Nikole Kampik, Kessara Chang, Linto Thomas, Daniela Spichtig Pedro Henriques and Eva Maria Pastor for helping me overcome frustrating times during my Ph.D. A special thanks goes to Thomas Knöpfel, my running partner, for all our silly and serious conversations.

Many cheers to the J floor “gang” for keeping a nice working atmosphere and organizing extra-lab activities. I would like to thanks Julia for helping me with my thesis German abstract.

I am grateful for my parents and sisters support through out my life. I am also grateful to my husband for being an excellent listener and for always being there for me.

Curriculum Vitae

MARTA FIGUEIREDO

martarakel@gmail.com | +41 774734644 |

Ottenbergstrasse, 39 8049- Zurich; Switzerland

Personal Information

Nationality: Portuguese

Date of birth: 1983-07-19

Marital state: Married

Education

University of Zurich, Physiology Institute — Since 02.2012

Graduation date: May 2016

PhD thesis "**New Insights into (P)RR/ATP6ap2 Function in the Kidney**"

University of Porto, Faculty of Pharmacy — 09.2009-02.2010

Postgraduate training in Clinical Analysis

Major subjects: clinical biochemistry, clinical microbiology and hematology

University of Porto, Faculty of Pharmacy — 10.2001-12.2008

Master in Pharmaceutical Sciences

Major subjects: microbiology, physiology, pharmaceutical organic chemistry, pharmacology

Work experience

Teaching laboratory practicals: University of Zurich; BIO 401

09.2013-11.2013

Laboratory assistant

Course coordinator: Prof. Thierry Hennet

- Functions of the human body (muscle contractions and blood circulation)

Guidance, supervision and report evaluation.

University of Zurich, Institute of Virology 03.2011-12.2011

VetSuisse Faculty, Winterthurerstrasse 266a, CH-8057 Zürich, Switzerland

Research assistant

Supervisor: Prof. Dr. Mathias Ackermann; Dr.Catherine Eichwald

- Cloning on *Bacillus subtillis* spores to develop a rotavirus oral vaccine
- Performed an immunization protocol for oral vaccine in mice
- Set up an ELISA for detecting rotavirus antibodies

University of Zurich, Institute of pharmacology and toxicology

03.2010-12.2010

University of Zurich, Winterthurerstrasse 190, CH-8057 Zürich, Switzerland

Research assistant

Supervisor: Prof. Jean-Marc Fritschy; Dr. Florence Crestani

- Behavioural characterization of α2 knock-out mice by using two behavioural paradigm
- Developed *in-situ* hybridization for brain mice sections
- Performed the behavioural data analysis and brain morphology data collection.

Farmàcia da Misericordia 01.2009-09.2009

Rua Correia de Oliveira, 62, 3660 - 442 S. Pedro do Sul, Portugal

Pharmaceutical assistant

Employer: Dr. Isabel Serra

- Oversee medical precriptions and patient conseling for medicinal usage.
- Oversee patient queries and complaints.
- Support and aid during health information campaings (e.g heart day)

Farmàcia da Mouro 09.2008-11.2008

Quinta Galo Lote 1-B, 3500-223 Viseu, Portugal

Community pharmacy internship

Supervisor: Dr. Ana Pipa

- Receive stocks and log inventory of all medications.
- Read and verify information contained in the prescriptions.
- Compile precriptions, patient information and other relevant information for the pharmacy.
- Drug formulation according with doctor's prescription or Portuguese pharmacopoeia.

University of Aberdeen, College of Physical Sciences - Chemistry

04.2008-08.2008

Trace Element Speciation Laboratory (tesla), Meston Walk Aberdeen AB24 3UE, Scotland UK Erasmus Project

Supervisor: Prof. Jorg Felman

- Stablish the best post-separation treatment for metalloproteins from sheep's liver and kidnes tissue.
- Detection of metals conjugated to metaloproteins from sheep's liver and kidney by using Laser ablation- inductively coupled plasma mass spectometry

Scholarships and Awards

- Travel Grant: Swiss Physiological Society 2015
- Travel grant: Epithelial Transport Group, American Physiological Society 2015
- StudEx scholarship (Leonardo Da vinci grant) 03.2010-12.2010
- National Contest: Third place " Advising patients 2007", Portuguese Association of Pharmacy´s Students (APEF- Associação Portuguesa de Estudantes de Farmácia)

Academic conferences

- Deutsche Physiologische Gesellschaft, Lübeck, Germany (Presentation) 03.2016
- Experimental Biology, Boston, U.S.A (Presentation/Poster) 04.2015
- (P)RR meeting, Roterdam, Netherland (Presentation) 11.2014
- Swiss Physiological Society, Fribourg, Switzerland (Poster) 09.2014
- Deutsche Physiologische Gesellschaft, Heidelberg Germany (Presentation) 03.2012

Publications:

- Daryadel A, Bourgeois S, Figueiredo MFL, Gomes Moreira A, Kampik NB, Oberli L, et al. (2016) Colocalization of the (Pro)renin Receptor/Atp6ap2 with H^+-ATPases in Mouse Kidney but Prorenin Does Not Acutely Regulate Intercalated Cell H^+-ATPase Activity. PLoS ONE 11(1): e0147831. doi:10.1371/journal.pone.0147831
- Figueiredo MFL, Sihn G, Daryadel A, Müller DN, Popova E, Rouselle A, Nguyen G, Bader M, Wagner CA , The (pro)renin receptor (ATP6ap2) facilitates receptor-mediated endocytosis and lysosomal function in the renal proximal tubule, Kidney International, submitted.